

Synthesis of Metallocene Derivatives:
Precursors for the Preparation
of [1]Metallocenophanes

A Thesis Submitted to the College of
Graduate Studies and Research
in Partial Fulfillment of the Requirements
for the Degree of Master of Science
in the Department of Chemistry
University of Saskatchewan
Saskatoon

By

Jonathon D. Martell

Permission to Use

In presenting this thesis in partial fulfilment of the requirements for a Postgraduate degree from the University of Saskatchewan, I agree that the Libraries of this University may make it freely available for inspection. I further agree that permission for copying of this thesis in any manner, in whole or in part, for scholarly purposes may be granted by the professor or professors who supervised my thesis work or, in their absence, by the Head of the Department or the Dean of the College in which my thesis work was done. It is understood that any copying or publication or use of this thesis or parts thereof for financial gain shall not be allowed without my written permission. It is also understood that due recognition shall be given to me and to the University of Saskatchewan in any scholarly use which may be made of any material in my thesis.

Requests for permission to copy or to make other use of material in this thesis in whole or part should be addressed to:

Head of the Department of Chemistry

University of Saskatchewan

Saskatoon, Saskatchewan (S7N 5C9), Canada

ABSTRACT

The planar-chiral C_2 -symmetrical dibromoferrocene derivatives, (S,S,S_p,S_p) -1,1'-dibromo-2,2'-di(2-butyl)ferrocene (**88**) and (S,S,S_p,S_p) -1,1'-dibromo-2,2'-bis{2-[1-(trimethylsilyl)propyl]}ferrocene (**92**), were synthesized using the well-established “Ugi’s amine” chemistry. The steric influences of the alkyl groups on ferrocenes **88** and **92** in salt-metathesis reactions were investigated. The reaction of **88** and **92** with $i\text{Pr}_2\text{NBCl}_2$ yielded mixtures of bora[1]ferrocenophanes (bora[1]FCPs) **94** and **99** and 1,1'-bis(boryl)ferrocenes **95** and **100** respectively. Ferrocene **92** was expected to yield the highest product ratio of bora[1]FCPs to 1,1'-bis(boryl)ferrocenes due to the significant amount of steric bulk on ferrocene from the alkyl groups; however, the product ratio was less than the product ratio obtained for the less bulky ferrocene **88**. The product ratios for **88** and **92** were compared to the known product ratios for (S_p,S_p) -1,1'-dibromo-2,2'-di(isopropyl)ferrocene (**78**) and (S_p,S_p) -1,1'-dibromo-2,2'-di(3-pentyl)ferrocene (**79**) to determine the effects of the alkyl groups in salt-metathesis reactions. To gain more insight into the effects of the alkyl groups on ferrocenes **88** and **92**, a series of conformational analyses of **78**, **88**, and **92** were performed using density functional theory (DFT) calculations. The DFT calculations aided in the explanation for the unexpectedly low product ratio obtained for ferrocene **92**.

In efforts to obtain new [1]ruthenocenophanes ([1]RCPs), the synthesis of the ruthenium analog of **78**, (S_p,S_p) -1,1'-dibromo-2,2'-di(isopropyl)ruthenocene (**105**), was attempted. To accomplish this, (R,R) -1,1'-bis(α -N,N-dimethylaminoethyl)ruthenocene (**109**) was prepared using the same chemistry that was used to prepare its ferrocene analog. However, the synthesis of (R,R,S_p,S_p) -1,1'-dibromo-2,2'-bis(α -N,N-dimethylaminoethyl)ruthenocene (**110**) via the dilithiation of **109** was unsuccessful.

The synthesis of dibromoferrocene derivatives using “Ugi’s amine” chemistry is a long and inflexible process. Therefore, a method to prepare dibromoferrocene derivatives through an alternative synthetic pathway was investigated. The synthesis of (*S_S,S_S*)-1,1'-bis(*p*-tolylsulfinyl)ferrocene (**118**) was accomplished by reacting dilithioferrocene·tmeda with (*1R,2S,5R*)-(-)-menthyl (*S_S*)-*p*-tolylsulfinate (**117**). The diastereoselective dilithiation and subsequent silylation of **118** to obtain (*S_S,S_S,S_p,S_p*)-2,2'-bis(trimethylsilyl)-1,1'-bis(*p*-tolylsulfinyl)ferrocene (**120**) proved to be problematic.

ACKNOWLEDGMENTS

First, I would like to thank my supervisor Dr. Jens Müller for his patience, support and guidance throughout my graduate studies.

I would like to thank the University of Saskatchewan and the Department of Chemistry for providing me the opportunity to study here and providing financial support. I am grateful for the advice of my advisory committee members and the assistance of the staff at the Saskatchewan Structural Science Centre. In particular, I would like to acknowledge Dr. Keith C. Brown for his help with NMR measurements, Ken Thoms for measuring mass spectra, and Dr. Wilson J. Quail for X-ray diffraction analysis.

I would like to acknowledge all past and present members of the Müller Research group for their support and comradery throughout my studies. It was a joy to work with you all and I wish you all the best with your studies.

I thank God for providing me all the opportunities that I have been given, I truly have been blessed.

I am very grateful to my loving parents Raymond and Sally Martell, as well as my brothers, who have always been there to support me through all my ups and downs. Lastly, I would like to thank all my friends for their support and friendship throughout the years.

TABLE OF CONTENTS

	<u>page</u>
ABSTRACT.....	ii
ACKNOWLEDGMENTS	iv
LIST OF FIGURES	ix
LIST OF SCHEMES.....	x
LIST OF TABLES	xiv
LIST OF ABBREVIATIONS.....	xv
CHAPTER 1: INTRODUCTION	1
1.1 [n]Metallocenophanes.....	3
1.1.1 [1]Ferrocenophanes.....	7
1.1.1.1 Group-13-Bridged [1]Ferrocenophanes.....	8
1.1.1.2 Group-14-Bridged [1]Ferrocenophanes.....	11
1.1.1.3 Group-15-Bridged [1]Ferrocenophanes.....	14
1.1.2 [1]Ruthenocenophanes.....	15
1.2 Metallopolymers via Ring-Opening Polymerization of [n]Metallocenophanes.....	18
1.2.1 Ring-Opening Polymerization Methodologies	21
1.2.1.1 Thermal ROP	21
1.2.1.2 Anionic ROP	22
1.2.1.3 Transition-Metal-Catalyzed ROP	23
1.2.1.4 Photolytic ROP	24
1.2.2 Poly(metallocene)s.....	27
1.2.2.1 Poly(ferrocene)s.....	28
1.2.2.2 Poly(ruthenocene)s	30

1.3 Planar-Chiral Ferrocenes	33
1.3.1 Derivatization of Ferrocene	34
1.3.2 <i>Ortho</i> -Directed Metalation of Ferrocene	36
1.3.3 Diastereoselective <i>ortho</i> -Directed Metalation of Ferrocene	38
1.4 Research Objectives	43
CHAPTER 2: RESULTS AND DISCUSSION	47
2.1 Synthesis of C_2 -Symmetrical Dibromoferrocene Derivatives	47
2.1.1 Synthesis of (<i>S,S,S_p,S_p</i>)-1,1'-Dibromo-2,2'-di(2-butyl)ferrocene	50
2.1.2 Synthesis of (<i>S,S,S_p,S_p</i>)-1,1'-Dibromo-2,2'-bis{2-[1-(trimethylsilyl)propyl]}	
ferrocene	52
2.2 Dibromoferrocene Derivatives as Precursors to Strained Bora[1]ferrocenophanes	57
2.2.1 Author Contribution	57
2.2.2 Salt-Metathesis Reactions of Dibromoferrocene Derivatives	57
2.2.3 Mechanism of Salt-Metathesis Reactions with Aminoboranes	62
2.2.4 DFT Calculations	64
2.3 Synthesis of C_2 -Symmetrical Dibromoruthenocene Derivatives	73
2.3.1 Synthesis of 1,1'-Diacetyl ruthenocene	74
2.3.2 Synthesis of (<i>R,R</i>)-1,1'-Bis(α -hydroxyethyl)ruthenocene	74
2.3.3 Synthesis of (<i>R,R</i>)-1,1'-Bis(α -N,N-dimethylaminoethyl)ruthenocene	75
2.3.4 Dilithiation of (<i>R,R</i>)-1,1'-Bis(α -N,N-dimethylaminoethyl)ruthenocene	76
2.3.5 Future Outlook	78
2.4 Alternate Pathway to C_2 -Symmetrical Dibromoferrocene Derivatives	79
2.4.1 Synthesis of (<i>S_S,S_S</i>)-1,1'-Bis(<i>p</i> -tolylsulfinyl)ferrocene	82

2.4.2 Dilithiation of (<i>S,S,S,S</i>)-1,1'-Bis(<i>p</i> -tolylsulfinyl)ferrocene	84
2.4.3 Future Outlook	85
CHAPTER 3: SUMMARY AND CONCLUSIONS	86
3.1 Synthesis and Application of <i>C</i> ₂ -Symmetrical Dibromoferrocene Derivatives in the Synthesis of Strained Bora[1]ferrocenophanes	86
3.2 Synthesis of <i>C</i> ₂ -Symmetrical Dibromoruthenocene Derivatives	87
3.3 Alternate Pathway to <i>C</i> ₂ -Symmetrical Dibromoferrocene Derivatives	88
CHAPTER 4: EXPERIMENTAL	89
4.1 General Procedures	89
4.2 Reagents	89
4.3 Computational Details	90
4.4 Syntheses	91
4.4.1 Synthesis of (<i>S,S,S_p,S_p</i>)-1,1'-Dibromo-2,2'-di(2-butyl)ferrocene (88)	91
4.4.2 Attempted synthesis of (<i>S,S,S_p,S_p</i>)-1,1'-Dibromo-2,2'-bis[2-(4-methylpentyl)] ferrocene (90)	92
4.4.3 Synthesis of [(Trimethylsilyl)methyl]lithium	93
4.4.4 Synthesis of Tris[(trimethylsilyl)methyl]aluminum	93
4.4.5 Synthesis of (<i>S,S,S_p,S_p</i>)-1,1'-Dibromo-2,2'-bis{2-[1-(trimethylsilyl)propyl]} ferrocene (92)	94
4.4.6 Synthesis of 1,1'-Diacetyl ruthenocene (106)	95
4.4.7 Synthesis of (<i>R,R</i>)-1,1'-Bis(α -hydroxyethyl)ruthenocene (107)	96
4.4.8 Synthesis of (<i>R,R</i>)-1,1'-Bis(α -acetoxyethyl)ruthenocene (108)	97
4.4.9 Synthesis of (<i>R,R</i>)-1,1'-Bis(α -N,N-dimethylaminoethyl)ruthenocene (109)	97

4.4.10 Synthesis of a Mixture of (<i>R,R,S_p,S_p</i>)-1,1'-Dibromo-2,2'-bis(α -N,N-dimethyl-aminoethyl)ruthenocene (110) and (<i>R,R,S_p</i>)-1-Bromo-2,2'-bis(α -N,N-dimethyl-aminoethyl)ruthenocene (111)	98
4.4.11 Synthesis of a Mixture of (<i>S_p,S_p</i>)-1,1'-Dibromo-2,2'-di(isopropyl)ruthenocene (105) and (<i>S_p</i>)-1-Bromo-2,2'-di(isopropyl)ruthenocene (112)	99
4.4.12 Synthesis of (<i>S_S,S_S</i>)-1,1'-Bis(<i>p</i> -tolylsulfinyl)ferrocene (118)	100
4.4.13 Attempted Synthesis of (<i>S_S,S_S,S_p,S_p</i>)-2,2'-Bis(trimethylsilyl)-1,1'-bis(<i>p</i> -tolylsulfinyl) ferrocene (120)	101
REFERENCES	102

LIST OF FIGURES

<u>Figure</u>	<u>page</u>
Figure 1-1. Metallocyclophanes.....	2
Figure 1-2. Geometric angles of [n]MCPs.....	4
Figure 1-3. [n]MCPs with varying metal atoms and bridging elements	5
Figure 1-4. Sila[1]FCPs with substituted Cp rings	13
Figure 1-5. Chiral phospho[1]FCPs	14
Figure 1-6. Assigning planar chirality for 1,2-heterodisubstituted ferrocenes using the R_p and S_p stereodescriptors, as defined by Schlögl, where X has a higher priority than Y	33
Figure 1-7. Substituted ferrocene derivatives used for <i>ortho</i> -directed metalation	38
Figure 1-8. Amount of available space for the bridging moiety, ER _x	43
Figure 1-9. Illustration of the space restrictions in galla[1.1]FCP 14b . The coloured-in hydrogen atoms highlight the group of hydrogen atoms in close proximity to each other.....	44
Figure 2-1. Molecular structure of 92 with thermal ellipsoids at the 50% probability level. Hydrogen atoms are omitted for clarity	54
Figure 2-2. Dibromoferrocene derivatives in increasing order of product ratios (bora[1]FCPs to 1,1'-bis(boryl)ferrocenes) of salt-metathesis with <i>i</i> Pr ₂ NBCl ₂ : (a) order predicted by sterics, (b) order observed experimentally	64
Figure 2-3. Dibromoferrocene derivatives that could potentially increase product ratios between bora[1]FCPs and 1,1'-bis(boryl)ferrocenes in salt-metathesis reactions	72

LIST OF SCHEMES

<u>Scheme</u>	<u>page</u>
Scheme 1-1. Synthetic pathways for [n]MCPs via (a) a salt-methathesis reaction, or (b) the “flytrap” route	4
Scheme 1-2. Synthesis of poly(ferrocenylsilane)s via thermal ROP of sila[1]FCPs	7
Scheme 1-3. Synthesis of bora[1]FCPs	8
Scheme 1-4. Synthesis of alumina[1]FCPs and galla[1]FCPs	9
Scheme 1-5. Synthesis of alumina[1.1]FCP and galla[1.1]FCP	10
Scheme 1-6. Reaction of dilithioferrocene·tmeda with (Mam _x)ECl ₂ (E = Al, Ga)	10
Scheme 1-7. Synthesis of sila[1]FCPs via salt-metathesis	11
Scheme 1-8. Substitution reactions with (a) dichlorosila[1]FCP and (b) chloromethylsila[1]FCPs	12
Scheme 1-9. Synthesis of stanna[1]FCPs	13
Scheme 1-10. Synthesis of phospho[1]FCPs	14
Scheme 1-11. Synthesis of stanna[1]RCP and zircona[1]RCP	15
Scheme 1-12. Synthesis of alumina[1]RCP and galla[1]RCP	16
Scheme 1-13. Reaction of dilithioruthenocene·tmeda and (Mam _x)ECl ₂ (E = Al, Ga)	17
Scheme 1-14. Synthesis of poly(ferrocenylsilane)s via polycondensation reactions	18
Scheme 1-15. Synthesis of poly(ferrocenylphenylphosphine)s via polycondensation reactions	19
Scheme 1-16. Attempted anionic ROP of phospho[1]FCP 32	20
Scheme 1-17. Synthesis of poly(ferrocenylpersulfide)	20
Scheme 1-18. Synthesis of amorphous poly(ferrocenylsilane) 18_n via thermal ROP of 18	21

Scheme 1-19. Synthesis of poly(ferrocenylsilane) 10^{Me}_n via anionic ROP	22
Scheme 1-20. Synthesis of a block co-polymer through living anionic ROP	23
Scheme 1-21. Proposed heterogeneous mechanism for transition-metal-catalyzed ROP	24
Scheme 1-22. Photolytic ROP of metallized phospho[1]FCPs	25
Scheme 1-23. The reaction of phospho[1]FCP 37 with phosphines under UV irradiation	25
Scheme 1-24. Proposed mechanism of photolytic ROP of phospho[1]FCP 37	26
Scheme 1-25. Living photolytic ROP mechanism of sila[1]FCP 10^{Me}	26
Scheme 1-26. Thermal ROP of boro[1]FCPs	29
Scheme 1-27. Reaction of alumina[1]FCP 12a with <i>n</i> BuLi	29
Scheme 1-28. Thermal ROP of dicarba[2]RCPs	31
Scheme 1-29. Thermal ROP of stanna[1]RCP 28	31
Scheme 1-30. Ir/Xyliphos-catalyzed enantioselective hydrogenation of imine 44	34
Scheme 1-31. Friedel-Crafts acylation of 1,1'-disubstituted ferrocenes	35
Scheme 1-32. Lithiation of isopropylferrocene followed by silylation	36
Scheme 1-33. <i>Ortho</i> -directed lithiation of ferrocene 51	36
Scheme 1-34. <i>Ortho</i> -directed lithiation of ferrocene 53	37
Scheme 1-35. Nucleophilic substitution of NMe ₂ in <i>rac</i> - 54	37
Scheme 1-36. Diastereoselectivity of “Ugi’s amine” (<i>R</i>)- 66 (the electrophiles (E = SiMe ₃ , CH ₂ OH, and CPh ₂ OH) all have a higher priority compared to the Ugi amine substituent) ...	39
Scheme 1-37. Diastereoselective lithiation (<i>S</i>)- 69 and (<i>R,R</i>)- 71 followed by quenching with Ph ₂ PCl	40
Scheme 1-38. Nucleophilic substitution of (<i>R</i>)- 66	40
Scheme 1-39. Synthesis of (<i>R_S</i>)- <i>p</i> -tolylsulfinylferrocene	41

Scheme 1-40. Diastereoselective lithiation of (<i>R_S</i>)- 73 and subsequent quenching with an electrophile.....	41
Scheme 1-41. Synthesis of planar-chiral 1,2-disubstituted ferrocenes with no stereogenic centres	42
Scheme 1-42. Synthesis of [1]FCPs with substituted ferrocene derivatives 78 and 79	45
Scheme 2-1. Synthesis of dibromoferrocene derivatives 78 and 79	47
Scheme 2-2. Salt-metathesis reactions between dibromoferrocenes 78 and 79 with <i>i</i> Pr ₂ NBCl ₂	49
Scheme 2-3. Synthesis of (<i>S,S,S_p,S_p</i>)-1,1'-dibromo-2,2'-di(2-butyl)ferrocene (88).....	51
Scheme 2-4. Test dilithiation of the dibromoferrocene derivative 88	51
Scheme 2-5. Reaction of diacetate 85a with TiBA	52
Scheme 2-6. Synthesis of tris[(trimethylsilyl)methyl]aluminum	53
Scheme 2-7. Synthesis of (<i>R,R,S_p,S_p</i>)-1,1'-dibromo-2,2'-bis{2-[1-(trimethylsilyl)propyl]} ferrocene (92).....	53
Scheme 2-8. Test dilithiation of the dibromoferrocene derivative 92	56
Scheme 2-9. Salt-metathesis reaction of 88 with <i>i</i> Pr ₂ NBCl ₂	58
Scheme 2-10. Synthesis of (<i>R,R,S_p,S_p</i>)-1,1'-dibromo-2,2'-di(2-butyl)ferrocene (96).....	59
Scheme 2-11. Salt-metathesis reaction of 96 with <i>i</i> Pr ₂ NBCl ₂	59
Scheme 2-12. Salt-metathesis reaction of 92 with <i>i</i> Pr ₂ NBCl ₂	60
Scheme 2-13. Mechanism of salt-metathesis reactions of ferrocene derivatives with <i>i</i> Pr ₂ NBCl ₂	62
Scheme 2-14. Proposed synthesis of new [1]RCPs using a dibromoruthenocene derivative (105).....	73

Scheme 2-15. Synthesis of 1,1'-diacetyl ruthenocene (106).....	74
Scheme 2-16. Synthesis of (<i>R,R</i>)-1,1'-bis(α -hydroxyethyl)ruthenocene (107)	75
Scheme 2-17. Esterification of diol 107	75
Scheme 2-18. Synthesis of (<i>R,R</i>)-1,1'-bis(α -N,N-dimethylaminoethyl)ruthenocene (109)	76
Scheme 2-19. Attempted synthesis of (<i>R,R,S_p,S_p</i>)-1,1'-dibromo-2,2'-bis(α -N,N-dimethylamino ethyl)ruthenocene (110)	77
Scheme 2-20. Attempted synthesis of (<i>S_p,S_p</i>)-1,1'-dibromo-2,2'-di(isopropyl)ruthenocene (105)	78
Scheme 2-21. Synthesis of dibromoferrocenes 88 and 92	79
Scheme 2-22. Synthesis of planar-chiral 1,2-disubstituted ferrocenes via (<i>S_S</i>)- 75	81
Scheme 2-23. Proposed synthetic pathway for obtaining dibromoferrocene precursors for the preparation of new [1]FCPs via 113	82
Scheme 2-24. Synthesis of (<i>S_S</i>)- <i>p</i> -tolylsulfinylferrocene	83
Scheme 2-25. Synthesis of (<i>S_S,S_S</i>)-1,1'-bis(<i>p</i> -tolylsulfinyl)ferrocene (118)	83
Scheme 2-26. Attempted synthesis of (<i>S_S,S_S,S_p,S_p</i>)-2,2'-bis(trimethylsilyl)-1,1'- bis(<i>p</i> -tolylsulfinyl)ferrocene (120).....	84
Scheme 2-27. Proposed synthesis of dibromoferrocene 121 via ferrocene 120	85
Scheme 3-1. Salt-metathesis reactions of 88 and 92 with <i>i</i> Pr ₂ NBCl ₂	86
Scheme 3-2. Proposed synthesis of dibromoruthenocene 105 via ruthenocene 109	88
Scheme 3-3. Proposed synthesis of dibromoferrocene 121	88

LIST OF TABLES

<u>Table</u>	<u>page</u>
Table 2-1. Crystal and structural refinement data for 92	55
Table 2-2. Measured product ratios of bora[1]FCPs and 1,1'-bis(boryl)ferrocenes.....	61
Table 2-3. Calculated conformers of 78 and distributions of conformers through the rotation of the C2-C11 bond. Hydrogens atoms are omitted for clarity	66
Table 2-4. Calculated conformers of 88 and distributions of conformers through the rotation of the C11-C12 bond. Hydrogens atoms are omitted for clarity	68
Table 2-5. Calculated conformers of 92 and distributions of conformers through the rotation of the C11-C12 bond. Hydrogens atoms are omitted for clarity	70

LIST OF ABBREVIATIONS

Abbreviation

Ar'	2-[(dimethylamino)methyl]phenyl
cod	1,5-cyclooctadiene
Cp	cyclopentadienyl
DFT	density functional theory
DIBALH	diisobutylaluminum hydride
DLS	dynamic light scattering
DSC	differential scanning calorimetry
FCP	ferrocenophane
FD	field desorption
GPC	gel permeation chromatography
HOMO	highest occupied molecular orbital
LDA	lithium diisopropylamide
LUMO	lowest unoccupied molecular orbital
Mamx	2,4-di- <i>tert</i> -butyl-6-[(dimethylamino)methyl]phenyl
MCP	metallocenophane
Me ₂ Ntsi	[(dimethylamino)dimethylsilyl]bis(trimethylsilyl)methyl
M _w	molecular weight
ODG	<i>ortho</i> -directing group
PDI	poly dispersity index
PFSs	poly(ferrocenylsilane)s
pmdta	N,N,N',N',N''-pentamethyldiethylenetriamine

Pytsi	[dimethyl(2-pyridyl)silyl]bis(trimethylsilyl)methyl
r.t.	room temperature
RCP	ruthenocenophane
R _h	hydrodynamic radius
ROP	ring-opening polymerization
TiBA	triisobutylaluminum
tmeda	N,N,N',N'-tetramethylethylenediamine
XRD	X-Ray Diffraction

CHAPTER 1: INTRODUCTION

Many significant advancements have been made in the field of synthetic polymers over the last century and have had a long lasting impact on society.¹⁻³ Without these materials, many modern day essentials would cease to exist, making the world a very different place. The majority of these materials are carbon-based organic polymers which have been studied extensively. Strained cyclic organic compounds have attracted much attention for their use as starting materials for obtaining organic polymers via ring-opening polymerization (ROP), and have been painstakingly studied over many years.⁴ In comparison, the use of strained cyclic organometallic compounds to prepare polymers with metals in the backbone has not been investigated as thoroughly. However, this area of study has gained considerable traction over the last couple of decades, taking advantage of the approximately 80% of elements that have been neglected for making polymers.⁵

Metallocyclophanes are a class of strained cyclic organometallic compounds that contain a transition metal sandwich complex. In these compounds, the two π -hydrocarbon rings of the sandwich complex are linked together by some elements. Among the many metallocyclophanes that have been discovered recently, [n]metallocenophanes ([n]MCPs) (**1**, Figure 1-1) have emerged as an important group of strained cyclic organometallic compounds. [n]MCPs are compounds that contain two η^5 -cyclopentadienyl (Cp) rings that sandwich a transition metal M through π -bonds, and are connected together by n bridging elements through σ -bonds. The first strained [n]MCP, a [2]ferrocenophane ([2]FCP), was prepared in 1960 by Rinehart *et al.*⁶ (**2**, Figure 1-1), containing C₂Me₄ in the bridging position. Due to the amount of strain that was present in this compound, it was speculated that similar compounds with only one element in the bridging position would be impossible to prepare. Despite this claim, a sila[1]FCP (**3**, Figure 1-1) was synthesized by Osborne and Whiteley in 1975.⁷ This led to the discovery of other [1]FCPs with different bridging elements,

such as germanium and phosphorus.^{8,9} Due to the interesting structure of these compounds, this chemistry was extended to the preparation of a wide variety of metallocyclophanes with varying transition metals, π -hydrocarbon rings and bridging elements. [n]Metalloarenophanes (**4**, Figure 1-1), [n]metalloarenocenophanes (**5**, Figure 1-1), [n]troticenophanes (**6** M=Ti, Figure 1-1) and [n]trovacenophanes (**6** M=V, Figure 1-1) are just some of the many examples of metallocyclophanes that have reported.

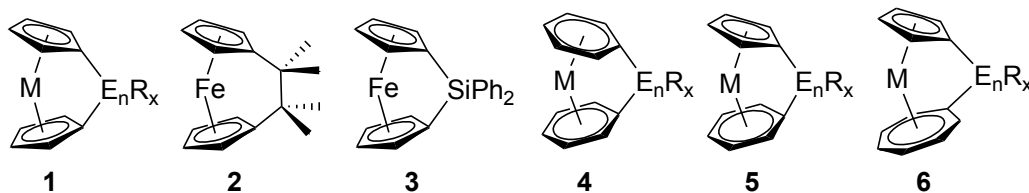
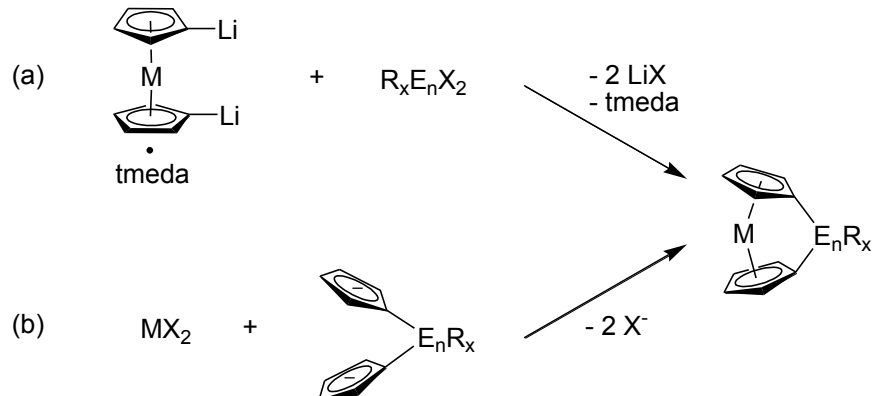


Figure 1-1. Metallocyclophanes.

1.1 [n]Metallophenes

As the number of reports of metallocyclophanes grew, [n]metallophenes ([n]MCPs) emerged as an important, thus widely investigated, group of compounds. These compounds are of interest due to their unique structure and reactivity. There are two well-known routes to synthesize [n]MCPs: through a salt-metathesis reaction, or through what is known as the “flytrap” route (Scheme 1-1). The salt-metathesis method is the reaction of a dilithiometallocene with an element dihalide that is equipped with an appropriate ligand; this route is the most commonly used pathway for preparing [n]MCPs. The most important step in this route is the preparation of the dilithiometallocene, which is typically accomplished by using butyllithium and an amine base, e.g. N,N,N',N'-tetramethylethylenediamine (tmeda) or N,N,N',N',N''-pentamethyldiethylenetriamine (pmdta).^{10, 11} This method has been used extensively for preparing [1]MCPs with bridging elements ranging from group 13 (B, Al, Ga), group 14 (Si, Ge, Sn), group 15 (P, As), group 16 (S, Se) and many more. The “flytrap” route is a much less used pathway for synthesizing [n]MCPs. This method requires the preparation of a dianionic compound which consists of two cyclopentadienide (Cp^-) rings linked together by some bridging moiety (E_xR_y). The dianionic compound is then reacted with an appropriate metal(II) dihalide to give an [n]MCP. This method is typically used to prepare [n]MCPs ($n \geq 2$); for example, dicarba[2]FCP (**2**) was obtained through this pathway.⁶ However, salt-metathesis reactions are usually used to prepare [1]MCPs, and was employed to synthesize sila[1]FCP (**3**), the first [1]MCP.⁷

Scheme 1-1. Synthetic pathways for [n]MCPs via (a) a salt-methathesis reaction, or (b) the “flytrap” route.



Comparing [n]MCPs to metallocenes (with $d > 2$ electrons), their parent compound, it is evident that there is a strain present in the molecule due to the tilted Cp rings. In a metallocene, such as ferrocene, the two Cp rings are parallel to each other; the introduction of a short *ansa* [n] bridge ($n = 1, 2$) causes the Cp rings to tilt, thus introducing strain to the molecule. The angle between the two planes of the Cp rings in an [n]MCP is known as the tilt angle α , and gives an indication to the amount of strain present in an [n]MCP. Additionally, the β ($\text{C}_{\text{pcentroid}}\text{-C}_{\text{ipso}}\text{-E}$), θ ($\text{C}_{\text{ipso}}\text{-E-C}'_{\text{ipso}}$), and δ ($\text{C}_{\text{pcentroid}}\text{-M-C}'_{\text{centroid}}$) angles help describe the ring-tilted structure of [n]MCPs (Figure 1-2).

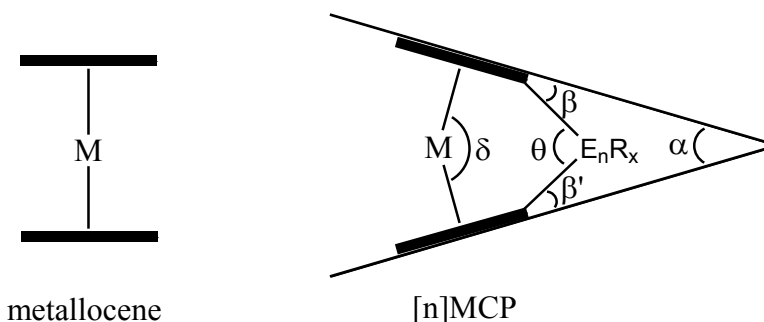


Figure 1-2. Geometric angles of [n]MCPs.

The angles in [n]MCPs become subject to change as the metal atoms (M) and the bridging moieties (E_nR_x) are altered. The tilt angle α is directly proportional to the size of the metal atom;

for example, the α angle of a [1]FCP (**7**: M = Fe) and a [1]ruthenocenophane ([1]RCP) (**7**: M = Ru) with tin in the bridging position are approximately 15° ¹² and 20° ¹³, respectively (Figure 1-3). On the other hand, the tilt angle α is inversely proportional to the size of the bridging element; smaller bridging elements result in larger α angles. The size of each element decreases along each row and increases down each group of the periodic table, therefore, the tilt angle α increases across the periodic table and decreases down the periodic table. For instance, a sila[1]FCP (**8**) has an α angle of 20.8° ¹⁴ and, going across the periodic table, a thia[1]FCP (**9**) has larger α angle of 31.0° ,¹⁵ whereas going down the periodic table, a stanna[1]FCP (**7**: M = Fe) has a smaller α angle of around 15° (Figure 1-3).¹² Furthermore, as more elements of the same kind are bridged between the two Cp rings, the tilt angle α decreases; for example, thia[1]FCP ($\alpha = 31.0^\circ$)¹⁵ has a much larger tilt angle than trithia[1]FCP ($\alpha = 4.5^\circ$).¹⁶ All of these α angles for [n]MCPs are used to express the amount of relative strain that is present in each molecule, which, in turn, gives some indication of the relative stability of each [n]MCP. The degree of tilting causes the energy gap between the highest occupied molecular orbital (HOMO) and lowest unoccupied molecular orbital (LUMO) to change, which is observable by the colour of the compounds. For instance, as the α angle increases due to decreasing the size of a bridging moiety, the HOMO-LUMO energy gap decreases, which can be observed by the colour changes of [1]FCPs from red (sila[1]FCP) to dark red (phospha[1]FCP) to purple (thia[1]FCP).¹⁷

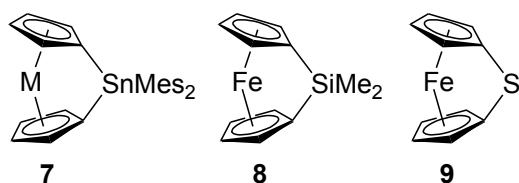
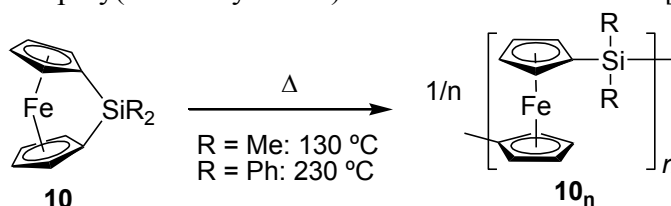


Figure 1-3. [n]MCPs with varying metal atoms and bridging elements.

The tilted ring structure of [n]MCPs imposes a strain on the molecule, which can be relieved by undergoing ROP to produce poly(metallocene)s. When the Cp rings are more tilted, there is more strain present in the [n]MCP; therefore, its tendency to undergo ROP increases. Density functional theory (DFT) calculations show that the tilt angle α gives a good indication of an [n]MCPs susceptibility to ROP.¹⁸ The calculations determined that the energy that is needed to tilt Cp rings to an angle α of an [n]MCP is similar to its ΔH^{ROP} value. The ROP of these compounds follow a chain growth polymerization mechanism which results in the formation of high-molecular-weight metallopolymer.¹⁹ The other method for obtaining metallopolymer from organometallic compounds, which does not yield high-molecular-weight metallopolymer, is through polycondensation, a step-growth polymerization. This makes [n]MCPs valuable precursors for obtaining high-molecular-weight polymers with metals incorporated in the backbone of the polymer.

The first ROP of an [n]MCP was reported in 1992 by Manners *et al.*, who demonstrated that the thermal ROP of sila[1]FCPs (**10**) yields high-molecular-weight poly(ferrocenylsilane)s (PFSs) (**10n**) (Scheme 1-2).²⁰ This accomplishment inspired many investigations into the synthesis of new [n]MCPs and respective metallopolymer through ROP. Different ROP methodologies have been developed which have allowed access to different kind of metallopolymer. One particular ROP method developed is a living polymerization which has allowed access to the synthesis of block co-polymers. Block co-polymers form different nanoscopic aggregate morphologies such as cylinders, vesicles, and spherical micelles in block-selective solvents which are possibly valuable in nanoscience research.²¹⁻²⁵ Of the metallopolymer that have been studied, PFSs have been investigated extensively due to the many applications they have found in material science. The ROP of [n]MCPs will be discussed in more detail later on in this thesis (Chapter 1.2).

Scheme 1-2. Synthesis of poly(ferrocenylsilane)s via thermal ROP of sila[1]FCPs.



The field of [n]MCPs has grown immensely over the last two decades. This thesis will look at some of the interesting [n]MCPs that have been prepared to date and discuss some interesting results that came from the studies. By no means will this thesis be a comprehensive list of all [n]MCPs that are known; however, the reader can refer to the following review that provide details about the large number of [n]MCPs that have been discovered to date.²⁶ Of the many [n]MCPs that have been discovered, [1]MCPs with group 8 transition metals (i.e. M = Fe, Ru), have been the most widely investigated. This thesis will discuss selected examples of [1]FCPs and [1]RCPs from the literature to provide the proper context to help explain the significance of this contribution.

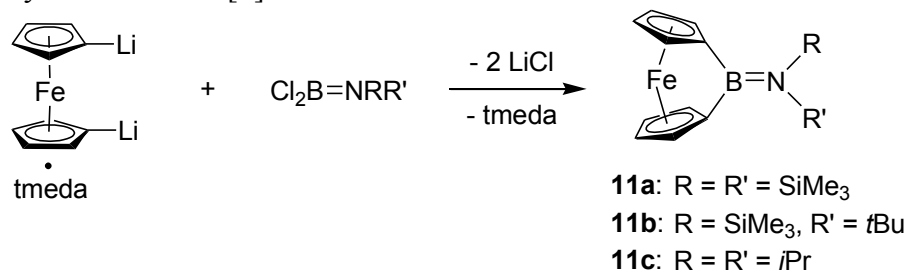
1.1.1 [1]Ferrocenophanes

The first reported [1]MCP was the silicon-bridged [1]FCP **3**, which was prepared by Osborne and Whiteley in 1975.⁷ Investigations into [1]MCPs remained relatively rare until 1992, when Manners *et al.* reported the first ROP of sila[1]FCPs **10** (Scheme 1-2).²⁰ This discovery initiated intensive studies into the synthesis and ROP of [1]MCPs, with [1]FCPs being the most heavily studied. The salt-metathesis route (Scheme 1-1a) has been used extensively to synthesize many [1]FCPs with different elements in the bridging position; this is due to the fact that dilithioferrocene·tmeda is easy to prepare and produces high yields. To get an overview of the chemistry that is relevant to this thesis, selected examples of [1]FCPs with group 13, 14, and 15 elements in the bridging positions will be discussed.

1.1.1.1 Group-13-Bridged [1]Ferrocenophanes

Boron-bridged [1]FCPs were the first group-13-bridged [1]FCPs, which were reported by Braunschweig and Manners *et al.* in 1997.²⁷ To date, bora[1]FCPs remain the only [1]FCP with a second period element in the bridging position. The synthesis of bora[1]FCPs (**11**) was completed by reacting dilithioferrocene·tmeda and aminodichloroboranes with bulky alkyl groups on nitrogen (Scheme 1-3).^{27, 28} It was found that sterically bulky alkyl groups on nitrogen are needed to yield bora[1]FCPs. If non-sterically demanding alkyl groups are employed, such as NMe₂, N(Me)Ph, and N(Me)*n*Bu, insoluble material was obtained in salt-metathesis reactions instead of the intended strained bora[1]FCP.

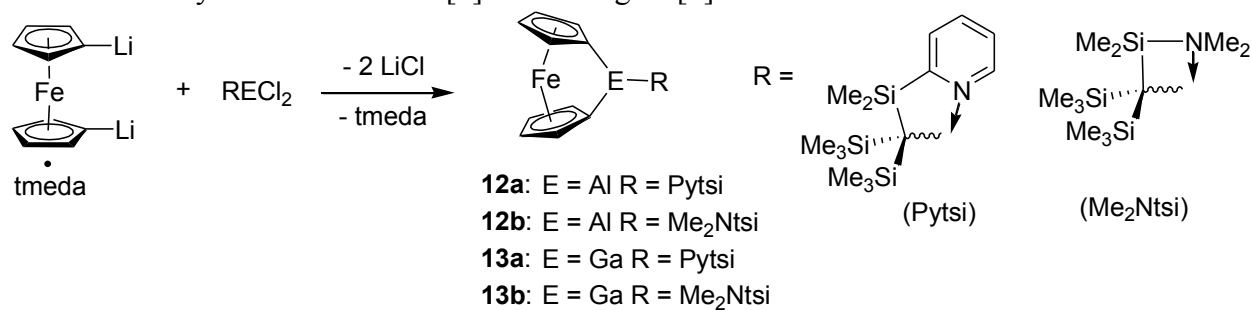
Scheme 1-3. Synthesis of bora[1]FCPs.



Boron is the smallest element that has been used to bridge a [1]FCP to date; it is for this reason that bora[1]FCPs exhibit the largest α angles ($\sim 32^\circ$) reported amongst all [1]FCPs. This highly ring tilted structure was confirmed with ¹³C NMR and UV-visible spectroscopy. The chemical shift for the carbon attached to boron (the *ipso*-carbon) in bora[1]FCP (**11a**: $\delta = 45.0$ ppm, **11b**: $\delta = 45.2$ ppm, **11c**: $\delta = 44.2$ ppm) was substantially downfield of the chemical shift of the Cp carbons in ferrocene ($\delta = 68.2$ ppm). Furthermore, each of the bora[1]FCPs also displayed a noticeable red shift of the absorption maximum in the visible range (**11a**: $\lambda_{\text{max}} = 479$ nm, **11b**: $\lambda_{\text{max}} = 489$ nm, **11c**: $\lambda_{\text{max}} = 489$ nm) compared to that of ferrocene ($\lambda_{\text{max}} = 440$ nm).

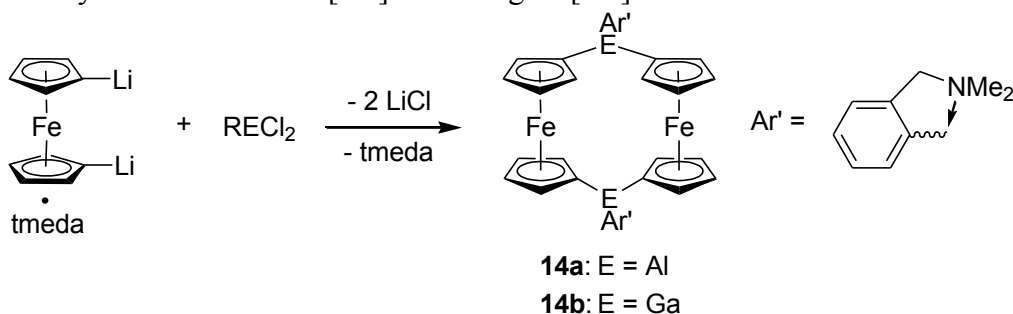
Following the synthesis of bora[1]FCPs, Müller *et al.* reported the preparation of aluminum- and gallium-bridged [1]FCPs, beginning in 2005.²⁹⁻³³ In comparison to bora[1]FCPs, which use bulky amino-stabilized boron dichlorides to prepare [1]FCPs, aluminum and gallium bridged [1]FCPs were obtained by reacting dilithioferrocene·tmeda with aluminum and gallium dihalides coordinated to bulky trisyl-based ligands with an intramolecularly donating nitrogen group (Scheme 1-4). The strain present in alumina[1]FCPs and galla[1]FCPs is significantly less than that in bora[1]FCPs; this can be seen by the much smaller α angles of alumina[1]FCPs (**12a**: $\alpha = 14.9^\circ$, **12b**: $\alpha = 14.3^\circ$) and galla[1]FCPs (**13a**: $\alpha = 15.7^\circ$, **13b**: $\alpha = 15.8^\circ$).²⁹⁻³¹ This is expected since aluminum and gallium are larger atoms than boron, therefore, the Cp rings will not tilt as much to form [1]FCPs. This is observed by the higher chemical shifts of the *ipso*-carbons in the ^{13}C NMR spectra of alumina[1]FCPs (**12a**: $\delta = 52.9$ ppm, **12b**: $\delta = 53.0$ ppm) and galla[1]FCPs (**13a**: $\delta = 47.2$ ppm, **13b**: $\delta = 47.3$ ppm) compared to those of bora[1]FCPs.

Scheme 1-4. Synthesis of alumina[1]FCPs and galla[1]FCPs.



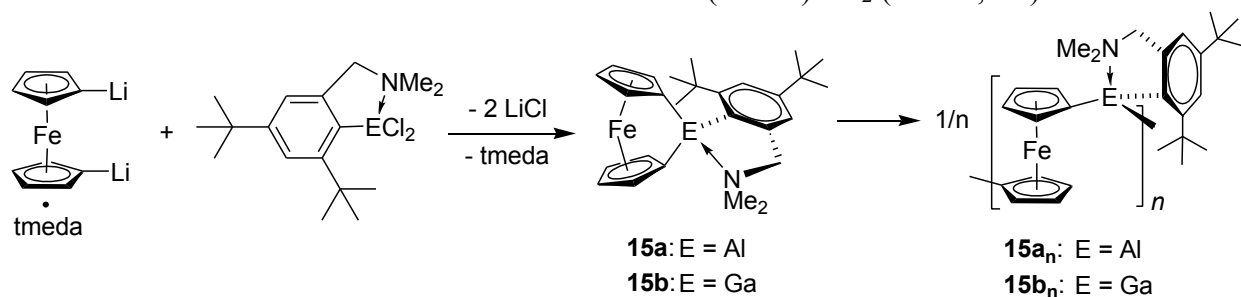
The steric bulk of the trisyl-based ligands were found to be essential to obtain alumina[1]FCPs and galla[1]FCPs. When aluminum and gallium dihalides with the flat Ar' ligand (Ar' = 2-[(dimethylamino)methyl]phenyl) were employed, [1]FCPs were not obtained and instead, [1.1]FCPs (**14a,b**) were obtained (Scheme 1-5).^{34, 35} Steric bulk is required to favour the formation of [1]FCPs over other products, such as [1.1]FCPs and oligomers.

Scheme 1-5. Synthesis of alumina[1.1]FCP and galla[1.1]FCP.



In efforts to prepare alumina[1]FCPs and galla[1]FCPs with less sterically demanding ligands, the Ar' ligand was altered to include some steric protection to facilitate the formation of [1]FCPs; thus, the Mamx ligand (Mamx = 2,4-di-*tert*-butyl-6-[(dimethylamino)methyl]phenyl) was synthesized. The Mamx ligand includes two additional *tert*-butyl groups on the phenyl ring in the *ortho* and *para* positions with respect to the aluminum or gallium atom. The *tert*-butyl group in the *ortho* position provides some steric protection to the aluminum and gallium atom, and should help facilitate the formation of [1]FCPs. The salt-metathesis reaction of (Mamx)ECl₂ (E = Al, Ga) with dilithioferrocene·tmeda resulted in the formation of expected [1]FCPs (**15a,b**), however, these [1]FCPs polymerized immediately in solution and were not isolable (Scheme 1-6).^{32, 33}

Scheme 1-6. Reaction of dilithioferrocene·tmeda with (Mamx)ECl₂ (E = Al, Ga).



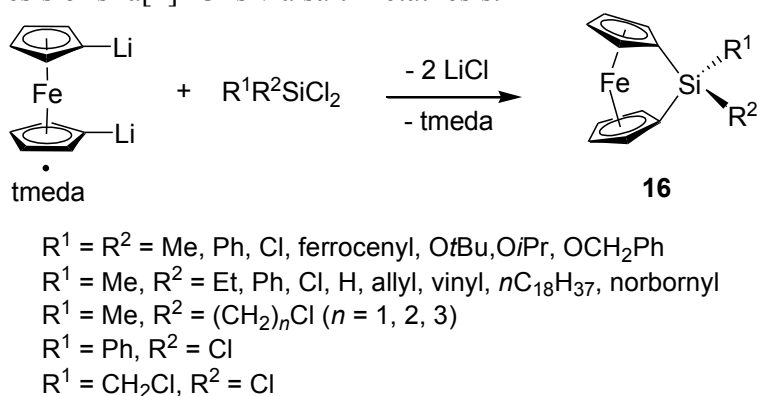
From the investigations into the synthesis of group-13-bridged [1]FCPs, it was found that sterics play a major role in the outcome of salt-metathesis reactions. If the ligand on the bridging element does not have sufficient steric protection, a [1]FCP will not be obtained. However,

[1]FCPs with large steric protection lead to fairly stable compounds, which can pose difficulties in ROP studies. Therefore, it is important to fine tune the sterics to favour the formation of [1]FCPs that can be isolated, as well as be reactive enough to allow for ROP.

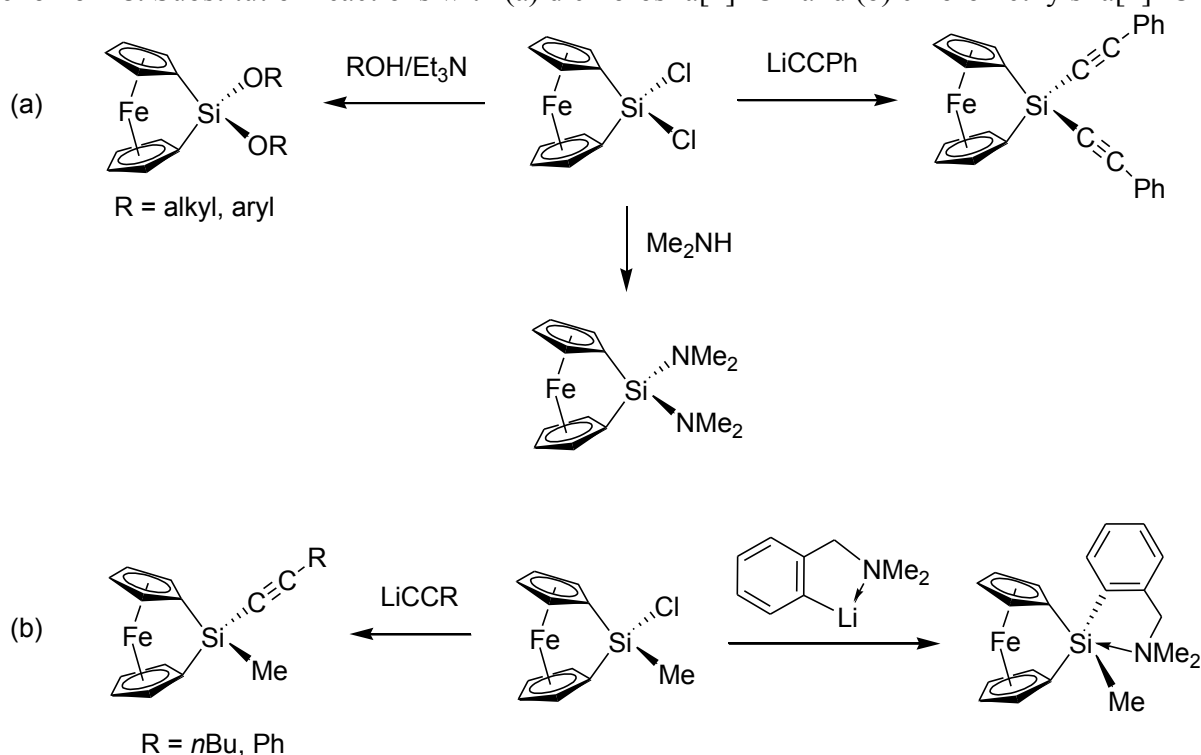
1.1.1.2 Group-14-Bridged [1]Ferrocenophanes

As mentioned earlier, the first [1]FCP that was successfully synthesized was a silicon-bridged [1]FCP, sila[1]FCP **3** (Figure 1-1).⁷ However, not much was done with this discovery until Manners *et al.* reported the successful ROP of sila[1]FCPs **10** (Scheme 1-2).²⁰ Due to this major breakthrough, sila[1]FCPs received much attention which lead to numerous reports of different sila[1]FCPs. The majority of these compounds were obtained through the salt-metathesis of dilithioferrocene·tmeda with various dichlorosilanes with a variety of substituents to yield symmetrically and unsymmetrically substituted sila[1]FCPs (**16**) with α angles ranging from 19 to 22° (Scheme 1-7).³⁶⁻⁴² Below are just some of the many examples of sila[1]FCPs that have been prepared. Other sila[1]FCPs have been synthesized by derivatizing chloro-substituted sila[1]FCPs with various reagents to yield new sila[1]FCPs (Scheme 1-8).^{12, 39, 40, 43}

Scheme 1-7. Synthesis of sila[1]FCPs via salt-metathesis.



Scheme 1-8. Substitution reactions with (a) dichlorosila[1]FCP and (b) chloromethylsila[1]FCPs.



Sila[1]FCPs with substituted Cp rings have also been prepared following similar pathways as discussed previously (**17-23**, Figure 1-4).^{14, 44-46} As the Cp rings are substituted with alkyl groups, their donor character increases due to the Cp rings becoming electron enriched. As a consequence, Fe-Cp distances decrease because of the increased bonding, which results in sila[1]FCPs with smaller α angles.⁴⁷ Introducing sterically bulky groups on the Cp rings can have some interesting effects on the resulting sila[1]FCPs. For instance, when the sterically bulky groups on the Cp rings are forced to stack on top of each other, like in sila[1]FCP **21**, the α angle increases to 26.3° due to steric repulsion of the trimethylsilyl substituted Cp rings.⁴⁶ When bulky groups are staggered with respect to one another, like in sila[1]FCPs **22** and **23**, steric protection is provided to the iron centre and the air and moisture stability of the sila[1]FCPs increase.^{44, 46}

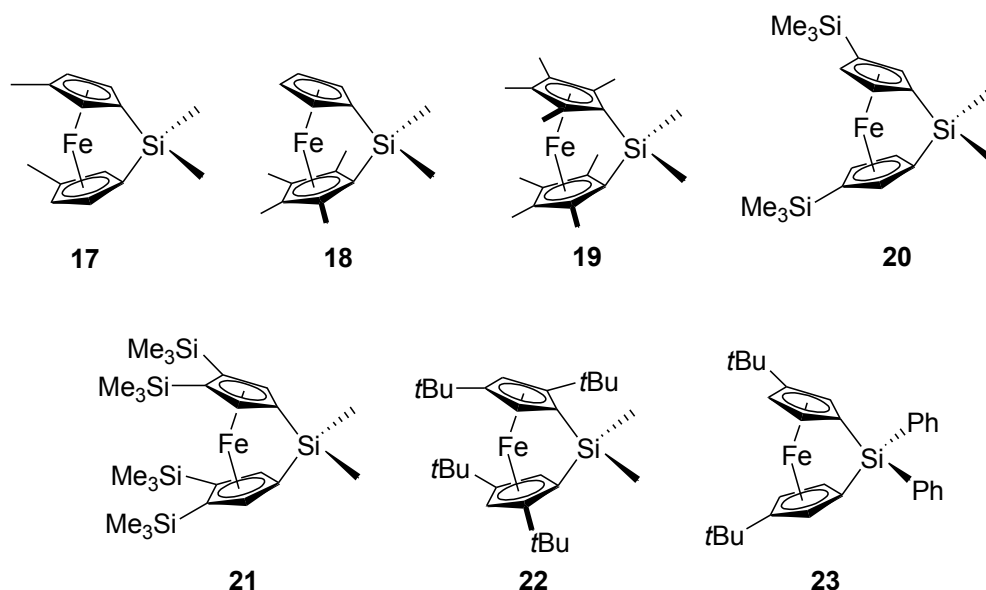
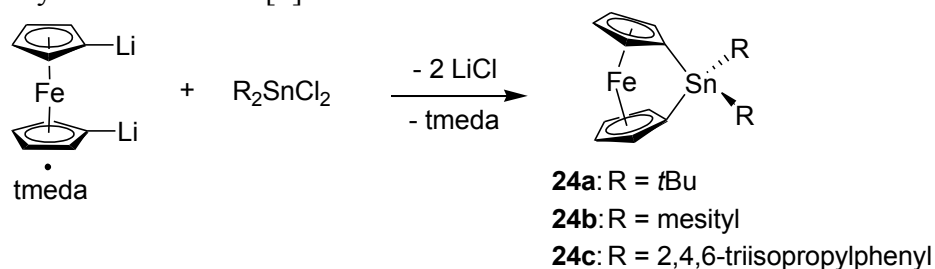


Figure 1-4. Sila[1]FCPs with substituted Cp rings.

Tin-bridged [1]FCPs have not been reported as much as sila[1]FCPs, however, three stanna[1]FCPs (**24**) have been prepared through salt-metathesis reactions (Scheme 1-9).^{12, 48, 49} Like alumina[1]FCPs and galla[1]FCPs, stanna[1]FCPs could only be obtained when there are sterically demanding substituents on the tin centre. Substituents that do not provide steric protection for the tin centre, such as Me, Et, *n*Bu, or Ph groups, yield oligomeric material and stanna[1.1]FCPs in salt-metathesis reactions, rather than the desired stanna[1]FCPs.⁵⁰

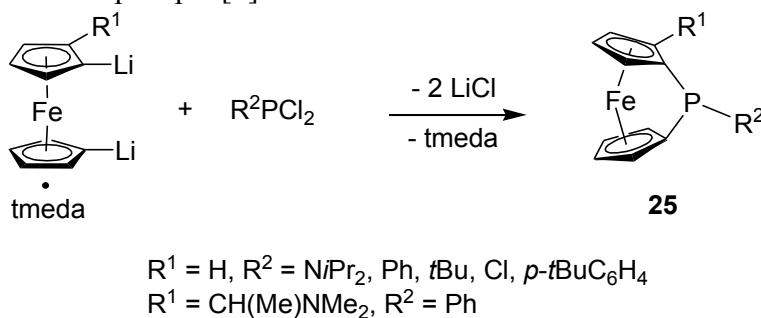
Scheme 1-9. Synthesis of stanna[1]FCPs.



1.1.1.3 Group-15-Bridged [1]Ferrocenophanes

Phosphorus-bridged [1]FCPs have been developed quite extensively and have emerged as a very important group of [1]FCPs. Just like the [1]FCPs previously discussed, phospho[1]FCPs (**25**) are synthesized via salt-metathesis reactions of dilithioferrocene·tmeda and dichlorophosphines with various substituents (Scheme 1-10).^{8, 9, 51-53} The use of dichlorophosphines with chiral substituents yield chiral phospho[1]FCPs; for example, phospho[1]FCPs **26** and **27** (Figure 1-5).⁵⁴ The α angle for phospho[1]FCPs fall within a narrow range of 26.9° and 27.9°.

Scheme 1-10. Synthesis of phospho[1]FCPs.



These compounds, particularly chiral phospho[1]FCPs, and respective ring-opened polymers have been found to be useful as ligands in catalytic reactions and as supports for transition-metal catalysts. For instance, phospho[1]FCP **26** and its respective poly(ferrocenylphosphine)s, were used as ligands in the Rh-catalyzed asymmetric hydrogenation of folic acid.⁵⁴ Therefore, the synthesis of phospho[1]FCPs and respective poly(ferrocenylphosphine)s have attracted much due to their potential application in these areas.

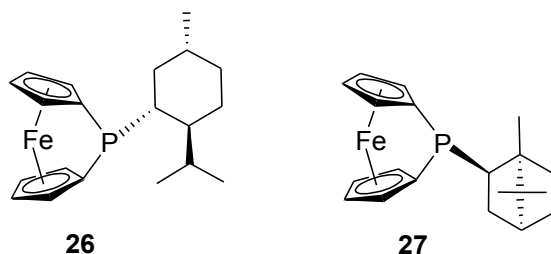
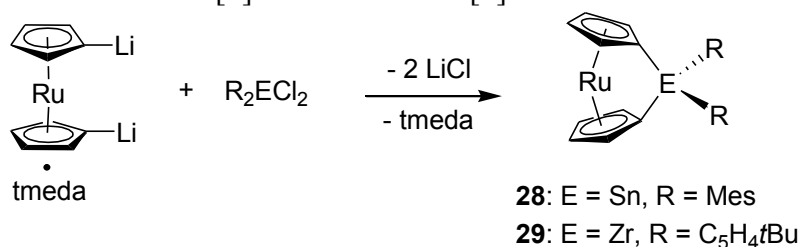


Figure 1-5. Chiral phospho[1]FCPs.

1.1.2 [1]Ruthenocenophanes

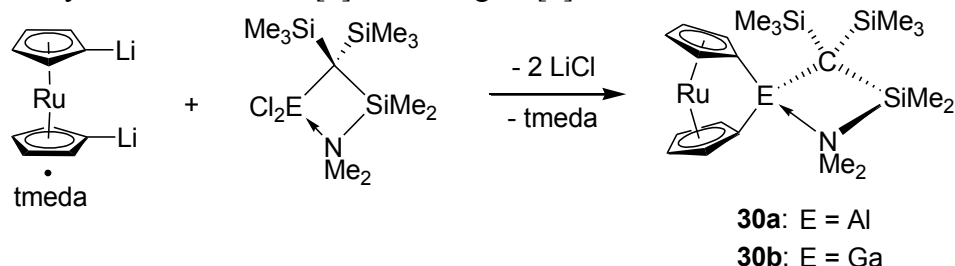
To date, [1]FCPs have been the most widely studied group of strained sandwich compounds. As mentioned before (Chapter 1.1.1), there have been many different [1]FCPs synthesized with a variety of different elements in the bridging position, including elements from group 13 (B, Al, Ga), group 14 (Si, Ge, Sn), group 15 (P, As), group 16 (S, Se) and many more. On the other hand, there have been very few studies of [1]MCPs where iron has been replaced by one of its group 8 family members such as ruthenium. [1]MCPs with ruthenium as the metal centre ([1]RCPs) are not as abundant as [1]FCPs. The size of a ruthenium atom is much larger than an iron atom, therefore, the two Cp rings in ruthenocene (3.68 Å) are further apart than in ferrocene (3.32 Å). Consequently, to synthesize [1]RCPs, the Cp rings need to tilt more than in [1]FCPs. Unlike the vast number of sila[1]FCPs that have been prepared, synthesis of sila[1]RCP have not been successful. The first [1]RCPs were synthesized by Manners *et al.* in 2004, employing the large bridging elements tin (**28**) and zirconium (**29**).¹³ These compounds were obtained through salt-metathesis reactions between the respective tin and zirconium dichlorides with dilithioruthenocene·tmeda (Scheme 1-11). For stanna[1]FCP **28**, the α angle of three independent molecules in its asymmetric unit were found to be 20.2, 20.8 and 20.9°,¹³ which are significantly larger than its [1]FCP analog **24b** (α = 14.5, 15.3 and 15.7°).¹² A similar difference was observed between the zircona[1]RCP **29** (α = 10.4°)¹³ and its zircona[1]FCP analog (α = 6.0°).⁵⁵

Scheme 1-11. Synthesis of stanna[1]RCP and zircona[1]RCP.



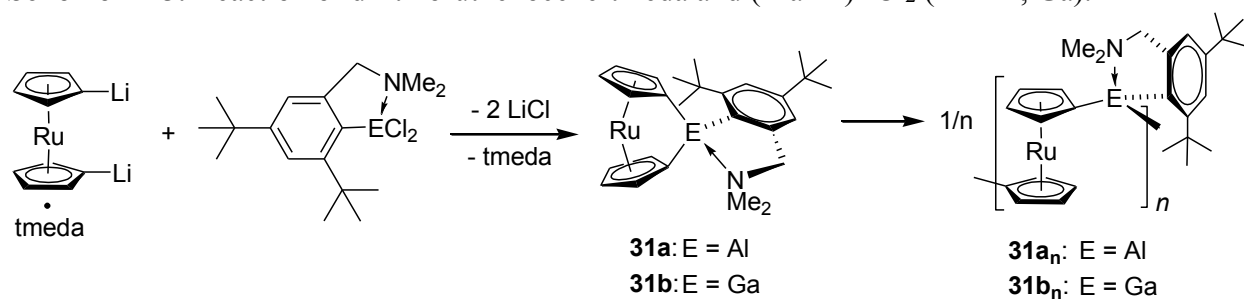
Müller *et al.* reported the only other known preparations of [1]RCPs, using aluminum and gallium in the bridging position.^{33, 56} The first alumina[1]RCP (**30a**) and galla[1]RCP (**30b**) were obtained by reacting dilithioruthenocene·tmeda with aluminum and gallium dichlorides stabilized by the bulky Me₂Ntsi ligand (Scheme 1-12). As expected, the group-13-bridged [1]RCPs (alumina[1]RCP **30a**: $\alpha = 20.31^\circ$, galla[1]RCP **30b**: $\alpha = 20.91^\circ$) were more strained compared to the group-13-bridged [1]FCP analogs (alumina[1]FCP **12b**: $\alpha = 14.33^\circ$, galla[1]FCP **13b**: $\alpha = 15.83^\circ$).⁵⁶

Scheme 1-12. Synthesis of alumina[1]RCP and galla[1]RCP.



Similar to the aluminum- and gallium-bridged [1]FCPs, the bulky trisyl-based ligand was found to be essential to obtain alumina[1]RCP and galla[1]RCP. When the less bulky Mamx ligand was employed to synthesize alumina[1]RCP **31a**, it behaved like [1]FCPs **15** and underwent ROP in solution and was not isolable.³³ Surprisingly, the galla[1]RCP **31b** was isolable as a powder with the Mamx ligand; however, after extended periods in solution, **31b** polymerized to yield **31b_n** (Scheme 1-13).³³ All attempts to crystallize **31b** failed, thus the α angle was unable to be measured, therefore, DFT calculations were used to approximate the ring-tilt angle to be 22.90° , which is similar to galla[1]RCP **30b** ($\alpha = 20.91^\circ$).

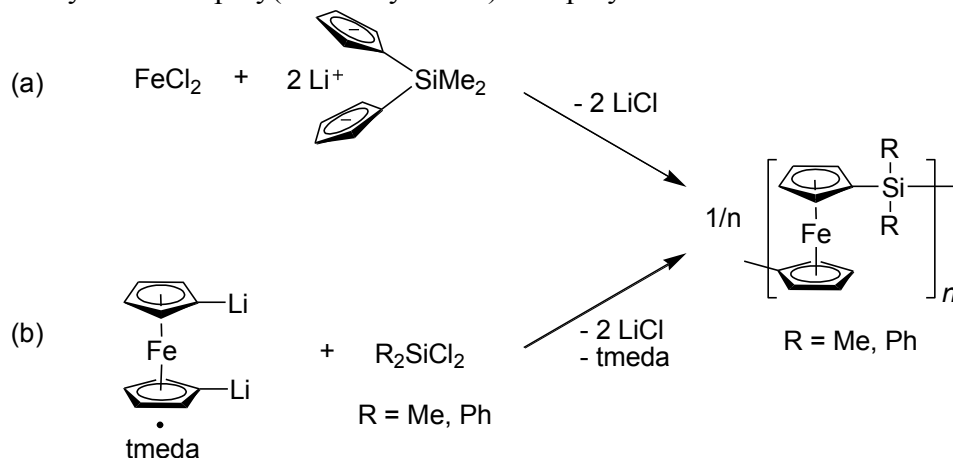
Scheme 1-13. Reaction of dilithioruthenocene·tmeda and (Mamx)ECl₂ (E = Al, Ga).



1.2 Metallopolymers via Ring-Opening Polymerization of [n]Metallocenophanes

Throughout history, polymers have been used extensively in everyday life. Over the last century, ways to synthesize polymers have been developed on industrial scale, resulting in many new materials that have been found to be absolutely essential in modern society. Many studies have been conducted to incorporate metals into either the backbone, or as a pendant in polymers to yield metallopolymers that could potentially display intriguing electronic properties. The first metallopolymer, poly(vinylferrocene), was synthesized at DuPont in 1955, and was prepared through the radical polymerization of vinylferrocene.⁵⁷ This inspired many investigations into the preparation of new metallopolymers, most of which were metallocene based and were obtained through polycondensation reactions. However, the majority of metallopolymers that were obtained through this method did not yield high-molecular-weight metallopolymers.

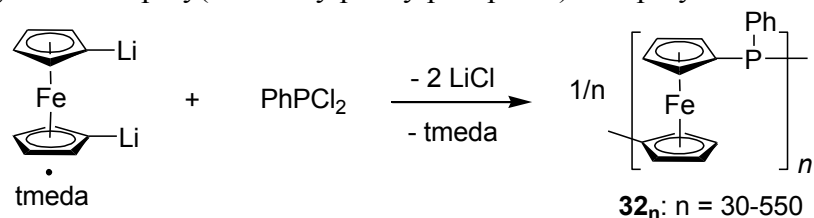
Scheme 1-14. Synthesis of poly(ferrocenylsilane)s via polycondensation reactions.



Beginning in the 1960s, metallopolymers, in particular PFSs, were being synthesized via polycondensation reactions of either (a) iron(II) chloride and $\text{Li}_2[(\text{C}_5\text{H}_4)_2\text{SiMe}_2]$ ⁵⁸ or (b) dilithioferrocene·tmeda and diorganosilicon dichlorides⁵⁹ (Scheme 1-14). This pathway exclusively yielded low-molecular-weight metallopolymers due to the strict requirements of polycondensation reactions. In order for polycondensation reactions to be successful, the starting

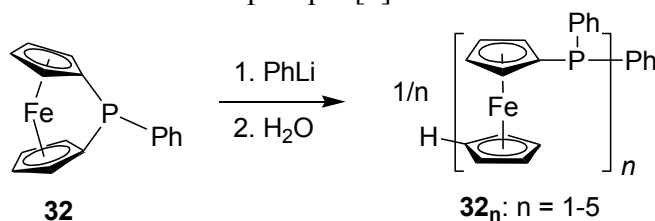
monomeric materials must be of high purity and be in precise stoichiometric ratios. It is nearly impossible to synthesize dilithioferrocene·tmeda free from ferrocene and with the exact equivalents of tmeda known (actual equivalents of tmeda range from 2/3 to 2). Due to the difficulty of obtaining highly pure starting materials, synthesizing high-molecular-weight PFSs via polycondensation reactions (i.e. a step-growth polymerization), is extremely difficult. In these reactions, various chain lengths exist and will react at random with each other or with monomers present in the reaction mixture; this results in polymers with various chain lengths. Therefore, metallopolymer obtained through polycondensation reactions are typically low-molecular-weight and have a wide distribution of molecular weights.

Scheme 1-15. Synthesis of poly(ferrocenylphenylphosphine)s via polycondensation reactions.



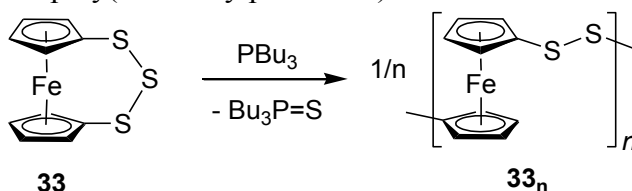
In 1982, Seyferth *et al.* reported the synthesis of a high-molecular-weight metallopolymer, poly(ferrocenylphenylphosphine) **32_n** ($M_w = 8.9\text{-}161$ kDa), via the polycondensation of dilithioferrocene·tmeda and dichlorophenylphosphine (Scheme 1-15).⁶⁰ This polycondensation reaction was surprising, since it yielded a high-molecular-weight polymer. No comments were made on the mechanism of the polymerization; however, it is highly likely that phosphat[1]FCP **32** was formed *in situ* and underwent anionic ROP initiated by dilithioferrocene·tmeda. In the same study, the anionic ROP of phosphat[1]FCP **32**, initiated by phenyllithium, was attempted and only yielded oligomeric material (Scheme 1-16).⁶⁰ The unsuccessful anionic ROP of phosphat[1]FCP **32**, was attributed to steric and solubility issues.

Scheme 1-16. Attempted anionic ROP of phospha[1]FCP **32**.



Due to the difficulty of obtaining high-molecular-weight metallopolymer, very few significant contributions were made until Rauchfuss and Brandt reported the synthesis of poly(ferrocenylpersulfide) **33_n** in 1992.⁶¹ This metallopolymer was obtained through the unique atom-abstraction based ROP of trithia[1]FCP **33** (Scheme 1-17). Tributylphosphine is used to desulfurize trithia[1]FCP **33** which triggers polymerization yielding the high-molecular-weight metallopolymer **33_n**.

Scheme 1-17. Synthesis of poly(ferrocenylpersulfide).



Not too long after, Manners *et al.* reported the synthesis of high-molecular-weight PFSs (**10_n**) via the thermal ROP of sila[1]FCPs **10** (Scheme 1-2).²⁰ High-molecular-weight PFSs (**10_n**) were attainable since the ROP of sila[1]FCPs (**10**) followed a chain-growth mechanism, rather than a step-growth mechanism. Chain-growth mechanisms allow for more controlled polymerizations, which can lead to high-molecular-weight metallopolymer with potentially narrow distributions of molecular weights. This discovery revolutionized the area of metallopolymer, and instigated numerous studies into synthesis and ROP of [n]MCPs to obtain new materials.

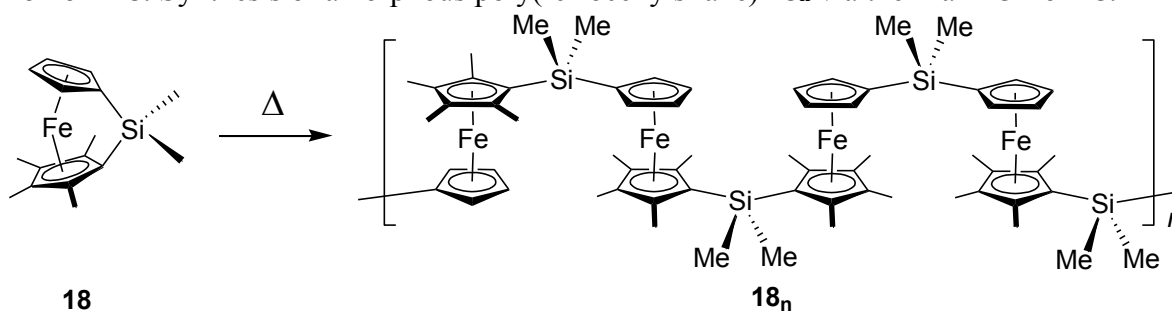
1.2.1 Ring-Opening Polymerization Methodologies

Since the groundbreaking report of thermal ROP of sila[1]FCPs made by Manners *et al.* in 1992,²⁰ many different ROP methodologies have been developed for [n]MCPs. Of these, thermal, anionic, transition-metal-catalyzed, and photolytic ROP have been found to be some of the more successful methods. The following section will briefly discuss how these ROP methodologies are applied to synthesize poly(metallocene)s from [n]MCPs.

1.2.1.1 Thermal ROP

The first successful methodology applied to obtain high-molecular-weight metallopolymer was the thermal ROP of [n]MCPs.²⁰ This method works for a wide variety of [n]MCPs, and is fairly tolerant of various functional groups, however, some [n]MCPs have been found to degrade under elevated temperatures. To perform thermal ROP, [n]MCPs are heated to high temperatures either in solution or as a bulk material. The most popular procedure is to heat a solid [n]MCP above its melting-point in a vacuum-sealed Pyrex tube, which typically produce high-molecular-weight metallopolymer with a wide range of molecular weights.

Scheme 1-18. Synthesis of amorphous poly(ferrocenylsilane) **18_n** via thermal ROP of **18**.



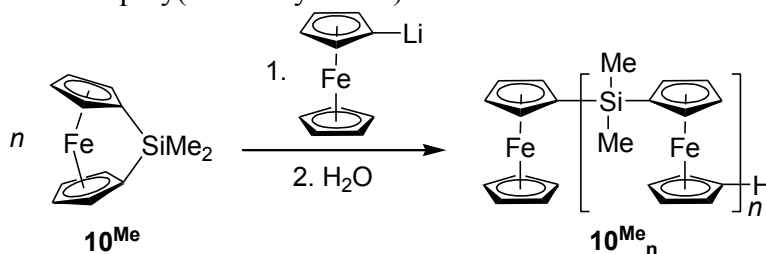
Investigations into the mechanism of thermal ROP have been made, but have not been very fruitful. Manners *et al.* studied the thermal ROP of sila[1]FCP **18** in attempts to understand the mechanism (Scheme 1-18).^{62, 63} This proved to be futile as Si-Cp^H and Si-Cp^{Me} bonds were cleaved

non-selectively, providing no clear insights for a mechanism for thermal ROP. Some investigations suggest that thermal ROP proceeds through a radical mechanism; however, no concrete evidence has been given, showing the need for more research to determine the mechanism of thermal ROP.

1.2.1.2 Anionic ROP

The first attempt at the anionic ROP of [n]MCPs, which was discussed earlier, was reported by Seyferth *et al.* in 1982.⁶⁰ In this study, phenyllithium was used as an anionic initiator to perform the anionic ROP of phospho[1]FCP **32**, however, only the oligomeric material **32_n** was obtained (Scheme 1-16). In 1994, Manners *et al.* described the first successful living carbanionic ROP of sila[1]FCP **10^{Me}**, using ferrocenyllithium as the anionic initiator, to yield poly(ferrocenylsilane) **10^{Me}_n** (Scheme 1-19).⁶⁴ Since this report, other anionic initiators, such as dilithioferrocene·2/3tmeda, *n*-butyllithium, and phenyllithium, have been employed successfully for the anionic ROP of [n]MCPs.

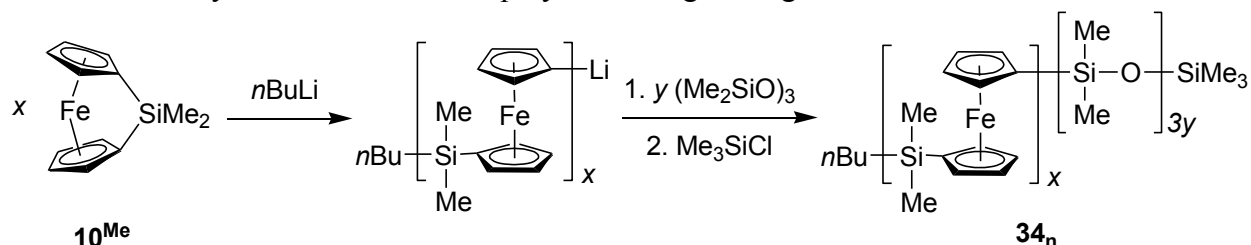
Scheme 1-19. Synthesis of poly(ferrocenylsilane) **10^{Me}_n** via anionic ROP.



The mechanism for the anionic ROP of [n]MCPs involves the initiator attacking the bridging element causing the bond between the *ipso*-carbon on the Cp ring and the bridging element to break.⁶⁵ The newly formed carbanion reacts with more monomer in the same way, thus continuing the polymerization process. The anionic ROP of [n]MCPs has been successful in obtaining high-molecular-weight metallocopolymers with a narrow distribution of molecular weights [Polydispersity Index (PDI) ~ 1], which can be controlled by changing the ratio of the initiator to

monomer. Furthermore, since this methodology is a living process, it can be used to prepare block copolymers, such as **34_n**, with a well-defined structure (Scheme 1-20).⁶⁶ Anionic ROP requires much milder conditions when compared to thermal ROP; however, reagents with the highest purity are needed to avoid early chain termination and [n]MCPs with functionalities resistant to carbanions are necessary.

Scheme 1-20. Synthesis of a block co-polymer through living anionic ROP.



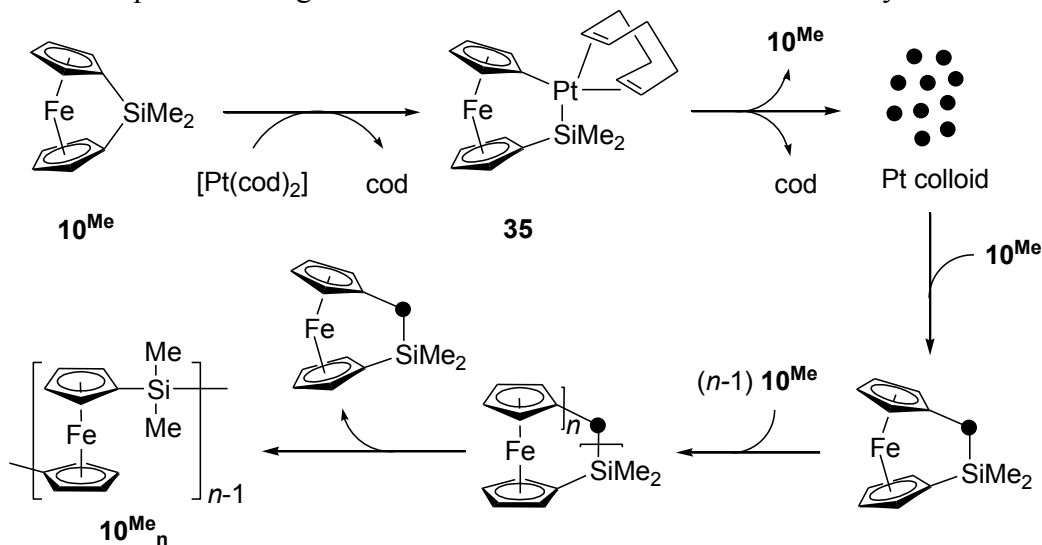
1.2.1.3 Transition-Metal-Catalyzed ROP

Transition-metal-catalyzed ROP was the next ROP methodology to be successfully applied to [n]MCPs to obtain high-molecular-weight metallocopolymers. It was first reported in 1995, by both Manners *et al.*⁶⁷ and Tanaka *et al.*,⁶⁸ independently from each other. Both authors found that platinum, palladium, and rhodium complexes could be used as catalysts for the ROP of sila[1]FCP **10^{Me}**. Changing the ligands of the transition metal complexes resulted in different reaction rates and molecular weights of resulting polymers. This ROP methodology was thought to proceed through a homogeneous polymerization pathway;⁶⁹ however, in 2001, Manners *et al.* proposed that it proceeds through heterogeneous polymerization mechanism (Scheme 1-21).⁷⁰

When $[\text{Pt}(\text{cod})_2]$ (cod = 1,5-cyclooctadiene) is added to **10^{Me}**, platinasila[2]FCP (**35**) forms via oxidative addition to the transition-metal complex. It was thought that **35** acts as a precatalyst in a homogeneous pathway, however, studies suggest that it does not get incorporated into the growing polymeric chain. Thus, it was suggested that **35** undergoes reductive elimination, followed by the

elimination of the cod ligand to form platinum colloids which act as the active catalytic species. This pathway was supported by experiments where the addition of mercury (a known inhibitor of heterogeneous reactions) to reaction mixtures slowed down ROP significantly. However, homogeneous reaction inhibitors were not investigated, thus, a homogeneous pathway cannot be ruled out as a possible mechanism for the transition-metal-catalyzed ROP of [n]MCPs.

Scheme 1-21. Proposed heterogeneous mechanism for transition-metal-catalyzed ROP.



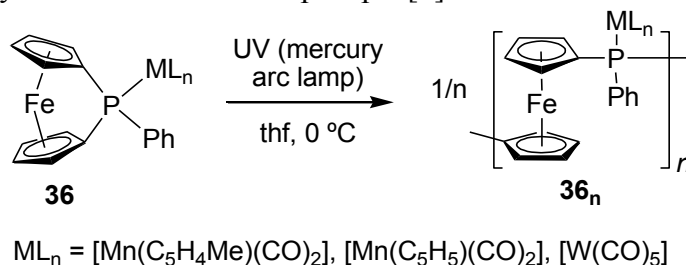
In comparison to other ROP methodologies, transition-metal-catalyzed ROP is performed under milder conditions, for instance, thermal ROP requires high temperatures. Additionally, highly purified starting materials are not necessary, whereas this is essential for anionic ROP. However, one downfall for this methodology is that it does not work at all for phosphazene[1]FCPs, most likely due to the coordination ability of the phosphorus atom to the transition-metal catalysts.

1.2.1.4 Photolytic ROP

More recently, photolytic ROP of [n]MCPs has been investigated as a useful methodology for obtaining metallopolymer.^{71, 72} In 2000, Miyoshi *et al.* described the ROP of metallized phosphazene[1]FCPs (**36**) in the presence of UV irradiation in donating solvents, such as acetonitrile

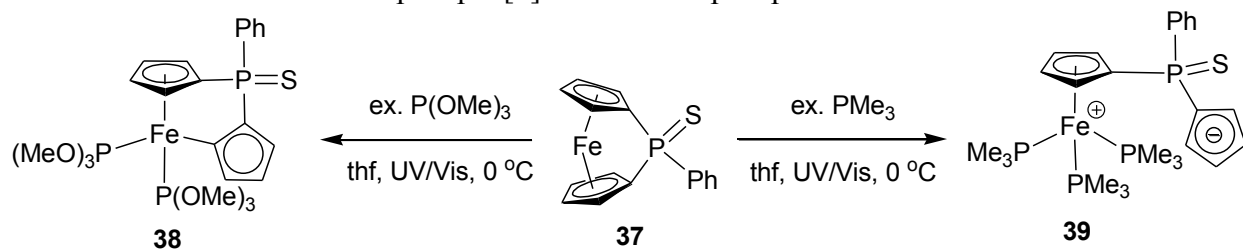
or tetrahydrofuran (thf), to yield high-molecular-weight poly(ferrocenylphosphine)s (**36_n**) (Scheme 1-22).⁷¹ This was the first report of a photolytic ROP, and the only one to successfully perform ROP on metallized [1]FCPs.

Scheme 1-22. Photolytic ROP of metallized phospho[1]FCPs.

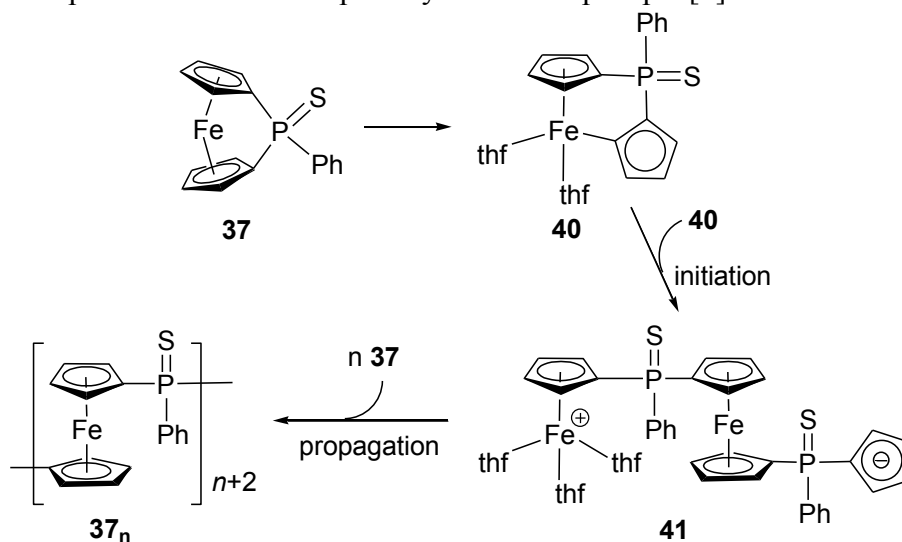


In order to understand the mechanism of this unique ROP of [n]MCPs, Miyoshi *et al.* synthesized the potential reaction intermediates **38** and **39** by reacting phospho[1]FCP **37** with phosphines under UV/Vis irradiation (Scheme 1-23).⁷³ For the intermediate **38**, one Cp ring underwent a haptotropic shift from η^5 to η^1 ; heating this intermediate yields the metallopolymer **37_n**. In contrast, the intermediate **39** has one Cp ring completely dissociated from the iron centre. Using what was observed by these intermediates, a mechanism for the photolytic ROP of **37** was proposed (Scheme 1-24). It is suggested that ROP initiates by the η^1 Cp of **40** attacking the iron centre of a second **40**, thus releasing its Cp ring to form the dimer **41**. This species then propagates the growth of the polymeric chain.

Scheme 1-23. The reaction of phospho[1]FCP **37** with phosphines under UV irradiation.

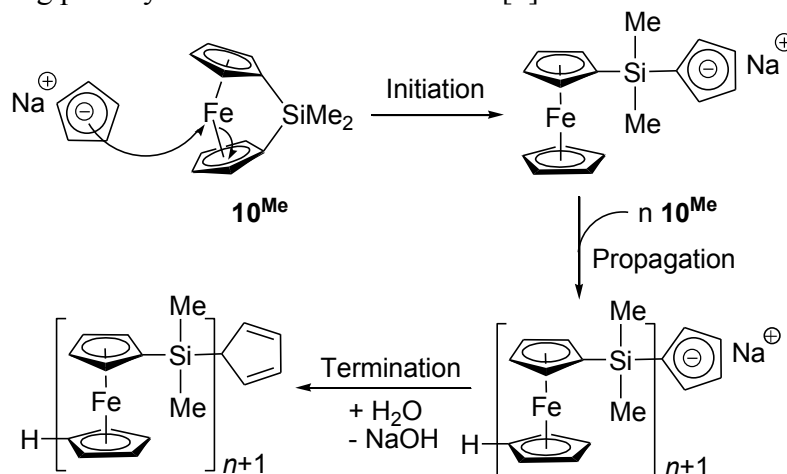


Scheme 1-24. Proposed mechanism of photolytic ROP of phospho[1]FCP **37**.



Following this, Manners *et al.* reported the living anionic photolytic ROP of sila[1]FCP **10^{Me}** in 2004.⁷⁴ Metallopolymers with controlled molecular weights and narrow distributions (PDI = 1.04-1.21) were obtained under UV radiation with NaCp as an anionic initiator (Scheme 1-25). NaCp is unable to perform anionic ROP on sila[1]FCP **10^{Me}**, however, when UV/Vis radiation is present, it weakens the Fe-Cp bond allowing NaCp to attack the iron centre, thus initiating the polymerization of **10^{Me}**.⁷⁵ Therefore, the results obtained by Miyoshi and Manners showed that photolytic ROP proceeds through the initial breaking of the Fe-Cp bond.

Scheme 1-25. Living photolytic ROP mechanism of sila[1]FCP **10^{Me}**.



1.2.2 Poly(metallocene)s

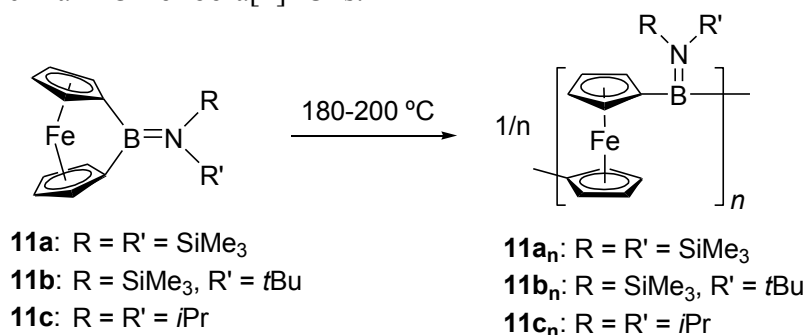
The ROP methodologies that have been developed have provided several options for attempting ROP on strained [n]MCPs to obtain new metallopolymer. Depending on the [n]MCP, certain ROP methodologies are more successful than others; thus, having a few possible routes for the ROP of [n]MCPs is useful. The most heavily investigated metallopolymer are PFSs, which have been successfully prepared through all of the common ROP methods (thermal,²⁰ anionic,⁶⁴ transition-metal-catalyzed,⁶⁷ and photolytic⁷⁴ ROP) starting from various sila[1]FCPs. PFSs have been widely studied due to the many potential applications that have been found for these materials.

The characteristics of a given [n]MCP determine its success to undergo ROP to yield metallopolymer. The compound needs to have a certain amount of ring strain that can be released to allow ROP to take place. For instance, sila[1]FCPs have a significant amount of Cp ring tilting with α angles ranging from 19 to 22°, introducing a substantial amount of ring strain, which makes sila[1]FCPs prone to ROP. This has also been confirmed by differential scanning calorimetry (DSC) analysis that showed the amount of energy released by sila[1]FCPs upon ring-opening is fairly high (70-80 kJ/mol).²⁰ The majority of the [n]FCPs that were discussed previously (Section 1.1.1), all possess significant amounts of ring strain which would suggest they should be prone to ROP. However, the amount of ring strain in an [n]MCP is not the only factor involved in determining whether or not a given compound will polymerize; sterics also play a major role. If the [n]MCP species has bulky groups attached to the bridging element, it becomes more difficult for ROP to occur. The following will be an examination of the ROP of selected [n]MCPs with various bridging elements.

1.2.2.1 Poly(ferrocene)s

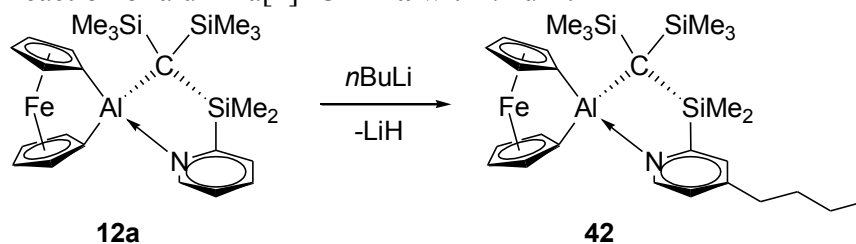
As stated earlier, several PFSs have been successfully synthesized with various ROP methodologies; however, the synthesis of other poly(ferrocene)s with different bridging elements via ROP have had varied success. Bora[1]FCPs possess highly ring-tilted structures (α angles around 32°), which makes these compounds potentially useful for obtaining poly(ferrocenylborane)s through ROP.^{27, 28} From DSC results, it was shown that all bora[1]FCPs **11** displayed ROP exotherms and melt endotherms similar to sila[1]FCPs. For example, the ROP exotherm for **11a** was at 190°C with a melt endotherm at 115°C . The calculated ROP enthalpy for **11a** ($\Delta H^{\text{ROP}} = 95 \text{ kJ/mol}$) was found to be greater than sila[1]FCPs ($\Delta H^{\text{ROP}} = 70\text{-}80 \text{ kJ/mol}$),²⁰ which readily undergo ROP to give high-molecular-weight PFSs. These results suggest that bora[1]FCPs are excellent candidates for ROP to obtain poly(ferrocenylborane)s. However, when thermal ROP of bora[1]FCPs **11** was attempted, mostly insoluble material was obtained for **11a** and **11b**, and a somewhat soluble metallopolymer was obtained for **11c** (Scheme 1-26). The characterization of these materials were attempted, however, due to the low solubility and high moisture sensitivity of the materials, it was difficult to fully characterize any metallopolymers present. Since **11c_n** was somewhat soluble, dynamic light scattering (DLS) was attempted to determine its molecular weight since it was too moisture sensitive for gel permeation chromatography (GPC); however, no signal was detected, which suggests **11c_n** has a hydrodynamic radius (R_h) $< 2.3 \text{ nm}$, consistent with a low-molecular-weight polymer. For instance, poly(ferrocenylsilane) **10^{Me}_n** with an R_h of $\sim 2.3 \text{ nm}$ has a molecular weight around 9000 Da , suggesting that **11c_n** has a lower molecular weight.⁷⁶ To date, high-molecular-weight poly(ferrocenylborane)s have not been synthesized via ROP, but they have been obtained through other methods.

Scheme 1-26. Thermal ROP of bora[1]FCPs.



The ROP of aluminum- and gallium-bridged [1]FCPs have also been examined for obtaining metallopolymer. These compounds have α angles (14-16°)²⁹⁻³¹ that are significantly lower than those of sila[1]FCPs (19-22°),³⁶⁻⁴² however, the amount of strain present should be sufficient for ROP to occur. The thermal ROP of alumina[1]FCP **12b** and galla[1]FCP **13b** was attempted and only resulted in oligomeric material with molecular weights around 1.5 kDa, as measured by DLS.⁵⁶ The [1]FCPs **12b** and **13b** were found to be completely resistant to anionic ROP, most likely due to sterics. When anionic ROP was attempted on alumina[1]FCP **12a** using MeLi, *n*BuLi, or *t*BuLi in various organic solvents at ambient and elevated temperatures, no polymeric material was obtained, instead unreacted **12a** and the new alumina[1]FCP **42** was obtained (Scheme 1-27).⁵⁶ The photolytic ROP of **12** and **13** using NaCp as an anionic initiator showed equally disappointing results. However, the transition-metal-catalyzed ROP of these [1]FCPs was successful, with galla[1]FCP **13a** giving the best result. The reaction of **13a** with a Pd(0) catalyst resulted in a metallopolymer with a molecular weight of 21.1 kDa (GPC relative to polystyrene).⁵⁶

Scheme 1-27. Reaction of alumina[1]FCP **12a** with *n*BuLi.



Overall, the ROP of alumina[1]FCPs **12** and galla[1]FCPs **13** were quite dismal, with the exception of transition-metal-catalyzed ROP. These results were attributed to the ligands on the bridging elements being too bulky. Thus, the synthesis of aluminum- and gallium-bridged [1]FCPs with less bulky ligands were attempted. As discussed earlier (Chapter 1.1.1.1), the synthesis of aluminum- and gallium-bridged [1]FCPs with less bulky ligands was not successful.^{32, 33, 35} The [1]FCPs **15** were synthesized, however, they were not able to be isolated as they were too reactive and resulted in the formation of metallopolymers **15_n** (Scheme 1-6).^{32, 33} These metallopolymers were isolated and were found to have a broad distribution of molecular weights (**15b**: $M_w = 48$ kDa, PDI = 3.3, GPC relative to polystyrene), due to the fact that ROP was uncontrolled. If less bulky aluminum and gallium bridged [1]FCPs could be isolated, followed by controlled ROP, high-molecular-weight metallopolymers with narrow distributions of molecular weights should be attainable.

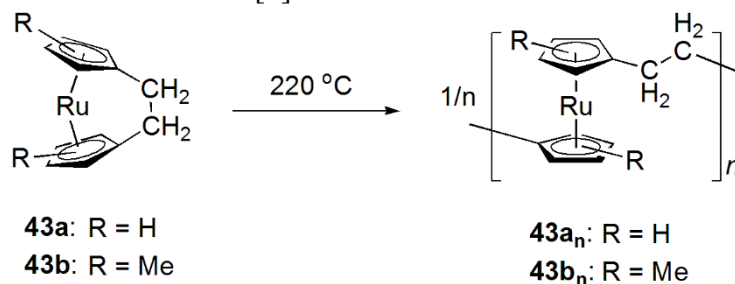
These results show that not all [1]FCPs with ring strain will be effective in obtaining poly(ferrocene)s via ROP. Solubility and steric factors need to be considered for the ROP of [1]FCPs to be successful.

1.2.2.2 Poly(ruthenocene)s

The ROP of [n]RCPs have not been studied as extensively as that of [n]FCPs, mainly due to the low availability of [n]RCPs. The larger metal atom increases the distance between the two Cp rings, causing the rings to tilt more to obtain strained [n]RCPs. In 1994, Manners *et al.* reported the synthesis of dicarba[2]RCPs **43**, which possess significant amounts of ring strain ($\alpha = 29-30^\circ$) making these compounds excellent candidates for ROP.⁷⁷ The thermal ROP of **43a** was attempted, however, insoluble material was obtained making it difficult to characterize the polymer. In order to overcome solubility issues, dicarba[2]RCP **43b** was synthesized with one methyl group on each

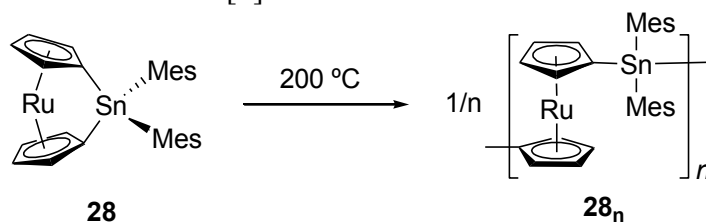
Cp ring, and its subsequent thermal ROP produced a soluble metallopolymer (Scheme 1-28). The poly(ruthenocenylethylene) **43b_n** was found to have a bimodal molecular weight distribution ($M_w = 43.1$ kDa and 12.7 kDa).

Scheme 1-28. Thermal ROP of dicarba[2]RCPs.



In order to obtain [1]RCPs, bridging elements with bulky ligands are employed to stabilize the formation of these species. In 2004, Manners *et al.* studied the first ROP of [1]RCPs with tin (**28**) and zirconium (**29**) in the bridging positions.¹³ Stanna[1]RCP **28** has a significant amount of ring strain ($\alpha = 20.2$ - 20.9°), and thermal ROP lead to the synthesis of poly(ruthenocenylnstannane) **28_n** (Scheme 1-29). GPC analysis indicated that metallopolymer **28_n** had a high-molecular-weight relative to polystyrene (615 kDa), with a broad distribution of molecular weights (PDI = 2.28). Zircona[1]RCP **29** had a much smaller amount of ring strain ($\alpha = 10.4^\circ$) and, as expected, all ROP attempts were unsuccessful.

Scheme 1-29. Thermal ROP of stanna[1]RCP **28**.



As mentioned earlier, Müller *et al.* reported the only other syntheses of [1]RCPs.^{33, 56} Alumina[1]RCP **30a** and galla[1]RCP **30b** were obtained using the bulky Me₂Ntsi ligand on the

bridging element (Scheme 1-12).⁵⁶ These compounds were considerably more ring tilted (**30a**: $\alpha = 20.31^\circ$, **30b**: $\alpha = 20.91^\circ$) compared to [1]FCP analogs (**12b**: $\alpha = 14.33^\circ$, **13b**: $\alpha = 15.83^\circ$), which suggest that **30a** and **30b** should be good candidates for obtaining poly(ruthenocene)s via ROP. However, all attempts to obtain metallopolymer via common ROP methodologies (thermal, anionic, transition-metal-catalyzed, and photolytic ROP) were unsuccessful.

As discussed earlier (Chapter 1.2.2.1), the fairly unsuccessful ROP of [1]FCP analogs **12b** and **13b** were attributed to the large bulkiness of the ligand attached to the bridging elements. Presumably, steric problems are most likely the same reason for the failed ROP of **30a** and **30b**. Therefore, the synthesis of [1]RCPs **31a** and **31b**, with less sterically demanding ligands was attempted.³³ The alumina[1]RCP **31a** behaved like its [1]FCP analogs **15a,b** and spontaneously polymerized in solution. The metallopolymer **31a_n** was found to have a molecular weight of 8.07 kDa, as determined by DLS. Interestingly, the galla[1]RCP **31b** could be isolated as a powder, however, if left for extended periods in solution it would polymerize like **31a** (Scheme 1-13). The metallopolymer **31b_n** obtained through spontaneous ROP in solution was found to have a molecular weight of 10.1 kDa (DLS analysis). Since **31b** could be isolated, transition-metal-catalyzed ROP, using Karstedt's catalyst, was attempted and resulted in the metallopolymer **31b_n** with a molecular weight of 28.6 kDa (DLS analysis), which is three times larger than the metallopolymer obtained through spontaneous ROP in solution.

1.3 Planar-Chiral Ferrocenes

Since its discovery, ferrocene has been found to be a fascinating compound due to its interesting sandwich structure. The unique properties of ferrocene, such as its ability to undergo electrophilic aromatic substitution, its simple lithiation and dilithiation, and its ability to stabilize carbocations in benzylic-like positions allow for the easy synthesis of substituted derivatives. Furthermore, due to its three-dimensional structure, multiple substitution on a Cp ring creates derivatives which lack a plane of symmetry, thus creating planar-chiral ferrocenes. The stereodescriptors “ R_p ” and “ S_p ” are used, according to Schlögl’s definition, to indicate the planar chirality of substituted ferrocene derivatives (Figure 1-6).

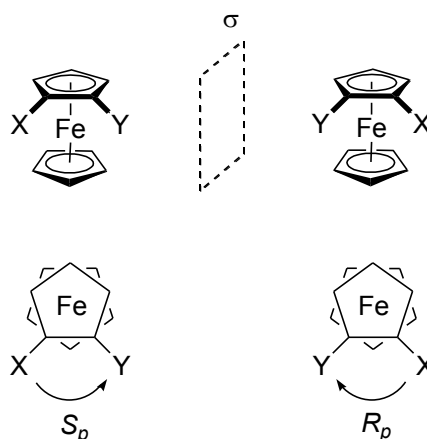
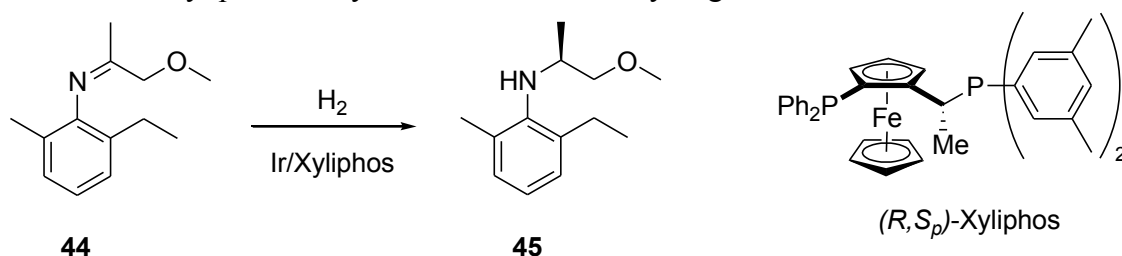


Figure 1-6. Assigning planar chirality for 1,2-heterodisubstituted ferrocenes using the R_p and S_p stereodescriptors, as defined by Schlögl, where X has a higher priority than Y.

Planar-chiral ferrocenes are very important compounds and have found great applicability as chiral ligands in asymmetric catalysis. For example, the industrial production of a precursor to the herbicide (*S*)-metolachlor, amine **45**, is prepared through the asymmetric Ir/Xyliphos-catalyzed hydrogenation of imine **44** (Scheme 1-30).^{78, 79} This is a very efficient process (turnover numbers (TONs) of 2,000,000 and turnover frequencies (TOFs) of 600,000 h⁻¹) and is the largest known enantioselective catalytic process in industry, producing more than 10,000 tons annually. Due to

the many applications of planar-chiral ferrocenes, several ways to synthesize substituted ferrocene derivatives have been developed.

Scheme 1-30. Ir/Xyliphos-catalyzed enantioselective hydrogenation of imine **44**.



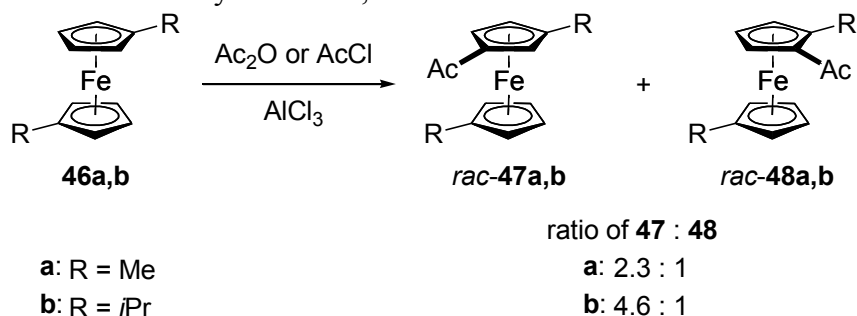
As discussed earlier, sterics play a major role in the synthesis and ROP of [n]MCPs. One can control the outcome of salt-metathesis reactions by tuning the sterics of the ligand(s) attached to the bridging element(s). Another way to tune the sterics of [n]MCPs, is by introducing substituents on the metallocene unit. Placing alkyl groups on the Cp rings also helps to increase the solubility of [n]MCPs and resulting metallopolymer. In order to tune the bulk properly, an understanding of how to control the substitution pattern on metallocenes is necessary. If substituents on a metallocene are to provide steric protection to the bridging element, they should be placed on the carbon atom adjacent to the *ipso*-carbon of resulting [n]MCPs (*ortho* position); therefore, metallocene derivatives would need to be designed appropriately. The synthesis of planar-chiral ferrocene derivatives and methodologies to control the resulting substitution pattern will be briefly discussed. Readers interested in a comprehensive overview of the synthesis and applications of planar-chiral ferrocenes are referred to the following review.⁸⁰

1.3.1 Derivatization of Ferrocene

There are two main methods for synthesizing substituted ferrocene derivatives, namely, electrophilic aromatic substitution or through metalation. Since ferrocene is aromatic, it is possible to perform Friedel-Crafts reactions to access substituted ferrocenes.^{81, 82} For instance, the acylation

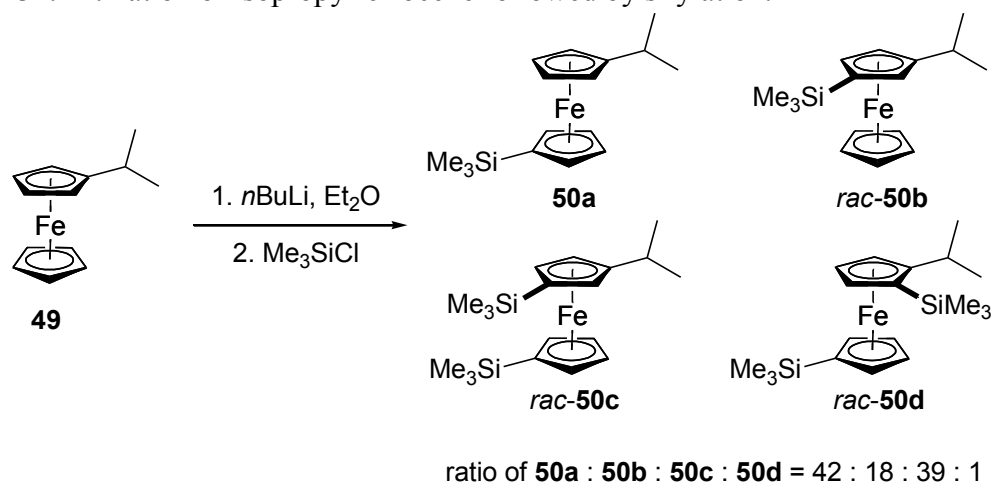
of 1,1'-disubstituted ferrocenes **46a,b** produces a mixture of acylated planar-chiral ferrocene derivatives **47a,b** and **48a,b** (Scheme 1-31). There is a slight preference for ferrocenes **47a,b** because of sterics, however, decent amounts of **48a,b** are also formed. These isomers are extremely difficult to separate, due to the structures being very similar. Therefore, the substitution reaction must somehow be controlled to obtain specifically substituted ferrocene derivatives, which is difficult through electrophilic aromatic substitution reactions.

Scheme 1-31. Friedel-Crafts acylation of 1,1'-disubstituted ferrocenes.



Metalation, particularly lithiation, is a commonly used route for obtaining substituted ferrocene derivatives. Well-established methods have been developed for the monolithiation^{83, 84} and 1,1'-dilithiation⁸⁵ of ferrocene. When substituted ferrocenes are lithiated followed by subsequent substitution with an electrophile, planar-chiral ferrocenes can be obtained. For instance, when isopropylferrocene (**49**) was lithiated with one equivalent *n*BuLi in ether followed by the addition of chlorotrimethylsilane, a mixture of substituted ferrocenes **50a-d** were obtained, including some planar-chiral ferrocenes (Scheme 1-32).⁸⁶ It is unavoidable to obtain a mixture of isomers, however, there does appear to be a preference for certain isomers, which is controlled by sterics.

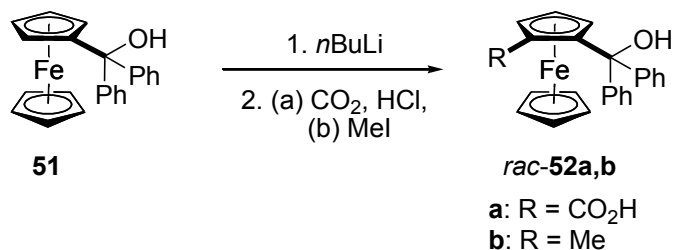
Scheme 1-32. Lithiation of isopropylferrocene followed by silylation.



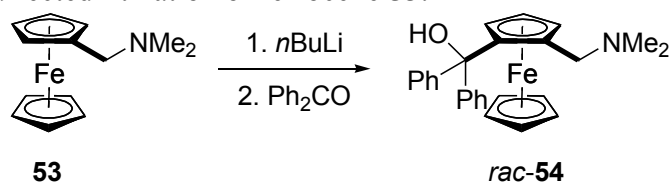
1.3.2 *Ortho*-Directed Metalation of Ferrocene

The substitution of ferrocene can be controlled by including *ortho*-directing groups (ODGs) on the Cp ring of ferrocene. If an ODG is present, it will direct lithiation to the position adjacent (α or *ortho* position) of the ODG. In 1961, Benkeser *et al.* reported the first use of an ODG (diphenylcarbinol) on ferrocene to obtain only 1,2-disubstituted ferrocenes.⁸⁷ In this report, the substituted ferrocene, diphenylferrocenylcarbinol **51**, was reacted with an excess of *n*BuLi in diethyl ether at room temperature followed by quenching with dry ice or methyl iodide to yield the 1,2-disubstituted ferrocenes *rac*-**52a,b** exclusively (Scheme 1-33).

Scheme 1-33. *Ortho*-directed lithiation of ferrocene **51**.

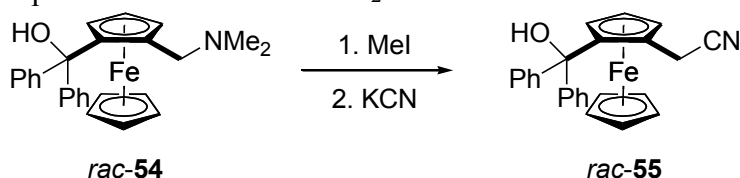


Scheme 1-34. *Ortho*-directed lithiation of ferrocene **53**.



In 1965, Slocum *et al.* reported the ability of N,N-dimethylaminomethylferrocene (**53**) to undergo *ortho*-directed lithiation to exclusively yield 1,2-disubstituted ferrocene *rac*-**54** (Scheme 1-34).⁸⁸ The solvent has a major influence on the *ortho*-directing ability of **53**; for instance, lithiation in hexane/diethyl ether mixtures exclusively yield *rac*-**54**, whereas hexane/thf mixtures result in a mixture of substituted ferrocenes. Compound **53** has been found to be very useful for preparing countless substituted ferrocenes, this is not only attributed to its *ortho*-directing ability, but also the ability to replace the NMe₂ moiety through nucleophilic substitution reactions, which follow an S_N1 mechanism.^{89, 90} For example, when *rac*-**54** is treated with methyl iodide, followed by the addition of a nucleophile, such as CN⁻, *rac*-**55** is obtained (Scheme 1-35).⁸⁸

Scheme 1-35. Nucleophilic substitution of NMe₂ in *rac*-**54**.



Over the years, several ferrocene derivatives (**56-65**) with various ODGs have been prepared and utilized to synthesize 1,2-disubstituted ferrocenes (Figure 1-7).^{80, 91-110} Each of the derivatives shown in Figure 7, require different metalation protocols employing various bases [e.g. *n*BuLi, *s*BuLi, *t*BuLi, or lithium diisopropylamide (LDA)], solvents (hexanes, Et₂O, or thf), and reaction temperatures (-78 °C up to refluxing temperatures). The majority of these derivatives lead to the synthesis of 1,2-disubstituted ferrocenes with reasonable yields and high regioselectivity.

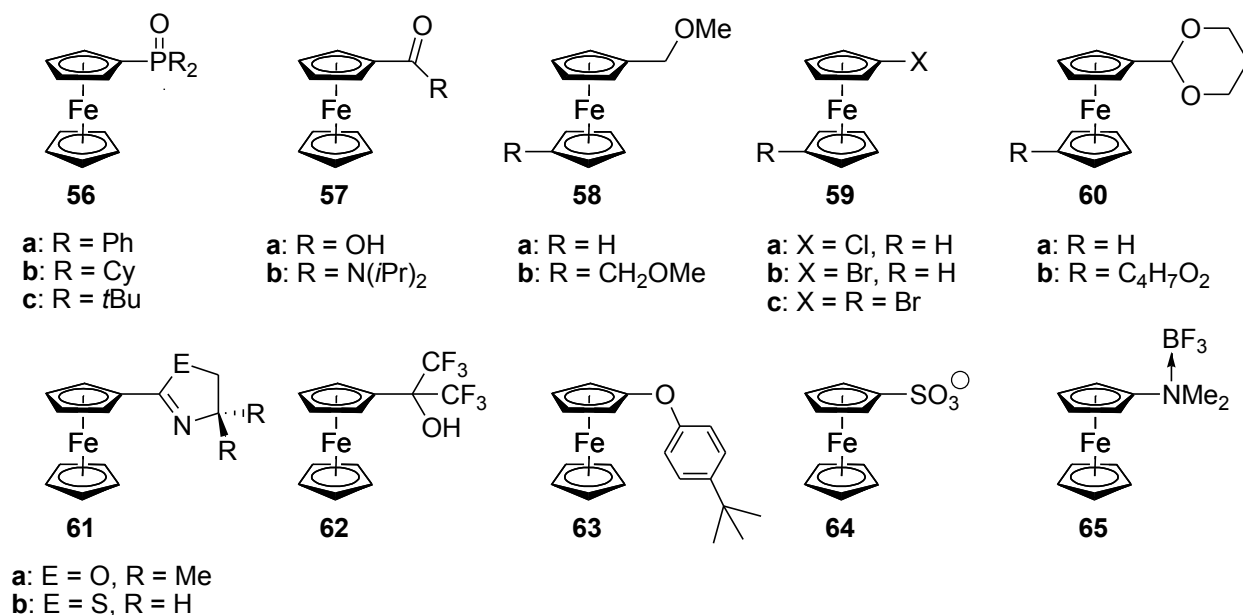


Figure 1-7. Substituted ferrocene derivatives used for *ortho*-directed metalation.

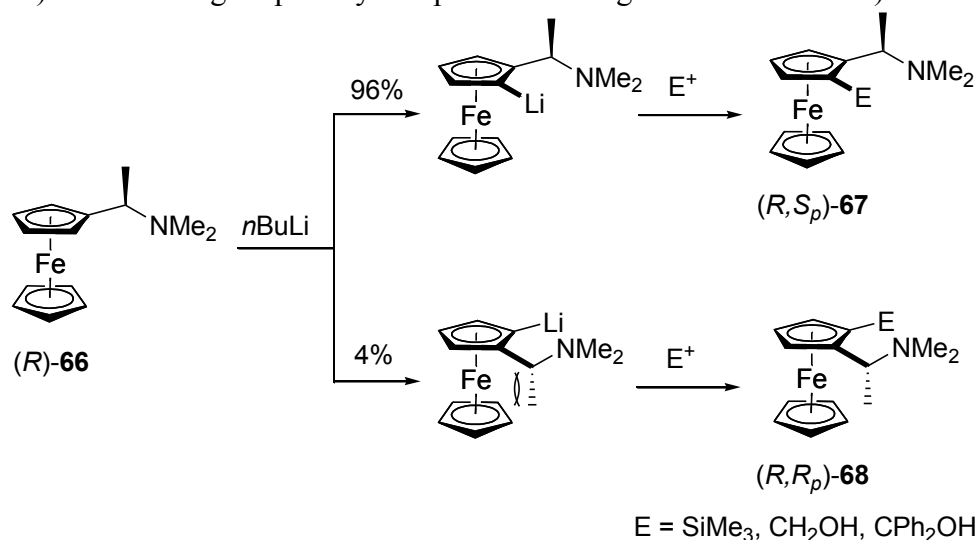
1.3.3 Diastereoselective *ortho*-Directed Metalation of Ferrocene

The products of 1,2-disubstituted ferrocene derivatives obtained through the *ortho*-directed lithiations discussed earlier (Chapter 1.3.2), are 50/50 mixtures of the two possible enantiomers, thus making a racemate. If an enantiopure planar-chiral ferrocene is desired, separating the racemic mixture could be a difficult process, depending on the ferrocene derivative. Ferrocene derivatives that contain chiral ODGs produce mixtures of diastereomers, instead of enantiomers. The chirality of the ODG typically favours a specific conformation so that all substituents on the group are oriented away from the ferrocene backbone. Therefore, the functionality that facilitates lithiation will orient itself to a particular *ortho*-position on ferrocene, producing only one diastereomer – this is known as diastereoselective *ortho*-directed lithiation.

In 1970, Ugi *et al.* introduced (*R*)- and (*S*)-N,N-dimethyl-1-ferrocenylethylamine (**66**, known as Ugi's amine), a well-known ferrocene derivative that performs diastereoselective *ortho*-directed lithiation in the synthesis of 1,2-disubstituted ferrocenes.¹¹¹ The two enantiomers, (*R*)-**66** and (*S*)-

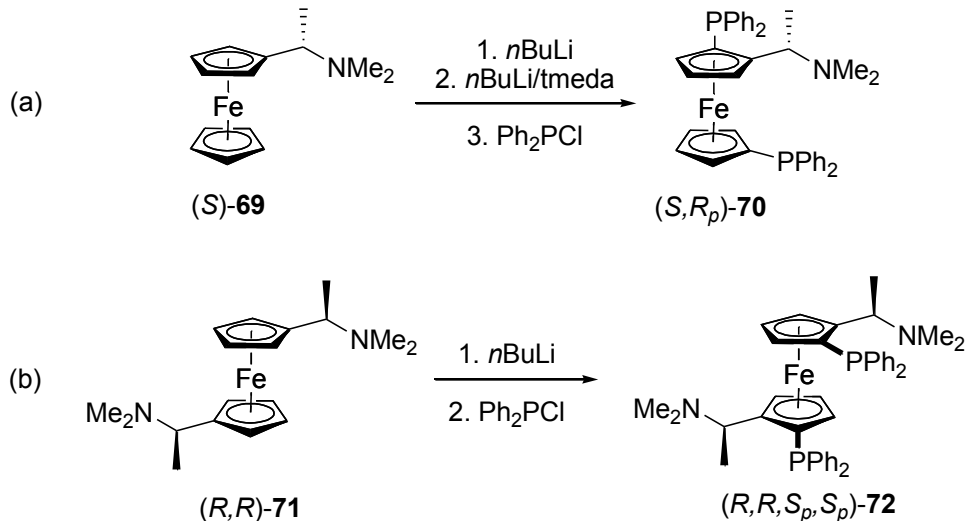
69, can be separated in high yields by resolution with (*R*)-(+)-tartaric acid. These compounds were revolutionary for the synthesis of ferrocene derivatives since they cause a high diastereoselectivity for lithiations, almost exclusively producing a single diastereomer. For example, the lithiation of (*R*)-**66** using *n*BuLi in diethyl ether at room temperature, followed by reaction with an electrophile yields (*R,S_p*)-**67** with 92% *de* (Scheme 1-36). The minor diastereomer, (*R,R_p*)-**68**, can usually be removed through standard purification methods. As demonstrated in Scheme 1-35, the chiral ODG favours lithiation of H² over H⁵, showing its diastereoselectivity.

Scheme 1-36. Diastereoselectivity of “Ugi’s amine” (*R*)-**66** (the electrophiles (E = SiMe₃, CH₂OH, and CPh₂OH) all have a higher priority compared to the Ugi amine substituent).



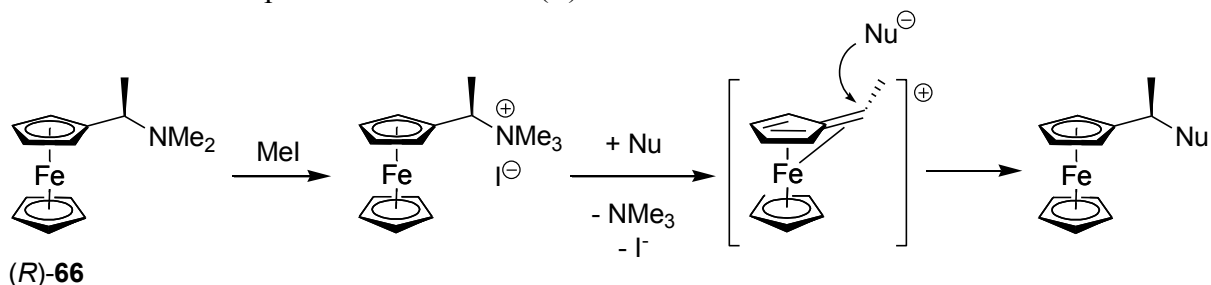
The other enantiomer of “Ugi’s amine”, (*S*)-**69**, can also be lithiated with the same diastereoselectivity following the same procedure. The dilithiation of (*S*)-**69** in the presence of tmeda followed by quenching with an electrophile, such as Ph₂PCl, results in the 1,2,1'-trisubstituted ferrocene (*S,R_p*)-**70** (Scheme 1-37a).¹¹² Similarly, the “double Ugi’s amine” (*R,R*)-**71** can be dilithiated diastereoselectively, without tmeda, and quenched with Ph₂PCl to yield the single diastereomer (*R,R,S_p,S_p*)-**72** (Scheme 1-37b).¹¹³⁻¹¹⁶

Scheme 1-37. Diastereoselective lithiation (*S*)-**69** and (*R,R*)-**71** followed by quenching with Ph₂PCl.

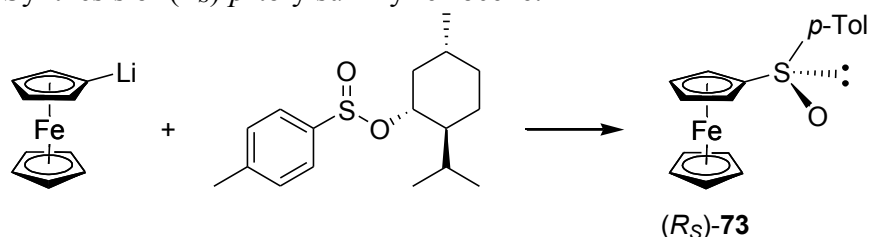


The NMe₂ moieties in “Ugi’s amine” and its various derivatives can be replaced through nucleophilic substitution reactions, similar to what was discussed for amine **53**.^{89, 90} It is noteworthy that this replacement occurs with full retention of configuration. The substitution of the NMe₂ moiety occurs through an S_N1 mechanism, therefore, when the carbocation intermediate is formed, it is stabilized by interactions with the iron centre. This intermediate only allows incoming nucleophiles to attack from the top of the Cp ring (i.e. away from iron), thus retaining configuration (Scheme 1-38).^{111, 117, 118}

Scheme 1-38. Nucleophilic substitution of (*R*)-**66**.

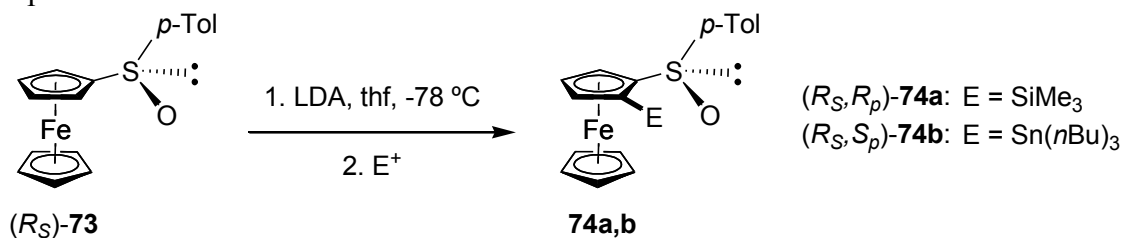


Scheme 1-39. Synthesis of (*R_S*)-*p*-tolylsulfinylferrocene.



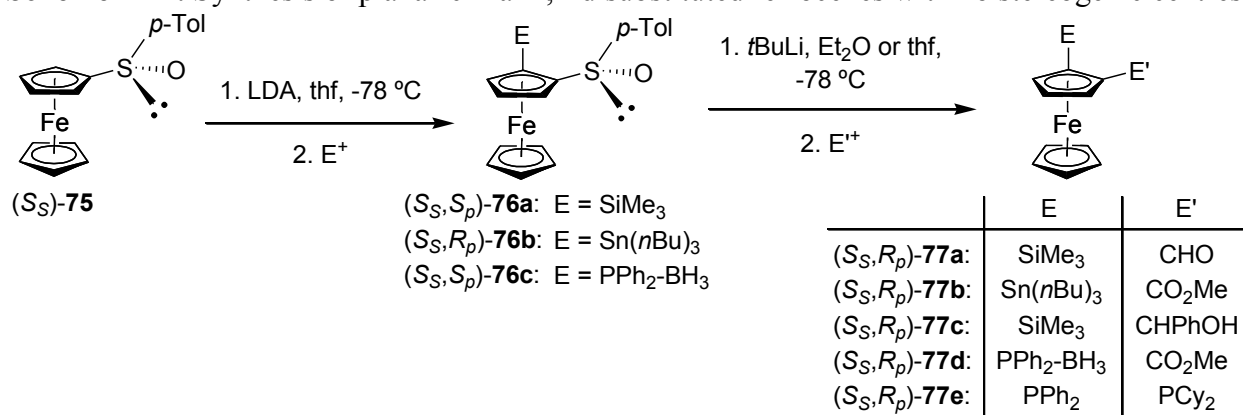
“Ugi’s amine” derivatives are not the only compounds with ODGs that can perform diastereoselective *ortho*-directed lithiation on ferrocene. In 1990, Kagan *et al.* reported the synthesis of chiral (*R_S*)-*p*-tolylsulfinylferrocene (*R_S*)-**73**, which is prepared by reacting monolithioferrocene with (+)-(1*S*)-menthyl (*R_S*)-*p*-tolylsulfinate (Scheme 1-39).¹¹⁹ A few years later, the same group reported that the lithiation and subsequent reaction of (*R_S*)-**73** with an electrophile, diastereoselectively (*de* ≥ 98%) yields planar-chiral ferrocenes **74a,b** when performed in thf at -78 °C using LDA (Scheme 1-40).¹²⁰ The enantiomer (*S_S*)-**75**, which displays similar reactivity, has been prepared following a similar procedure.^{84, 121}

Scheme 1-40. Diastereoselective lithiation of (*R_S*)-**73** and subsequent quenching with an electrophile.



What is unique about compounds (*R_S*)-**73** and (*S_S*)-**75** is that after obtaining 1,2-disubstituted ferrocenes, the *p*-tolylsulfinyl group can be removed and replaced with a second electrophile through a lithium exchange using *t*BuLi. For instance, various planar-chiral 1,2-disubstituted ferrocenes **77a-e**, which contain no stereogenic centres, were obtained after replacing the *p*-tolylsulfinyl group of ferrocenes **76a-c**, synthesized from (*S_S*)-**75** (Scheme 1-41).¹²¹

Scheme 1-41. Synthesis of planar-chiral 1,2-disubstituted ferrocenes with no stereogenic centres.



Compounds (*R*)-**66**, (*S*)-**69**, (*R_S*)-**73**, and (*S_S*)-**75** are just a few examples of ferrocene derivatives that can be used to synthesize a wide variety of 1,2-disubstituted ferrocenes diastereoselectively.

1.4 Research Objectives

Part 1. As discussed throughout Chapter 1, [n]metallocenophanes have found great utility as precursors for metallocopolymers, due to their intrinsic strain and susceptibility to ROP. To successfully isolate [1]MCPs, the appropriate amount of steric protection needs to be provided to favour the ring-tilted structures. For instance, when studying group-13-bridged [1]FCPs, the Müller group employed the bulky Me₂Ntsi and Pytsi ligands to successfully synthesize **12** and **13** (Scheme 1-4); however, the ROP of these compounds was fairly unsuccessful, which was attributed to the large bulk on the bridging element.²⁹⁻³¹ When the trisyl-based ligands were replaced with the non-bulky Ar' ligand, the unstrained [1.1]FCPs **14**, which are not prone to ROP, were obtained instead of the desired [1]FCPs (Scheme 1-5).^{34, 35} From these studies, it can be seen that the bulkiness of the ligand on the bridging element plays a major role in the outcome of salt-metathesis reactions (Figure 1-8). In these reactions, the thermodynamically favoured product is the [1.1]FCP, if the ER_x moiety is small enough. By utilizing larger bridging ER_x moieties, [1.1]FCPs can be blocked, thus favouring the formation of [1]FCPs. However, if the bridging moiety is too large, subsequent ROP of the [1]FCPs could be difficult, or impossible, since there is less space available for the bridging moiety in a metallocopolymer.

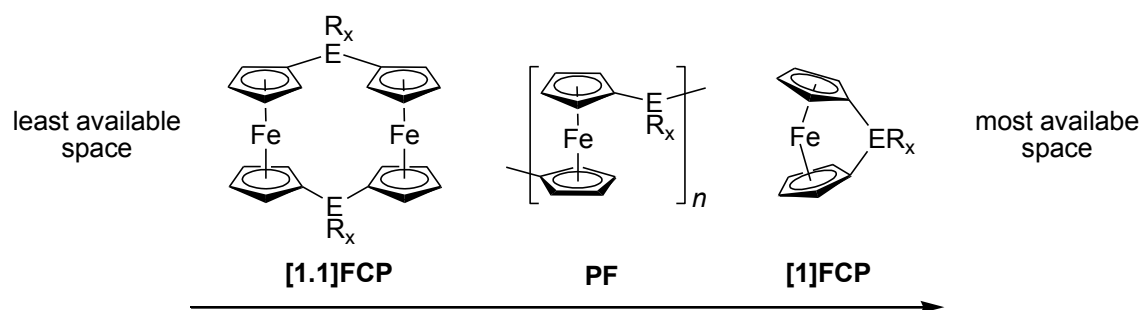


Figure 1-8. Amount of available space for the bridging moiety, ER_x.

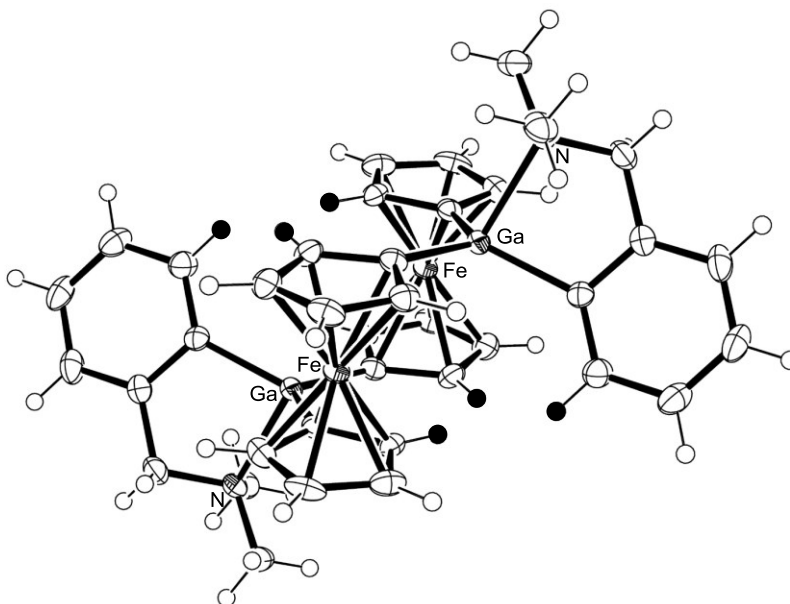
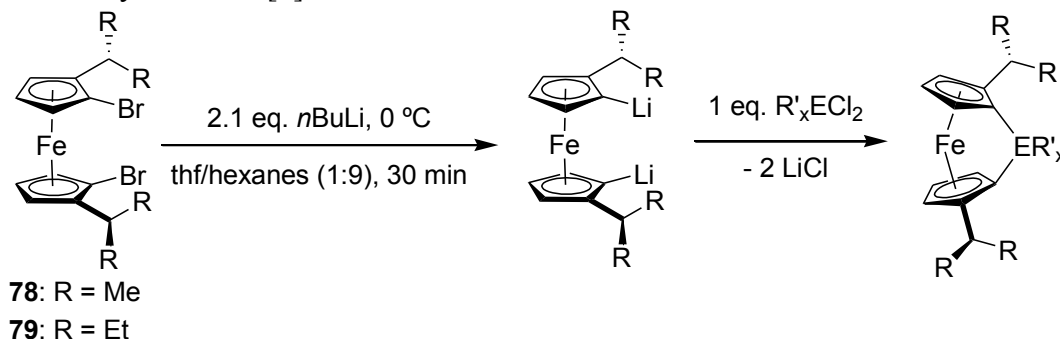


Figure 1-9. Illustration of the space restrictions in galla[1.1]FCP **14b**. The coloured-in hydrogen atoms highlight the group of hydrogen atoms in close proximity to each other.

Analyzing the crystal structure of galla[1.1]FCP **14b**, shows that there is some space restriction between the hydrogen atoms in the α position of the Cp rings and the *ortho* position of the phenyl ring, with respect to the gallium atom (Figure 1-9).³⁵ By placing a bulky group in this area, the formation of [1.1]FCPs will be blocked, thus facilitating the formation of [1]FCPs. Based on this observation, the Müller group developed two strategies for tuning the sterics to favour the formation of [1]FCPs over [1.1]FCPs. The first involved the synthesis of the Mamx ligand which contains a *t*Bu group in the *ortho* position of the phenyl ring. When this ligand was employed in salt-metathesis reactions, it resulted in the formation of [1]FCPs **15**, however, these compounds were too reactive and underwent spontaneous ROP in solution (Scheme 1-6).^{32, 33} More recently, the Müller group focused on shifting the bulkiness on the bridging moiety to the Cp rings on the ferrocene unit, thus developing the C_2 -symmetrical dibromoferrocene derivatives **78** and **79**.¹²²⁻¹²⁵ These derivatives can be lithiated cleanly, and used as the dilithioferrocene in salt-metathesis

reactions. These derivatives have successfully led to the synthesis of new [1]FCPs, which are prone to ROP (Scheme 1-42).

Scheme 1-42. Synthesis of [1]FCPs with substituted ferrocene derivatives **78** and **79**.



As was demonstrated earlier, the amount of steric bulk is key to isolating [1]FCPs, which is different for various bridging elements. Therefore, the bulk in the α positions, with respect to the bridging element, on the ferrocene unit could be altered to favour the formation of various [1]FCPs. In order to obtain these [1]FCPs, α -substituted 1,1'-dilithioferrocene derivatives are required. On this basis, my Master's work was to synthesize ferrocene derivatives with varying steric bulk, which can be used as precursors for obtaining [1]FCPs. Chapter 2.1 will discuss the research I did to prepare new dibromoferrocene precursors following the strategy that was developed by the Müller group; Chapter 2.2 will discuss the application of some of these derivatives.

Part 2. There have been many investigations into the synthesis and ROP of [1]FCPs, however, the same studies for [1]RCPs are relatively unexplored in comparison. To date, only five [1]RCPs have been successfully synthesized.^{13, 33, 56} Since the ruthenium atom is larger than iron, the Cp rings must tilt more to form [1]RCPs. For example, the galla[1]RCP **30b** has a higher tilt angle of 20.91° compared to its [1]FCP analog **13b**, with a tilt angle of 15.83°. As demonstrated in Chapter 1.1.2, to favour the formation of highly ring-tilted structures of [1]RCPs, bulky ligands on the bridging element were required. As shown earlier by the Müller group, steric bulk can be placed

on the ferrocene unit to help favour the formation of [1]FCPs (Scheme 1-42). Therefore, my second research objective was to apply this same strategy to [1]RCPs by preparing analogous ruthenocene derivatives. Chapter 2.3 will discuss my research to prepare a ruthenocene derivative for salt-metathesis reactions.

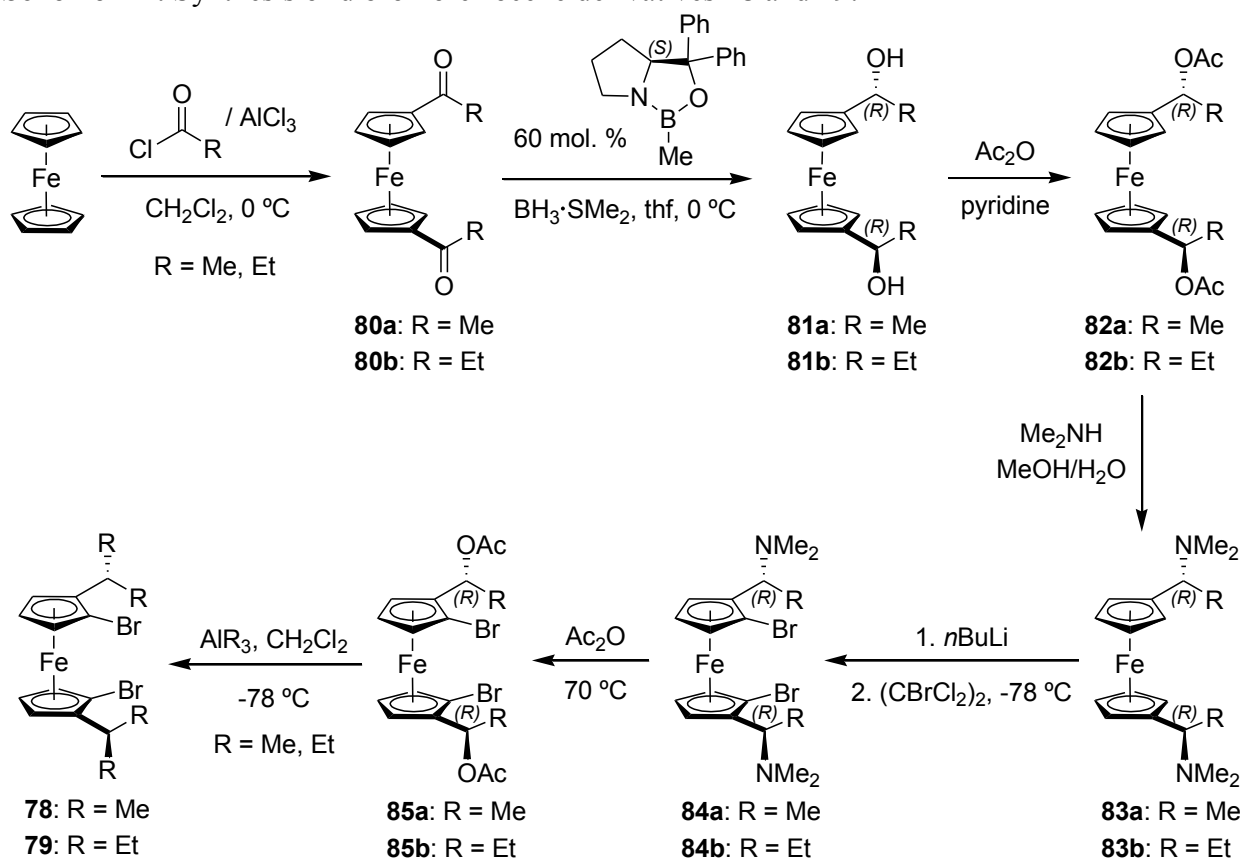
Part 3. As stated earlier, the Müller group has found success with employing dibromoferrocene derivatives **78** and **79** in salt-metathesis reactions to obtain new [1]FCPs (Scheme 1-42).¹¹⁷⁻¹²⁰ However, this method is a very long process and is not very flexible synthetically for obtaining dibromoferrocene derivatives. There are only two points in the synthetic pathway where the substituents on ferrocene can be altered. Therefore, my third research objective was to find an alternative method to obtain dibromoferrocene derivatives suitable for preparing [1]FCPs that is both shorter and more flexible. To accomplish this, chemistry that was developed by Kagan *et al.*¹¹⁵⁻¹¹⁶ to synthesize planar-chiral ferrocenes was adapted to synthesize C₂-symmetrical dibromoferrocene derivatives. Chapter 2.4 will discuss my research to develop a new method for synthesizing these derivatives.

CHAPTER 2: RESULTS AND DISCUSSION

2.1 Synthesis of C_2 -Symmetrical Dibromoferrocene Derivatives

The major objective of this Master's work was to synthesize ferrocene derivatives that could be used as precursors for [1]FCPs. Ferrocene derivatives containing substituents on the Cp rings in the α position with respect to the bridging element assist in favouring the formation of [1]FCPs. Therefore, the appropriate precursor to synthesizing [1]FCPs are α -substituted dilithioferrocene derivatives. As mentioned earlier (Chapter 1.4), the Müller group prepared the dibromoferrocene derivatives **78** and **79**, which were successfully used to synthesize a wide variety of [1]FCPs (Scheme 1-42).^{122, 124, 125} These derivatives were prepared by using the well-known "Ugi's amine" chemistry,^{111, 116} which is a fairly flexible synthetic pathway for obtaining C_2 -symmetrical, α -substituted dibromoferrocenes, which can be used as precursors for [1]FCPs (Scheme 2-1).

Scheme 2-1. Synthesis of dibromoferrocene derivatives **78** and **79**.

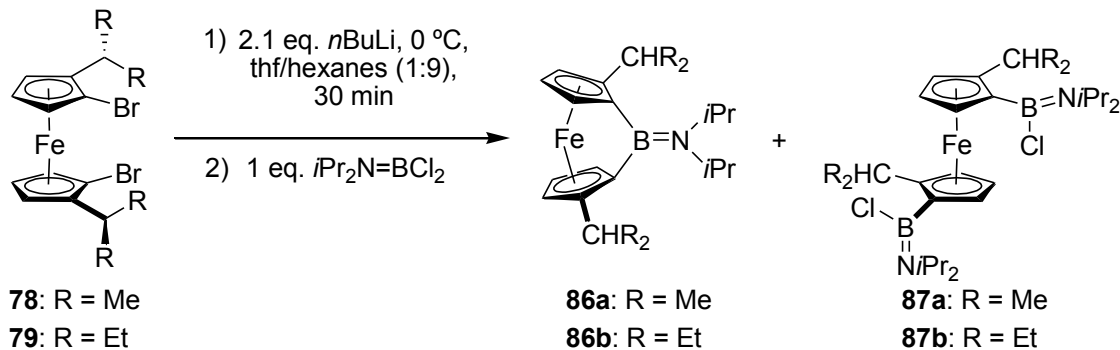


The most vital step in this synthesis route is the known asymmetric reduction of **80a,b**, using an oxazaborolidine catalyst to yield the known, enantiomerically pure diols **81a,b**.¹¹⁶ The diols can then be acetylated to yield acetates **82a,b**, followed by nucleophilic substitution reactions, similar to what was reported for “Ugi’s amine” (see Chapter 1.3.3), to yield the known compounds **83a,b** with full retention of configuration. Since the “double Ugi’s amines” **83a,b** are enantiomerically pure, they can be dilithiated diastereoselectively to yield only one 1,1'-2,2'-tetrasubstituted ferrocene isomer. The dilithiated **83a,b** can then be used in salt-metathesis reactions to obtain [1]FCPs, however, it is difficult to completely remove LiCl formed in the reaction due to the NMe₂ moieties. Therefore, it is advantageous to remove the NMe₂ moieties before performing salt-metathesis reactions. After lithiation, the compounds can be brominated to yield the known compounds **84a,b**.¹²⁶ Using known substitution chemistry,¹²⁷ the NMe₂ moieties can be replaced with alkyl groups to obtain dibromoferrocene derivatives **78** and **79**, which are excellent precursors for salt-metathesis reactions.¹²² This synthetic pathway can also be used to obtain other C₂-symmetrical dibromoferrocene derivatives with various amounts of steric bulk. This can be done by changing the R groups that are introduced in the first and last steps of this synthesis (Scheme 2-1).

To use these compounds for salt-metathesis reactions, the published quantitative lithium-bromine exchange procedure for lithiating aromatic bromides was used (Scheme 1-42).¹²⁸ The dibromoferrocene derivatives **78** and **79** were successfully employed for obtaining a wide variety of [1]FCPs.¹²² Very recently, the Müller group reported on the salt-metathesis reactions of dibromoferrocenes with various amino(dichloro)boranes, which resulted in different ratios of bora[1]FCPs and 1,1'-bis(boryl)ferrocenes.¹²⁵ For example, the reaction of **78** and **79** with

$i\text{Pr}_2\text{NBCl}_2$ yielded mixtures of the desired bora[1]FCPs **86a,b** and 1,1'-bis(boryl)ferrocenes **87a,b** with particular ratios (Scheme 2-2).

Scheme 2-2. Salt-metathesis reactions between dibromoferrocenes **78** and **79** with $i\text{Pr}_2\text{NBCl}_2$.



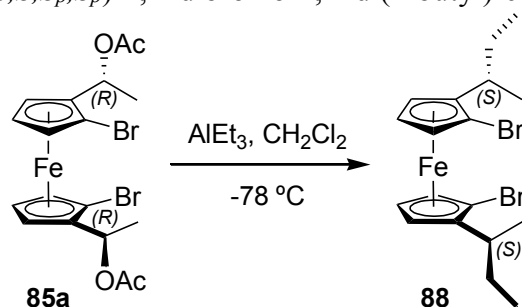
It was observed that the ratios between the bora[1]FCPs and the 1,1'-bis(boryl)ferrocene species changed dramatically depending on the alkyl group present on the Cp rings. The ratio between the two products was found to be 1.0:0.59 (**86a:87a**) and 1.0:0.30 (**86b:87b**) for the salt-metathesis reactions between respective ferrocene derivatives and $i\text{Pr}_2\text{NBCl}_2$.¹²⁵ This observation can be rationalized by analyzing the most stable conformation of the CHR_2 alkyl groups on the ferrocene unit. In all of these compounds, one of the R groups is roughly in the same plane as a Cp ring, while the other R group orients itself away from iron and almost perpendicular to a Cp ring. This is most likely the thermodynamically favoured conformation since repulsive interactions are minimized between the alkyl groups and iron when both R groups are oriented away from iron. It is believed that the size of the R group that is perpendicular to the Cp rings affects the rate of $i\text{Pr}_2\text{NBCl}_2$ reacting with the lithiated ferrocene since it is close to the reaction site; whereas the other R group, which is oriented away from the reaction site, has little to no effect. The alkyl groups have no effect on the rate of ring-closure to form bora[1]FCPs; therefore, the ratio between bora[1]FCPs and 1,1'-bis(boryl)ferrocenes should become larger as the R group perpendicular to the Cp rings becomes larger, which was observed for the ferrocene derivatives **78** and **79**.

The synthetic pathway shown in Scheme 2-1 can be manipulated to change the size of the R group that is perpendicular to the Cp rings on ferrocene unit. This group is introduced in the last step of the synthesis of dibromoferrocene derivatives. On this basis, I synthesized new dibromoferrocene derivatives by following the pathway in Scheme 2-1, where R = Me, and changed the R group that was introduced in the last step. The following subsections will discuss the synthesis of these new dibromoferrocene derivatives and Chapter 2.2 will discuss the outcomes of salt-metathesis reactions of the derivatives with $i\text{Pr}_2\text{NBCl}_2$.

2.1.1 Synthesis of (*S,S,S_p,S_p*)-1,1'-Dibromo-2,2'-di(2-butyl)ferrocene

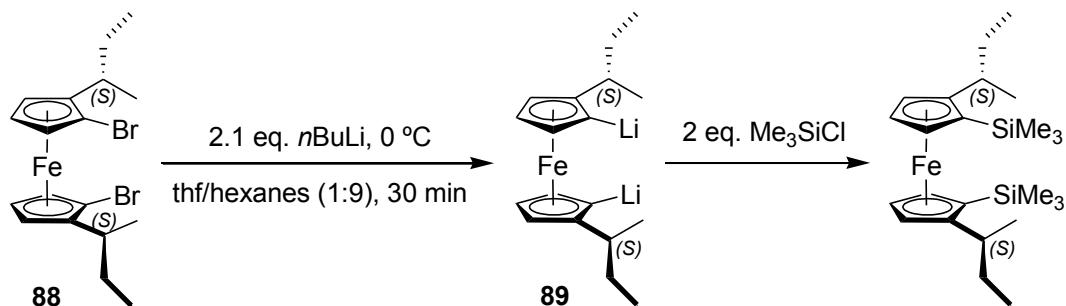
As mentioned earlier, it is believed that the R group that is roughly in the same plane as the Cp rings do not affect the outcome of salt-metathesis reactions. Therefore, similar product ratios between bora[1]FCPs and 1,1'-bis(boryl)ferrocene species should be observed for the salt-metathesis reactions where ferrocene moieties have different R groups in the same plane as the Cp ring, but the same R group perpendicular to the Cp rings. For this reason, the dibromoferrocene derivative **88**, where the R group that is roughly in the same plane as the Cp rings has been changed to a Me group compared to **79**, was targeted to confirm this speculation. The diacetate **85a** was prepared by following the synthetic pathway outlined in Scheme 2-1.^{116, 122} At this point, reaction with triethylaluminum at -78 °C yielded (*S,S,S_p,S_p*)-1,1'-dibromo-2,2'-di(2-butyl)ferrocene (**88**) (Scheme 2-3). Unlike the dibromoferrocene derivatives **78** and **79**, **88** has both central and planar chirality.

Scheme 2-3. Synthesis of (*S,S,S_p,S_p*)-1,1'-dibromo-2,2'-di(2-butyl)ferrocene (**88**).



The crude product was passed through a column of silica, which gave a reddish-brown oil with an 85% yield. Several attempts were made to crystallize **88** using different solvents and crystallization temperatures, however, crystals of **88** could not be obtained. The ^1H NMR spectroscopic data of **88** contained an extra set of signals in the Cp region, indicating the presence of a C_1 -symmetrical stereoisomer of **88** in a significant amount (~9%); this shows that the replacement of the acetoxy groups with an Et group using AlEt_3 does not occur with 100% retention of configuration. The dilithiation of **88** was tested by following the same lithium-bromine exchange procedure¹²⁸ that was used for **78** and **79**.¹²² After quenching the dilithioferrocene **89** with trimethylsilyl chloride (Me_3SiCl), the dilithiation was found to be quantitative (Scheme 2-4). Despite **88** containing some amount of another stereoisomer, the reaction of **89** with $i\text{Pr}_2\text{NBCl}_2$ was performed to observe the effects of the alkyl group on salt metathesis, which will be discussed later (Chapter 2.2).

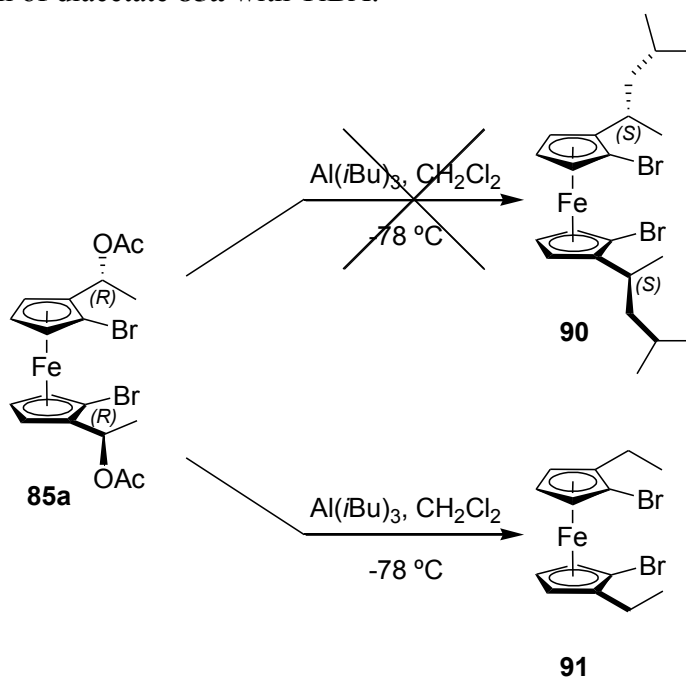
Scheme 2-4. Test dilithiation of the dibromoferrocene derivative **88**.



2.1.2 Synthesis of (*S,S,S_p,S_p*)-1,1'-Dibromo-2,2'-bis{2-[1-(trimethylsilyl)propyl]}ferrocene

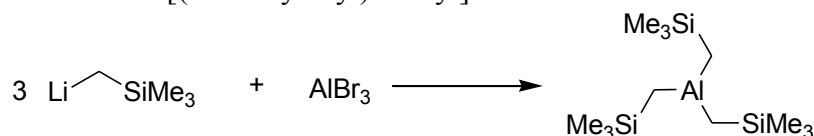
As mentioned earlier, it is believed that the size of the R group that is perpendicular to the Cp rings influence the ratio of the products in salt-metathesis reactions. Therefore, I decided to synthesize dibromoferrocene derivatives that have larger R groups in this position, compared to compounds **78** and **79**. As shown in Scheme 2-1, trialkylaluminum reagents are required to replace the acetoxy groups in **85a** with alkyl groups that are oriented perpendicular to the Cp rings; therefore, various trialkylaluminum reagents were surveyed for preparing new dibromoferrocene derivatives. The first reagent that was employed to obtain a bulkier dibromoferrocene derivative was triisobutylaluminum (TiBA), because it was commercially available. When attempting to replace the acetoxy groups using TiBA, the desired (*S,S,S_p,S_p*)-1,1'-dibromo-2,2'-bis[2-(4-methylpentyl)]ferrocene (**90**) was not obtained, and (*S_p,S_p*)-1,1'-dibromo-2,2'-diethylferrocene (**91**) was obtained instead. It is speculated that trace amounts of diisobutylaluminum hydride (DIBALH) present in the TiBA reagent causes this reaction (Scheme 2-5).

Scheme 2-5. Reaction of diacetate **85a** with TiBA.



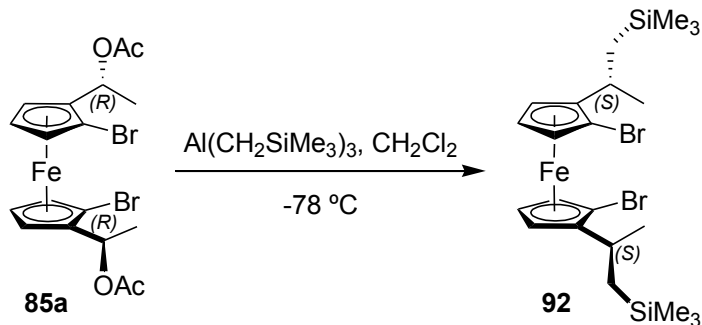
Trialkylaluminum reagents containing bulky alkyl groups are generally not commercially available, therefore, they must be synthesized. After trying to synthesize a few trialkylaluminum reagents, tris[(trimethylsilyl)methyl]aluminum $[\text{Al}(\text{CH}_2\text{SiMe}_3)_3]$ was successfully prepared from [(trimethylsilyl)methyl]lithium¹²⁹ and aluminum(III) bromide in 86% yield following literature procedures (Scheme 2-6).¹³⁰

Scheme 2-6. Synthesis of tris[(trimethylsilyl)methyl]aluminum.



After tris[(trimethylsilyl)methyl]aluminum was purified, it was reacted with **85a** at -78°C to yield (*S,S,S_p,S_p*)-1,1'-dibromo-2,2'-bis{2-[1-(trimethylsilyl)propyl]} ferrocene (**92**) (Scheme 2-7).

Scheme 2-7. Synthesis of (*S,S,S_p,S_p*)-1,1'-dibromo-2,2'-bis{2-[1-(trimethylsilyl)propyl]} ferrocene (**92**).



The crude product was passed through an alumina column to give an orange-brown oil with an 82% yield. Orange needles were obtained after allowing a solution of **92**, obtained by dissolving **92** in a minimal amount of CH_2Cl_2 and adding twice the amount of MeOH , to slowly evaporate. The crystallization was repeated to yield orange needles of **92** in 56% yield. The ^1H NMR spectroscopic data of **92** contained an extra six signals in the Cp region, indicating the presence of a C_1 -symmetrical stereoisomer of **92** in a significant amount (~9%); this shows that the

replacement of the acetoxy groups with CH_2SiMe_3 using $\text{Al}(\text{CH}_2\text{SiMe}_3)_3$ does not occur with 100% retention of configuration. The orange needles of **92** were analyzed by X-ray diffraction (XRD) analysis and its structure was determined (Figure 2-1, Table 2-1).

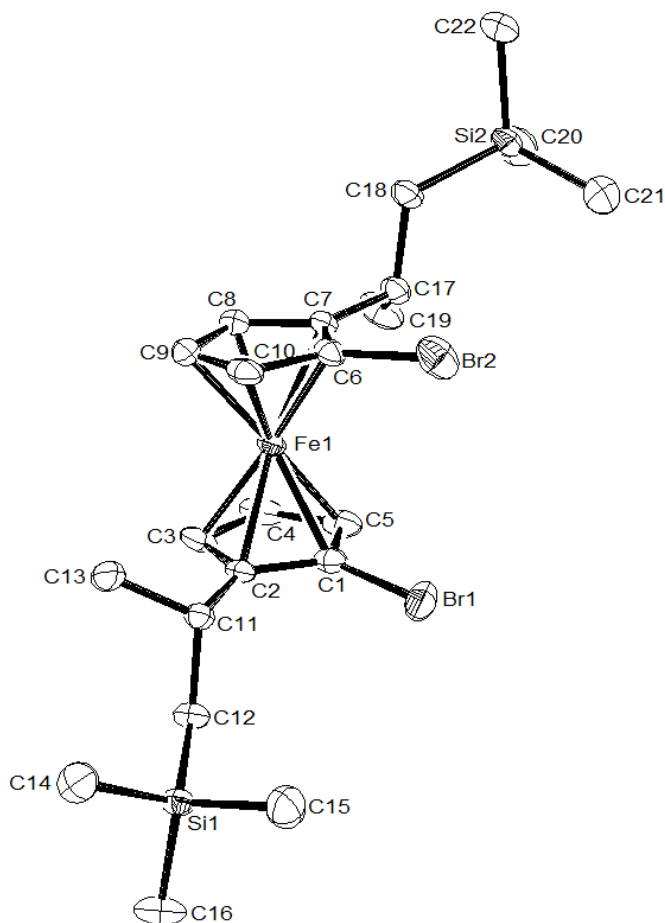


Figure 2-1. Molecular structure of **92** with thermal ellipsoids at the 50% probability level. Hydrogen atoms are omitted for clarity.

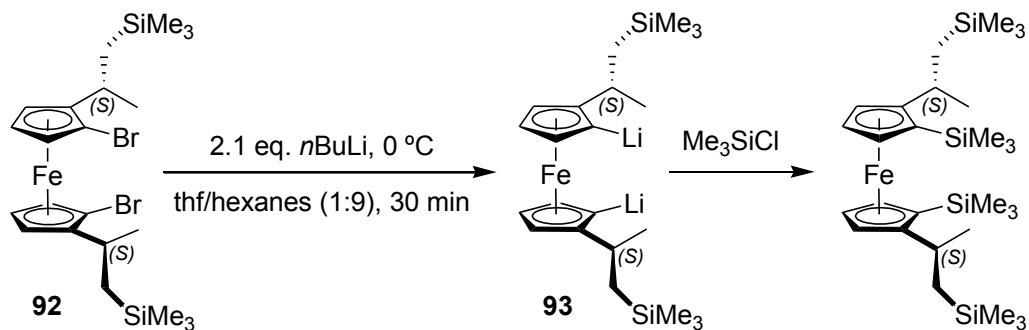
Table 2-1. Crystal and structural refinement data for **92**.

	92
empirical formula	C ₂₂ H ₃₆ Br ₂ FeSi ₂
fw	572.36
cryst. size / mm³	0.240 x 0.200 x 0.150
cryst. system, space group	orthorhombic, <i>P</i> 2 ₁ 2 ₁ 2 ₁
Z	4
a / Å	6.9388(2)
b / Å	16.7638(5)
c / Å	22.0514(7)
α / °	90
β / °	90
γ / °	90
volume / Å³	2565.03(13)
ρ_{calc} / mg m⁻³	1.482
temperature / K	173(2)
μ_{calc} / mm⁻¹	3.803
θ range / °	3.1 to 27.98
reflns collected / unique	7807 / 6870
absorption correction	multi-scan
data / restraints / params	7807 / 0 / 252
goodness-of-fit	1.018
R₁ [I > 2 σ(I)]^a	0.0343
wR₂ (all data)^a	0.0571
largest diff. peak and hole	0.341
Δρ_{elect} / [e Å⁻³]	-0.457

$$^a R_1 = [\Sigma||F_o| - |F_c||] / [\Sigma|F_o|] \text{ for } [F_o^2 > 2\sigma(F_o^2)], wR_2 = \{[\Sigma w(F_o^2 - F_c^2)^2] / [\Sigma w(F_o^2)^2]\}^{1/2} [\text{all data}].$$

The dilithiation of **92**, following the same lithium-bromine exchange procedure¹²⁸ used for other dibromoferrocene derivatives, was tested.¹²² The dilithioferrocene **93** was quenched with Me₃SiCl and the dilithiation was found to be quantitative (Scheme 2-8). Despite **92** containing some amount of another stereoisomer, the reaction of **93** with *i*Pr₂NBCl₂ was performed to observe the effects of the larger alkyl group on salt-metathesis, which will be discussed later (Chapter 2.2).

Scheme 2-8. Test dilithiation of the dibromoferrocene derivative **92**.



2.2 Dibromoferrocene Derivatives as Precursors to Strained Bora[1]ferrocenophanes

As mentioned earlier, when salt-metathesis reactions were performed between various dibromoferrocene derivatives and amino(dichloro)boranes, specific ratios of bora[1]FCPs and 1,1'-bis(boryl)ferrocenes would be obtained, depending on the starting materials that were used.¹²⁵ It was demonstrated that the bulkiness of the alkyl groups on the ferrocene unit affected the outcome of the salt-metathesis reactions. Therefore, I set out to understand how the sterics on the ferrocene unit affects salt-metathesis reactions by synthesizing dibromoferrocene derivatives with various alkyl groups (Chapter 2.1). The results of the salt-metathesis reactions of dibromoferrocenes **88** and **92** with *i*Pr₂NBCl₂ (Chapter 2.2.2), its mechanism (Chapter 2.2.3), as well as conformational analyses of **78**, **88**, and **92** using DFT calculations (Chapter 2.2.4) will be discussed.

2.2.1 Author Contribution

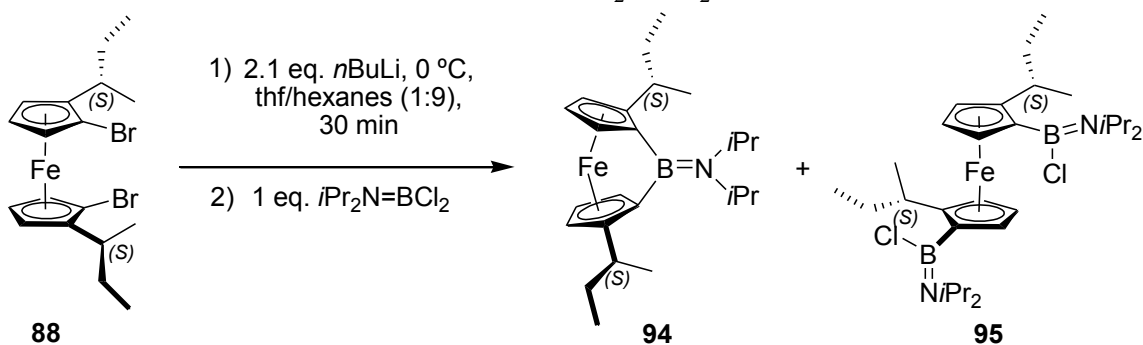
I worked with two colleagues to complete this project. I synthesized the dibromoferrocene derivatives **88** and **92**, and Elaheh Khozeimeh Sarbisheh synthesized the dibromoferrocene derivative **96**, which were all synthesized to test the speculations made earlier (Chapter 2.1). Hridaynath Bhattacharjee performed the salt-metathesis reactions of **88**, **92**, and **96** with *i*Pr₂NBCl₂ and measured their respective product ratios. To ensure consistency with these new results, the salt-metathesis reactions of **78** and **79** with *i*Pr₂NBCl₂ were repeated by Hridaynath Bhattacharjee to make sure the product ratios of all the salt-metathesis reactions were comparable.

2.2.2 Salt-Metathesis Reactions of Dibromoferrocene Derivatives

The outcome of salt-metathesis reactions between dibromoferrocene derivatives and amino(dichloro)boranes are affected by the alkyl groups on the ferrocene unit. In particular, it is believed that the R group that orients itself perpendicular to the Cp rings determines the ratios of

bora[1]FCPs and 1,1'-bis(boryl)ferrocenes that are obtained; whereas the R group that is roughly in the same plane as the Cp rings has little to no effect on the outcome of salt-metathesis reactions.¹²⁵ To test this theory, dibromoferrocenes **88** and **92** were employed in salt-metathesis reactions with $i\text{Pr}_2\text{NBCl}_2$. All salt-metathesis reactions were performed following the same procedure reported by Müller *et al.* for dibromoferrocenes **78** and **79**.^{122, 125} As expected, the salt-metathesis reaction between **88** and $i\text{Pr}_2\text{NBCl}_2$ produced a mixture of bora[1]FCP **94** and 1,1'-bis(boryl)ferrocene **95** (Scheme 2-9).

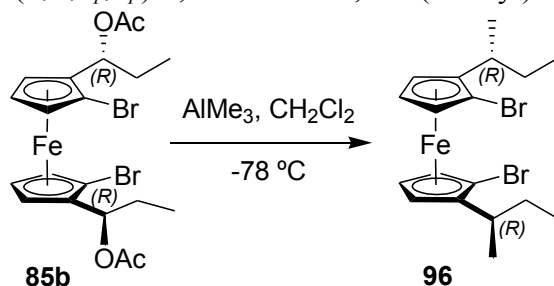
Scheme 2-9. Salt-metathesis reaction of **88** with $i\text{Pr}_2\text{NBCl}_2$.



As discussed earlier, it is proposed that the size of the R group that is perpendicular to the Cp rings influences the resulting ratios of bora[1]FCPs to 1,1'-bis(boryl)ferrocenes in salt-metathesis reactions with $i\text{Pr}_2\text{NBCl}_2$. Therefore, the salt-metathesis reactions of **79** and **88** with $i\text{Pr}_2\text{NBCl}_2$ should have the same product ratios since both **79** and **88** have ethyl groups that are perpendicular to the Cp rings. The ratio of bora[1]FCPs (**86b**, **94**) and 1,1'-bis(boryl)ferrocenes (**87b**, **95**) were found to be 1.0:0.27 and 1.0:0.30 for the reactions of **79** and **88** with $i\text{Pr}_2\text{NBCl}_2$ respectively; determined by ^1H NMR spectroscopy from sample aliquots from reaction mixtures after 20 minutes. The product ratio for **79** showed a slightly higher yield of bora[1]FCP to 1,1'-bis(boryl)ferrocene compared to **88**; however, the yield of bora[1]FCP to 1,1'-bis(boryl)ferrocene was much higher for **88** than it was for **78** (1.0:0.51). These results support the speculation that the

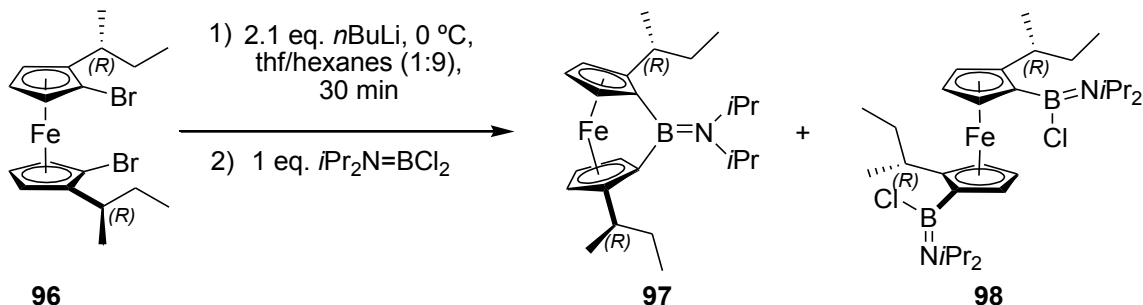
size of the R group that is perpendicular to the Cp rings is the main influence on the outcome of salt-metathesis reactions. To confirm that the R group that is roughly in the same plane as the Cp rings has a minimal effect on the result of salt-metathesis reactions, the dibromoferrocene derivative **96** was prepared (Scheme 2-10).

Scheme 2-10. Synthesis of (*R,R,S_p,S_p*)-1,1'-dibromo-2,2'-di(2-butyl)ferrocene (**96**).



After **96** was successfully synthesized, the salt-metathesis reaction of **96** with $i\text{Pr}_2\text{NBCl}_2$ was performed and yielded the expected mixture of bora[1]FCP **97** and 1,1'-bis(boryl)ferrocene **98** (Scheme 2-11).

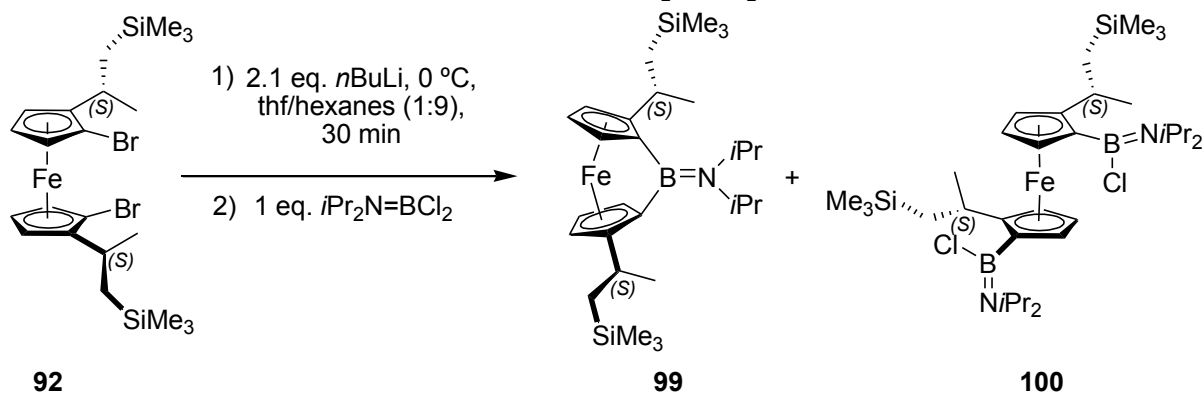
Scheme 2-11. Salt-metathesis reaction of **96** with $i\text{Pr}_2\text{NBCl}_2$.



The ratio between **97** and **98** was found to be 1.0:0.49, which is a slight improvement over the ratio observed between **86a** and **87a** (1.0:0.51) from the salt-metathesis reaction between **78** and $i\text{Pr}_2\text{NBCl}_2$. When comparing the effect of the two different R groups, it can be seen that the R group that is roughly in the same plane as the Cp rings has a very minimal effect on the outcome of salt-metathesis reactions, whereas the R group that is perpendicular to the Cp rings has a more

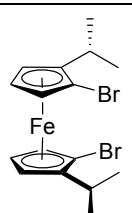
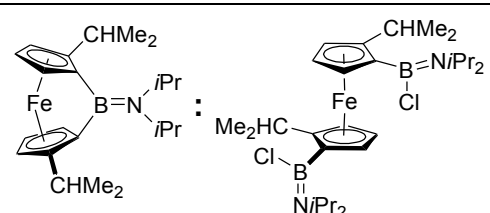
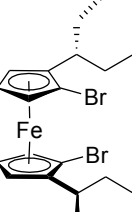
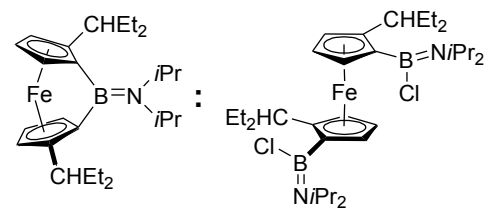
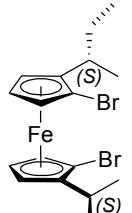
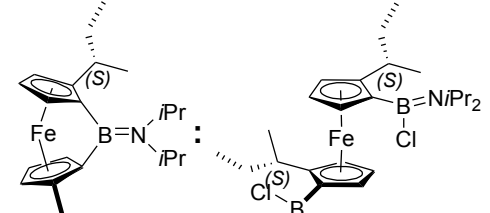
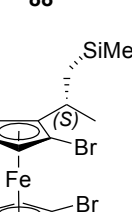
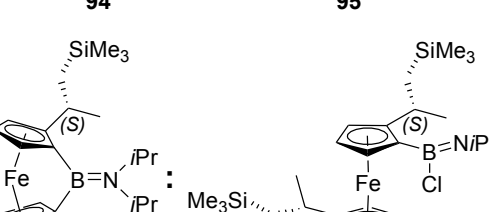
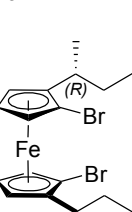
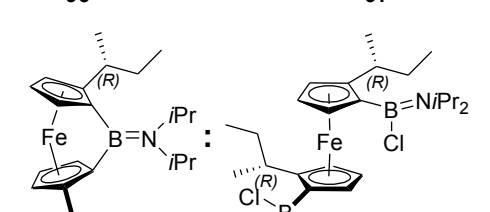
drastic effect. Therefore, the yield of bora[1]FCPs can mainly be improved by changing the bulkiness of the R groups that are perpendicular to the Cp rings. For this reason, as described before, dibromoferrocene derivative **92** was prepared in attempts to improve the yield of bora[1]FCPs (Scheme 2-7). The salt-metathesis reaction of **92** with $i\text{Pr}_2\text{NBCl}_2$ produced a mixture of bora[1]FCP **99** and 1,1'-bis(boryl)ferrocene **100** (Scheme 2-12).

Scheme 2-12. Salt-metathesis reaction of **92** with $i\text{Pr}_2\text{NBCl}_2$.



Surprisingly, the ratio between bora[1]FCP **99** and 1,1'-bis(boryl)ferrocene **100** was found to be 1.0:0.38. It was expected that the salt-metathesis reaction between **92** and $i\text{Pr}_2\text{NBCl}_2$ would yield a higher product ratio of **99** to **100** compared to the product ratios observed for dibromoferrocenes **79** (1.0:0.27) or **88** (1.0:0.30), instead the opposite occurred. In order to understand this surprising result, the mechanism of salt-metathesis reactions with (amino)boranes (Chapter 2.2.3) as well as the conformational analyses of dibromoferrocenes **78**, **88**, and **92** using DFT calculations (Chapter 2.2.4) will be discussed. The ratios between all bora[1]FCPs and 1,1'-bis(boryl)ferrocene species for the salt-metathesis reactions between dibromoferrocene derivatives **88**, **92**, and **96**, as well as the published derivatives **78** and **79**, with $i\text{Pr}_2\text{NBCl}_2$ are summarized in Table 2-2.

Table 2-2. Measured product ratios of bora[1]FCPs and 1,1'-bis(boryl)ferrocenes.

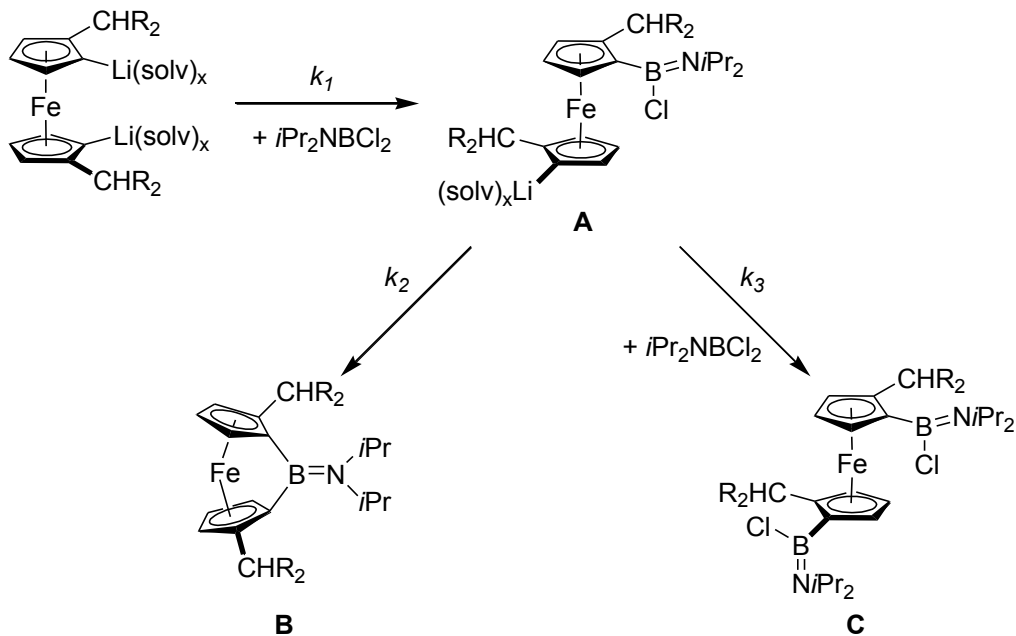
Dibromoferrocene Derivative Used	Products	Product Ratios ^a
 78	 86a : 87a	1.0 : 0.51 ^b (1.0 : 0.59) ^c
 79	 86b : 87b	1.0 : 0.27 ^b (1.0 : 0.30) ^c
 88	 94 : 95	1.0 : 0.30
 92	 96 : 97	1.0 : 0.38
 96	 97 : 98	1.0 : 0.49

^a Approximate ratios determined by ¹H NMR spectroscopy (sample aliquots taken from reaction mixture after 20 min). ^b New values determined by Hridaynath Bhattacharjee. ^c Values obtained from *J. Chem.-Eur. J.* **2014**, *49*, 16320-16330.

2.2.3 Mechanism of Salt-Metathesis Reactions with Aminoboranes

In order to understand how sterics play a role in the outcome of the salt-metathesis reactions of ferrocene derivatives with $i\text{Pr}_2\text{NBCl}_2$, one must review its reaction mechanism (Scheme 2-13). The formation of lithium chloride in these reactions is irreversible, therefore, the formation of all products is controlled by kinetics. The first step in this mechanism is the reaction of a dilithioferrocene derivative molecule with an $i\text{Pr}_2\text{NBCl}_2$ molecule to produce a monoborylated intermediate (**A**). After formation of intermediate **A**, it can either undergo intramolecular ring-closure to form bora[1]FCP **B**, or react intermolecularly with a second $i\text{Pr}_2\text{NBCl}_2$ molecule to produce 1,1'-bis(boryl)ferrocene **C**.

Scheme 2-13. Mechanism of salt-metathesis reactions of ferrocene derivatives with $i\text{Pr}_2\text{NBCl}_2$.



Müller *et al.* studied this mechanism thoroughly and proposed three different factors that affect the rates of the formation of **B** and **C**.¹²⁵ The first factor that was proposed to affect this mechanism was the concentrations of $i\text{Pr}_2\text{NBCl}_2$. It is believed that the rate of **A** to ring-close to form **B** is unaffected by the concentration of $i\text{Pr}_2\text{NBCl}_2$; whereas the rate of the formation of **C** increases with higher concentrations of $i\text{Pr}_2\text{NBCl}_2$. The second factor that is believed to affect the rates of these reactions is the temperature of the reaction mixture. Elevated temperatures greatly increase the rate of the formation of **B** because the activation barrier for ring-closure is higher than the reaction of **A** with a second equivalent of $i\text{Pr}_2\text{NBCl}_2$ to produce **C**, assuming both reactions have similar steric influences. Lastly, it is speculated that the bulkiness of the alkyl groups on the ferrocene unit has an affect on the rates of these reactions. The rate constants of ring-closure to form **B** (k_2) is relatively unaffected by the bulkiness of the alkyl groups, whereas the rate constants for the formation of **C** (k_3) decreases as the bulkiness of the alkyl groups increases. In particular, it was speculated that the bulkiness of the R group that is oriented perpendicular to the Cp ring affects the rate constant k_3 , decreasing the rate of formation of **B** with bulkier R groups in this position. The first two factors are controlled by the conditions of the salt-metathesis reactions, whereas the last factor is dependent on the properties of the starting materials; i.e., the sterics.

The salt-metathesis reactions that were investigated in Chapter 2.2.2 only look at the steric influences on the formation of bora[1]FCPs. The concentrations of $i\text{Pr}_2\text{NBCl}_2$ as well as the reaction temperatures were all held constant and should not influence the formation of bora[1]FCPs for the various dibromoferrocene derivatives. Based on what is known about the effects of sterics on salt-metathesis reactions, dibromoferrocene derivatives with bulkier R groups that are perpendicular to the Cp rings should have higher ratios of bora[1]FCPs to 1,1'-bis(boryl)ferrocenes. Looking at the dibromoferrocenes in Table 2-2, one could predict which

compounds would have higher ratios of bora[1]FCPs to 1,1'-bis(boryl)ferrocenes based on the bulkiness of the alkyl groups on the ferrocene derivatives (Figure 2-2a). However, after performing all of the salt-metathesis reactions, the product ratios did not follow the predicted trend (Figure 2-2b). As the dibromoferrocene derivative **92** did not produce the highest product ratio, DFT calculations were performed to understand the steric interactions in **92** (Chapter 2.2.4).

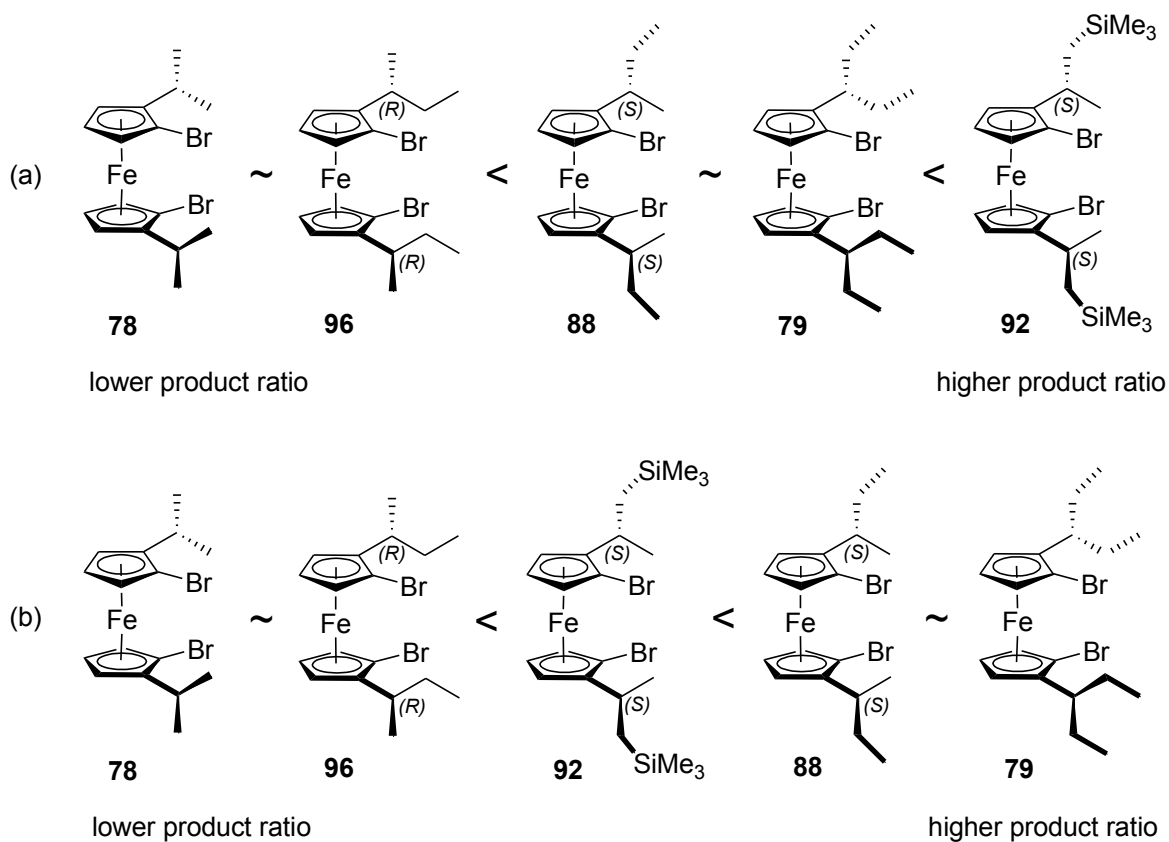


Figure 2-2. Dibromoferrocene derivatives in increasing order of product ratios (bora[1]FCPs to 1,1'-bis(boryl)ferrocenes) of salt-metathesis with $i\text{Pr}_2\text{NBCl}_2$: (a) order predicted by sterics, (b) order observed experimentally.

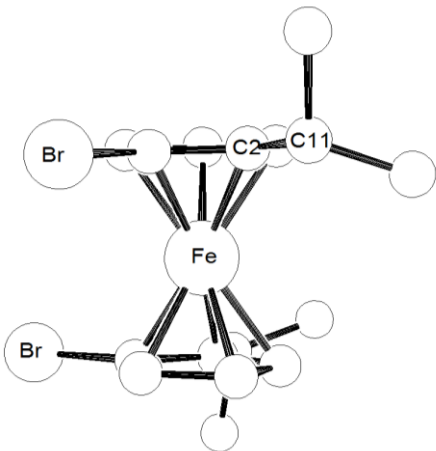
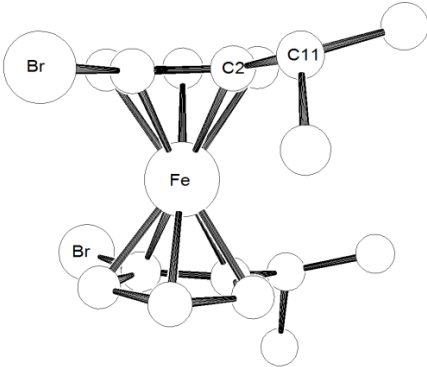
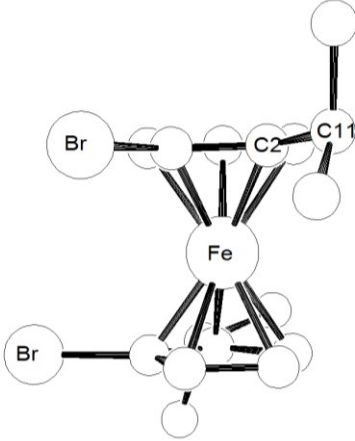
2.2.4 DFT Calculations

To gain a better understanding of how the steric interactions of the alkyl groups in dibromoferrocene derivatives affect the outcome of salt-metathesis reactions, a series of

conformational analyses of **78**, **88**, and **92** using DFT calculations were performed. All calculations were performed by Dr. Jens Müller using the B3LYP/6-31G(d) level of theory for all calculations (see Experimental Section for details).

To confirm the positions of the two R groups with respect to the Cp rings, a conformational analysis of **78**, with respect to a rotation of one of the isopropyl groups (C2-C11 bond) was performed. After observing all of the possible rotations around the C2-C11 bond, the calculations determined three different conformers of **78**, conformers **78_A**, **78_B**, and **78_C**. Using the relative Gibbs free energies calculated for each conformer under standard conditions (T = 298.15 K, P = 1 atm), the approximate amount of each conformer was calculated to be 98.5, 0.5, and 1.0% for **78_A**, **78_B**, and **78_C** respectively (Table 2-3). From these calculations, it can be concluded that **78_A** is the most stable conformation for the isopropyl groups in **78**, which agree with the conformation of the isopropyl groups observed in the crystal structure of **78**.¹²² This makes sense since **78_A** is the only conformation where unfavourable interactions are minimized by orienting both of the R groups away from the bromine and iron atoms.

Table 2-3. Calculated conformers of **78** and distributions of conformers through the rotation of the C2-C11 bond. Hydrogens atoms are omitted for clarity.

Conformer	Distribution of Molecules (%)
78_A 	98.5
78_B 	0.5
78_C 	1.0

Due to the highly unfavourable interactions of the isopropyl groups in conformers **78B** and **78C**, it can be assumed that all dibromoferrocene derivatives (**78**, **79**, **88**, **92**, and **96**) will adopt a similar conformation as **78A**, with respect to the rotation of the bonds between the alkyl groups and the Cp rings. To understand the surprising result that was obtained from the salt-metathesis reaction between **92** and *i*Pr₂NBCl₂ (Scheme 2-12), DFT calculations were used to compare the structures of **88** and **92**.

The conformational analysis of **88**, looking at the rotation around the C11-C12 bond, determined three different conformers of **88**, conformers **88A**, **88B**, and **88C**. Using the Gibbs free energies calculated for each conformer under standard conditions (T = 298.15 K, P = 1 atm), the approximate amount of each conformer was determined to be 38.8, 27.2, and 34.0% for **88A**, **88B**, and **88C** respectively (Table 2-4). From these calculations, it can be seen that there is no significant orientation preference for the methyl group attached to C12, and the distribution of these conformers under standard conditions are relatively equal.

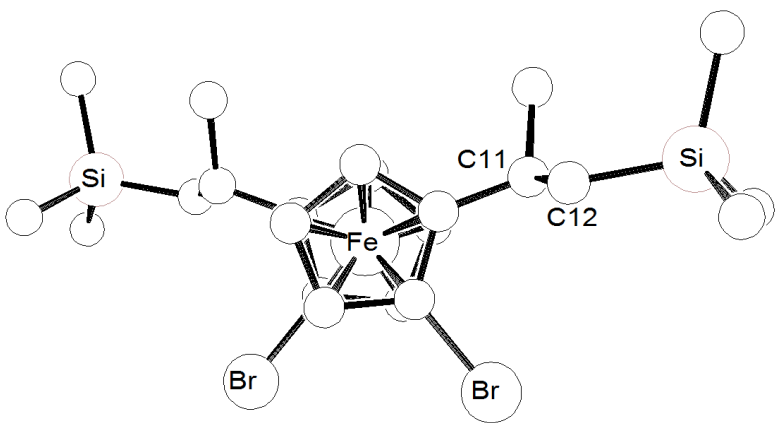
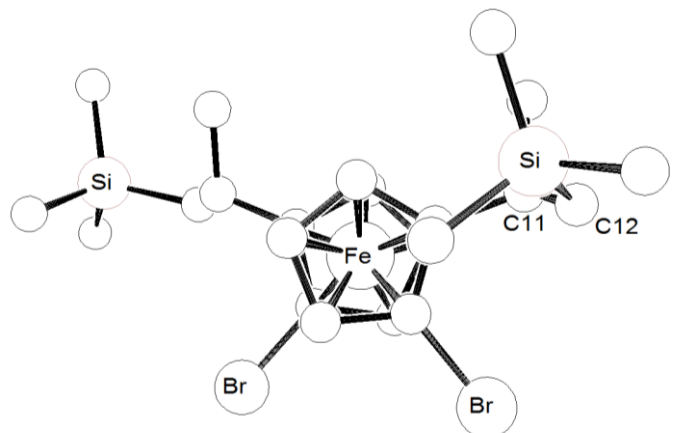
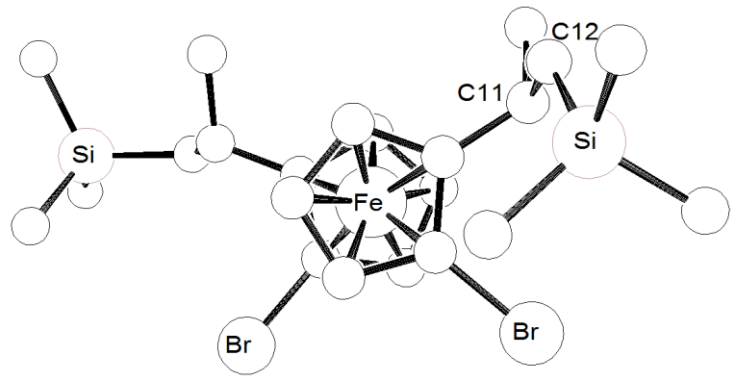
Table 2-4. Calculated conformers of **88** and distributions of conformers through the rotation of the C11-C12 bond. Hydrogens atoms are omitted for clarity.

	Conformers	Distribution of Molecules (%)
88A		38.8
88B		27.2
88C		34.0

The conformational analysis of **92**, looking at the rotation around the C11-C12 bond, determined three different conformers of **92**, conformers **92_A**, **92_B**, and **92_C**. Using the Gibbs free energies ($T = 298.15\text{ K}$, $P = 1\text{ atm}$), the approximate amount of each conformer was determined to be 70.6, 17.7, and 11.7% for **92_A**, **92_B**, and **92_C** respectively (Table 2-4). Unlike the calculations for the conformations of **88**, the calculations of the conformations of **92** showed a preference for conformer **92_A**. In this conformation, the bulky CH_2SiMe_3 group is oriented away from the Cp ring and the bromine atom. This helps to explain the unexpected result from the salt-metathesis reaction between **92** and $i\text{Pr}_2\text{NBCl}_2$.

In salt-metathesis reactions, the dilithioferrocene molecule reacts with $i\text{Pr}_2\text{NBCl}_2$ to give a monoborylated intermediate (see Scheme 2-13). This species can either react with a second $i\text{Pr}_2\text{NBCl}_2$ molecule to form a 1,1'-bis(boryl)ferrocene, or undergo ring-closure to yield a bora[1]FCP (see Chapter 2.2.3). In order to increase the ratio between bora[1]FCPs and 1,1'-bis(boryl)ferrocene species in salt-metathesis reactions using sterics, the steric bulk must be placed as close as possible to the site where salt-metathesis occurs. To accomplish this, it is believed that dibromoferrocene precursors with bulky alkyl groups close to the bromine atoms are required. As the steric protection around the bromine atoms increases, the rate of a second $i\text{Pr}_2\text{NBCl}_2$ molecule reacting with the ferrocene moiety decreases, thus decreasing the amount of 1,1'-bis(boryl)ferrocenes and increasing the amount of bora[1]FCPs. Dibromoferrocene **92** has bulky alkyl groups attached to the ferrocene unit, however, conformational analysis of **92** using DFT calculations show that the bulky CH_2SiMe_3 groups have a strong preference to orient itself away from the bromine atoms. Whereas the conformational analysis of **88** showed that the methyl group had no strong preference to orient itself away from the bromine atoms. Assuming that the

Table 2-5. Calculated conformers of **92** and distributions of conformers through the rotation of the C11-C12 bond. Hydrogens atoms are omitted for clarity.

	Conformers	Distribution of Molecules (%)
92A		70.6
92B		17.7
92C		11.7

conformation of the alkyl groups behave similarly in the transition state, **88** provides more steric protection, compared to **92**, to the site where salt-metathesis occurs. Therefore, it can be understood why the ratio observed between bora[1]FCP and 1,1'-bis(boryl)ferrocene from the salt-metathesis reaction of **92** and $i\text{Pr}_2\text{NBCl}_2$ was lower than expected, compared to the reaction of **88** with $i\text{Pr}_2\text{NBCl}_2$.

The DFT calculations show how the steric bulk on the alkyl groups of dibromoferrocene derivatives should be tuned to increase the ratio of bora[1]FCPs to 1,1'-bis(boryl)ferrocenes in salt-metathesis reactions. The R groups that are perpendicular to the Cp rings must not be able to orient its bulk away from the bromine atoms, since this will increase the formation of 1,1'-bis(boryl)ferrocenes in salt-metathesis reactions. To combat this, the R groups must be bulked up to force the alkyl groups to interact with the bromine atoms. For example, replacing the CH_2SiMe_3 groups in **92** with $\text{CH}(\text{SiMe}_3)_2$ (**101**) or $\text{C}(\text{SiMe}_3)_3$ (**102**) groups forces an SiMe_3 group to interact with the bromine atoms, potentially increasing the ratio of bora[1]FCPs to 1,1'-bis(boryl)ferrocenes in salt-metathesis reactions. Alternatively, replacing the CH_2SiMe_3 groups in **92** with either $i\text{Pr}$ (**103**) or $t\text{Bu}$ (**104**) groups could also potentially increase this product ratio (Figure 2-3). However, these derivatives could be hard to obtain synthetically due to the difficulty of preparing the bulky trialkylaluminum reagents required to synthesize these compounds.

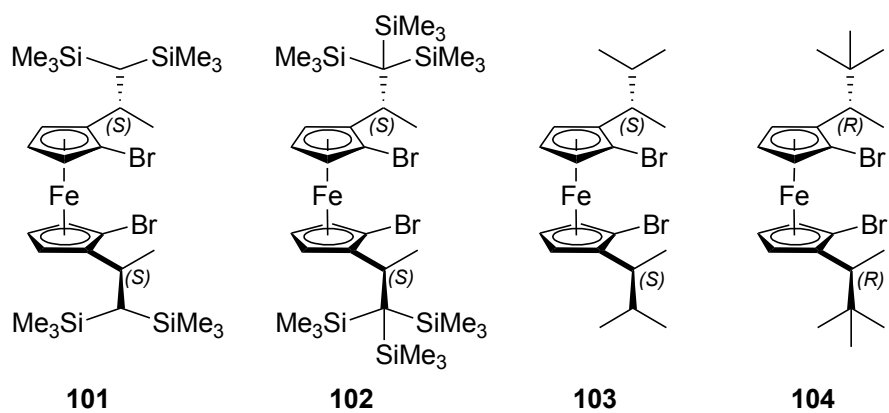
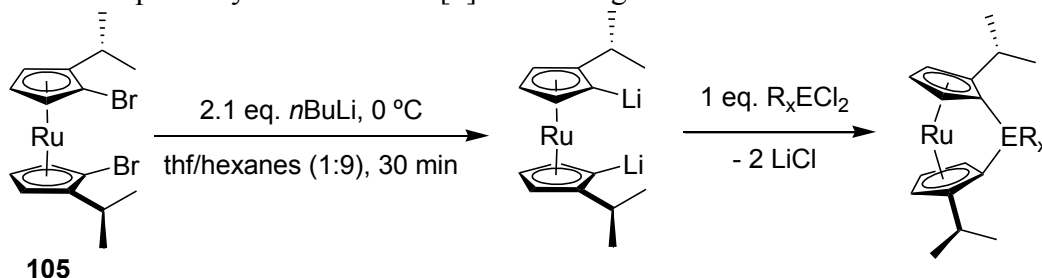


Figure 2-3. Dibromoferrocene derivatives that could potentially increase product ratios between bora[1]FCPs and 1,1'-bis(boryl)ferrocenes in salt-metathesis reactions.

2.3 Synthesis of C₂-Symmetrical Dibromoruthenocene Derivatives

As discussed earlier (Chapter 1.1.2), there are a large number of [1]FCPs, with a wide variety of bridging elements, that have been prepared, whereas, only a total of five [1]RCPs have been successfully synthesized to date.^{13, 33, 56} In ruthenocene (3.68 Å), the Cp rings are further apart when compared to ferrocene (3.32 Å), which is due to the larger size of the ruthenium atom. Therefore, the Cp rings in ruthenocene must tilt more compared to ferrocene, to accommodate a bridging element to make a [1]RCP. To synthesize [1]RCPs, bridging elements with extremely bulky ligands have been employed to help favour the formation of [1]RCPs. As mentioned earlier (Chapter 2.1), the Müller group had found much success in preparing [1]FCPs when employing ferrocene derivatives with alkyl substituents in the α -position with respect to the bridging element.^{122, 125} Therefore, the second objective of this Master's work was to synthesize a dibromoruthenocene analog (**105**) of **78**, following the synthetic pathway in Scheme 2-1, to employ in salt-metathesis reactions to obtain new [1]RCPs (Scheme 2-14).

Scheme 2-14. Proposed synthesis of new [1]RCPs using a dibromoruthenocene derivative (**105**).

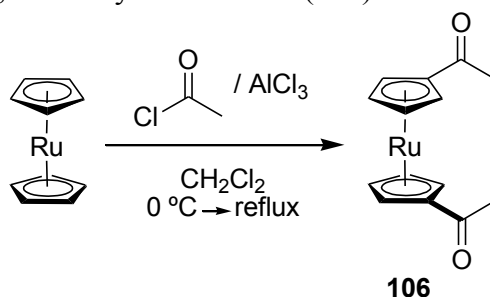


The synthesis of dibromoruthenocene **105** proved to be more difficult than expected and was not completed. Details of the attempted synthesis of **105** and the future of this project will be discussed in the following subsections.

2.3.1 Synthesis of 1,1'-Diacetylruthenocene

Following the synthetic pathway laid out in Scheme 2-1, the first step to synthesize **105** is preparing 1,1'-diacetylruthenocene (**106**), via a Friedel-Crafts acylation (Scheme 2-15).^{131, 132} When the reaction was performed the same way as for its ferrocene derivative, the conversion of ruthenocene to **106** was fairly low (reported yield: 34%);¹¹⁶ however, this could be improved by heating the reaction mixture to reflux for an extended period of time. After purification by column chromatography, **106** was obtained with a maximum yield of 55%. The ¹H NMR spectrum of **106** confirmed the presence of the acetyl groups with a singlet at $\delta = 2.20$ ppm.

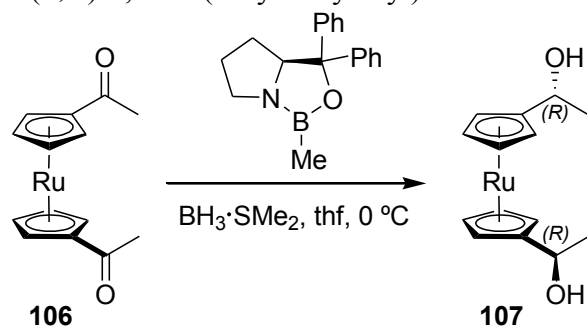
Scheme 2-15. Synthesis of 1,1'-diacetylruthenocene (**106**).



2.3.2 Synthesis of (*R,R*)-1,1'-Bis(α -hydroxyethyl)ruthenocene

The next step in the synthesis of **105** is the asymmetric reduction of **106** to produce (*R,R*)-1,1'-bis(α -hydroxyethyl)ruthenocene (**107**). In 1998, Knochel *et al.* adapted the asymmetric reduction method that Corey and Itsuno developed for ketones, to reduce several metallocenyl ketones to yield nearly enantiomerically pure metallocenyl diols with small amounts of *meso* diastereomers.¹¹⁶ This method has also been applied to selectively reduce **106** to **107** (Scheme 2-16); however, the reduction of **106** is not as selective as it was for **80a**, producing a diastereometric ratio *dl:meso* of 87:13.

Scheme 2-16. Synthesis of (*R,R*)-1,1'-bis(α -hydroxyethyl)ruthenocene (**107**).

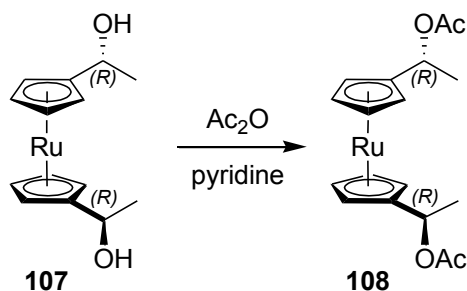


The diol **107** was isolated by column chromatography in 89% yield, however, as noted by Knochel, the *meso* isomer cannot be easily removed through column chromatography. Nevertheless, the *meso* isomer should be easier to remove in the later stages of the synthesis of **105**. The obtained 1H NMR spectroscopic data of **107** matched literature values.

2.3.3 Synthesis of (*R,R*)-1,1'-Bis(α -N,N-dimethylaminoethyl)ruthenocene

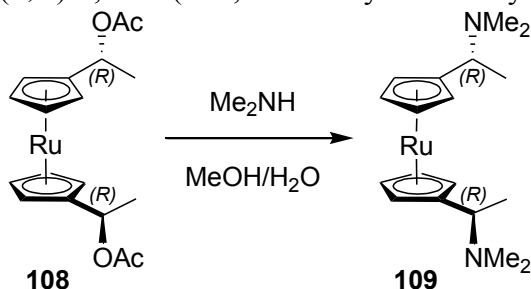
The next step in the synthetic pathway is to prepare (*R,R*)-1,1'-bis(α -N,N-dimethylaminoethyl)ruthenocene (**109**). As discussed earlier (Chapter 1.3), the NMe_2 moiety in “Ugi’s amine” can be replaced through nucleophilic substitution reactions with full retention of configuration, this is true for other heteroatoms in α -positions of metallocenes. In 1998, Knochel *et al.* showed that this can be applied to metallocenyl diols after esterification, which has not yet been performed on **107**.¹¹⁶ The diol **107** was esterified by reacting with acetic anhydride in pyridine to yield the new diacetate **108** (Scheme 2-17).

Scheme 2-17. Esterification of diol **107**.



The diacetate **108** was isolated by removing all of the volatiles under high vacuum. It was found that no further purification was needed for **108**, and the same reaction vessel could be used to substitute the acetate groups with NMe₂ moieties. The diacetate **108** was reacted with dimethylamine in a water/methanol solvent mixture to yield (*R,R*)-1,1'-bis(α -N,N-dimethylaminoethyl)ruthenocene (**109**) (Scheme 2-18). After aqueous work-up, **109** was obtained in a good yield (87%). The ¹H NMR spectrum of **109** showed that the reactions occurred with full retention of configuration.

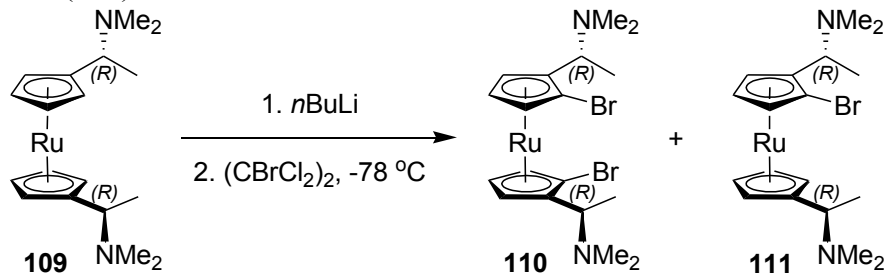
Scheme 2-18. Synthesis of (*R,R*)-1,1'-bis(α -N,N-dimethylaminoethyl)ruthenocene (**109**).



2.3.4 Dilithiation of (*R,R*)-1,1'-Bis(α -N,N-dimethylaminoethyl)ruthenocene

Continuing the synthesis of **105**, the next step is to prepare (*R,R,S_p,S_p*)-1,1'-dibromo-2,2'-bis(α -N,N-dimethylaminoethyl)ruthenocene (**110**). As discussed earlier (Chapter 2.1), the “double Ugi’s amine” can be cleanly dilithiated to yield only one 1,1'-2,2'-tetrasubstituted ferrocene isomer,¹¹⁶ this dilithiated compound is then brominated to yield a dibromoferrocene derivative (Scheme 2-1). Since **109** is analogous to the ferrocene “double Ugi’s amine” **83a**, it was assumed that **109** can undergo the same reactions to give the dibromoruthenocene **110**. However, after performing these reactions with **109**, significant amounts of the monobromoruthenocene **111** (~33%) were present (Scheme 2-19). Due to the difficulty of separating **110** and **111**, attempts were made to improve the conversion of **109** to **110**.

Scheme 2-19. Attempted synthesis of (*R,R,S_p,S_p*)-1,1'-dibromo-2,2'-bis(α -N,N-dimethylamino ethyl)ruthenocene (**110**).

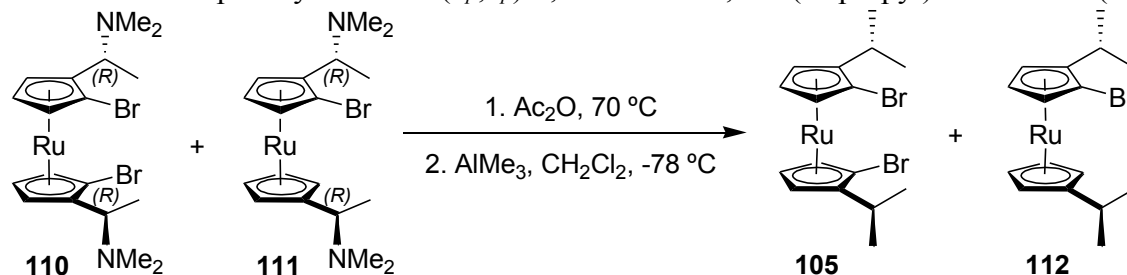


To determine if the problem with the reaction was the dilithiation or its subsequent bromination, Me_3SiCl and deuterium oxide (D_2O) were used as quenching reagents after dilithiating **109** instead of using the expensive brominating reagent. Quenching the reaction mixture with Me_3SiCl led to a messy ^1H NMR spectrum containing several by-products. Using D_2O as a quenching reagent produced a cleaner ^1H NMR spectrum that clearly showed that the complete dilithiation of **109** was unsuccessful, showing that the dilithiation of **109** does not work as well as its ferrocene counterpart. When **83a** is dilithiated, the reaction mixture remains homogeneous, however, when **109** is dilithiated, a precipitate forms after approximately an hour. It is speculated that this precipitate is not completely dilithiated and as it is no longer in solution it is difficult to react further with $n\text{BuLi}$ to become completely dilithiated. To combat this, efforts to improve the conversion of **109** to **110** using different reaction times, temperatures and solvents were made, however, all attempts were unsuccessful.

Despite not being able to improve the conversion of **109** to **110** or the separation of **110** and **111**, the synthesis of (*S_p,S_p*)-1,1'-dibromo-2,2'-di(isopropyl)ruthenocene (**105**) was carried out using the mixture of **110** and **111** (Scheme 2-20). This was done in hopes that the separation of the mixture obtained after substituting the NMe_2 moieties with methyl groups would be easier. The mixture was reacted with acetic anhydride at 70°C to first substitute the NMe_2 groups with acetate groups. Similar to the synthesis of **108**, the diacetate was isolated by removing all volatiles under

high vacuum and the same reaction flask could be used for the last substitution reaction. Finally, the diacetate was reacted with trimethylaluminum at -78 °C to yield a mixture of **105** and **112**. Unfortunately, it was not possible to separate the mixture to isolate the desired dibromoruthenocene **105**, and only a mixture of **105** and **112** was obtained.

Scheme 2-20. Attempted synthesis of (*S_p*,*S_p*)-1,1'-dibromo-2,2'-di(isopropyl)ruthenocene (**105**).



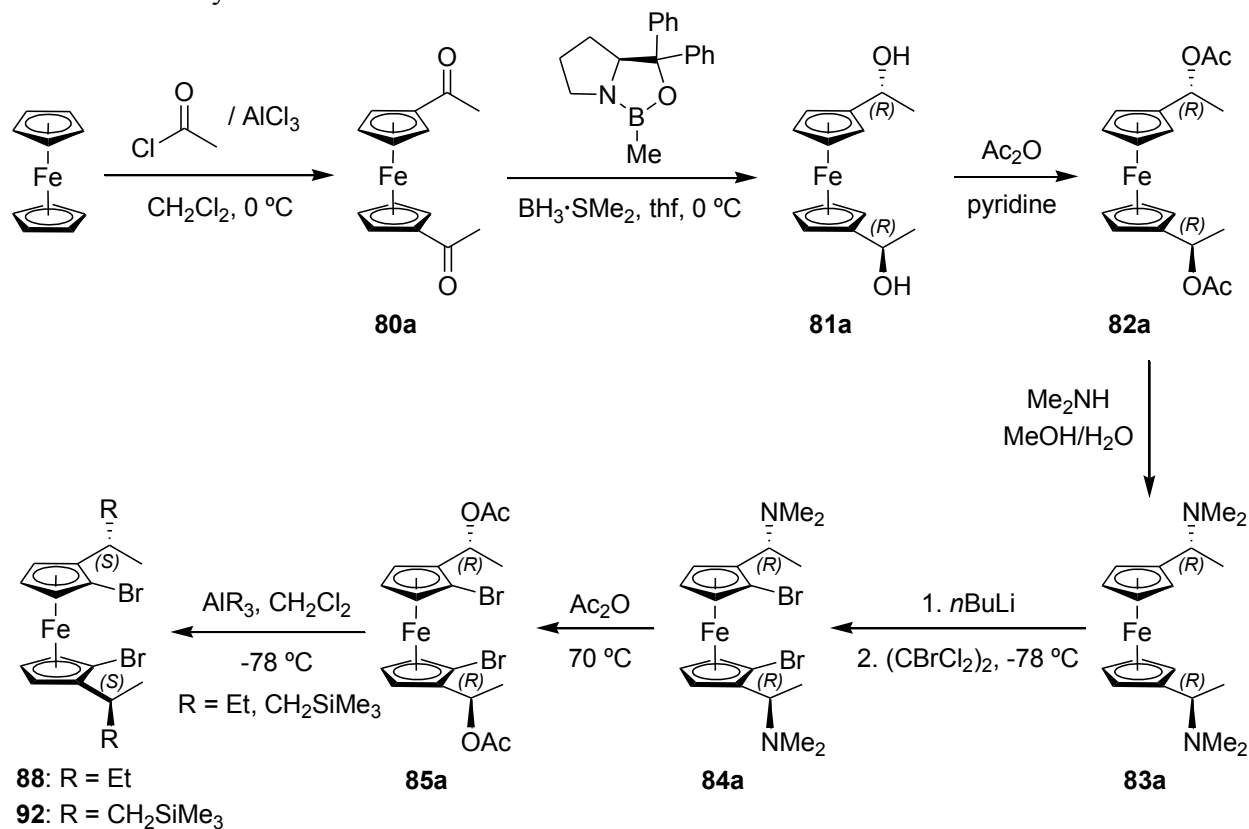
2.3.5 Future Outlook

As mentioned earlier, when compared to [1]FCPs, there are a limited number of [1]RCPs that are known in the literature. One strategy to obtain new [1]RCPs is to prepare the dibromoruthenocene derivative **105** to use as a precursor in salt-metathesis reactions. The alkyl groups on the Cp rings could potentially facilitate the formation of [1]RCPs in salt-metathesis reactions. The only hurdle in obtaining **105** is finding the correct conditions to quantitatively dilithiate **109** to synthesize the dibromoruthenocene **110**, or to find a method to separate the monobromo- and dibromoruthenocene. After solving this problem, the NMe₂ groups can be easily replaced through substitution reactions to yield **105**, which could potentially be an excellent precursor for salt-metathesis reactions for obtaining new [1]RCPs.

2.4 Alternate Pathway to C_2 -Symmetrical Dibromoferrocene Derivatives

The main aim of this Master's work was been to prepare dibromoferrocene derivatives that are suitable as precursors for salt-metathesis reactions to obtain new [1]FCPs. The C_2 -symmetrical dibromoferrocene derivatives prepared through the synthetic pathway used by the Müller group was applied for the synthesis of the new dibromoferrocenes **88** and **92** (Scheme 2-21).¹²² This method is a very long process and is not very flexible synthetically for obtaining new dibromoferrocene derivatives. There are only two points in this pathway where the alkyl groups can be altered, which require the use of certain reagents. Therefore, I set out to find an alternative method to synthesize C_2 -symmetrical dibromoferrocene derivatives suitable for preparing [1]FCPs that is shorter and allows for more synthetic flexibility.

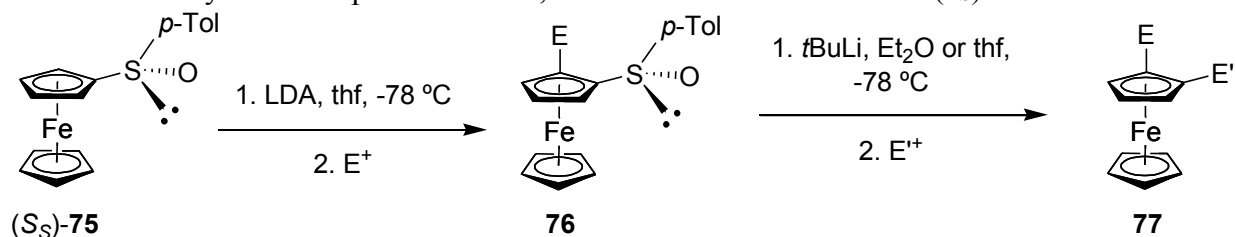
Scheme 2-21. Synthesis of dibromoferrocenes **88** and **92**.



In the synthesis of **88** and **92**, the “double Ugi’s amine” **83a** was prepared and subsequently substituted through a diastereoselective dilithiation to obtain the C_2 -symmetrical dibromoferrocene **84a**. The ODG in **83a**, i.e. the NMe_2 group, was required to place bromine atoms adjacent to the alkyl groups on the ferrocene unit. If ODGs are not present on a substituted ferrocene, the lithiation and subsequent bromination of the compound would yield a mixture of compounds with different substitution patterns. Therefore, ODGs on both Cp rings are required to synthesize dibromoferrocene derivatives with alkyl groups adjacent to the bromine atoms. Using an alternative synthetic pathway to prepare dibromoferrocene derivatives will still require ODGs on both Cp rings. As discussed earlier (Chapter 1.3.2), a wide variety of planar-chiral, 1,2-disubstituted ferrocenes have been synthesized using ferrocene derivatives with various ODGs (Figure 1-7). To obtain only one isomer of resulting 1,2-disubstituted ferrocenes, it is useful to use diastereoselective ODGs (Chapter 1.3.3). Otherwise, the racemic mixture of 1,2-disubstituted ferrocenes must be resolved through tedious methods. Therefore, to prepare C_2 -symmetrical dibromoferrocene derivatives through an alternative synthetic pathway, it would be advantageous to use diastereoselective ODGs on both Cp rings of ferrocene.

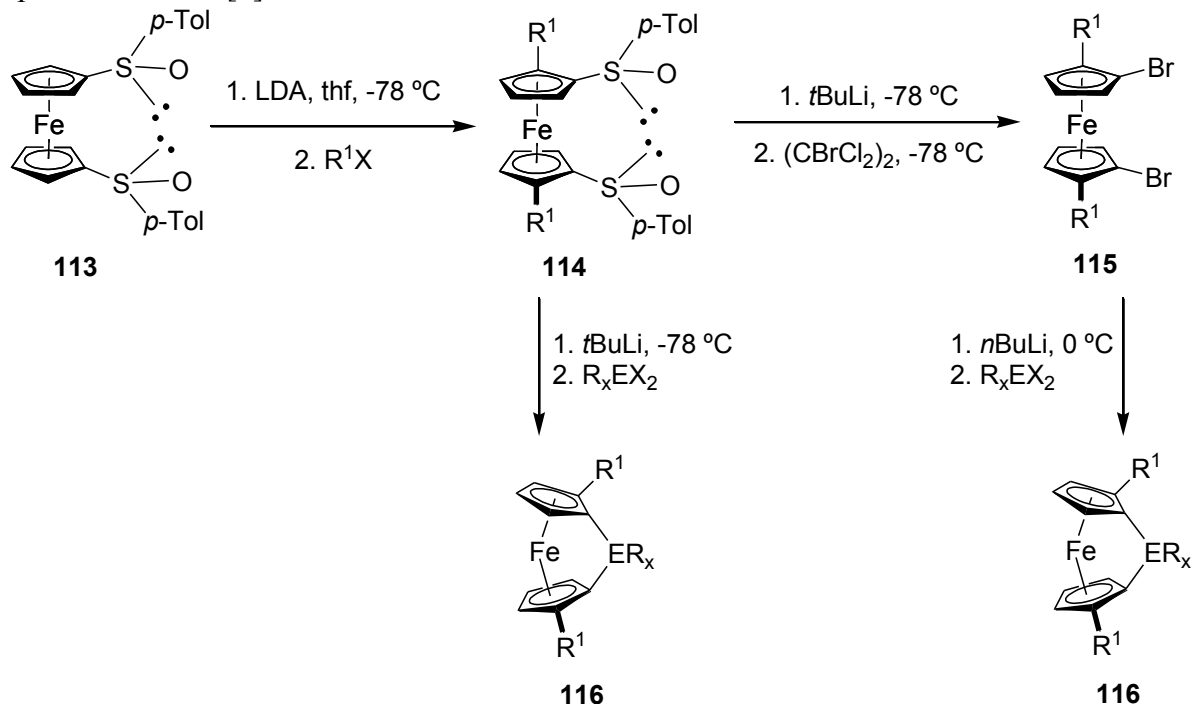
In 1990, Kagan and co-workers began to investigate the use of chiral ferrocenes (R_S)-**73** and (S_S)-**75** to prepare 1,2-disubstituted ferrocenes.¹¹⁹⁻¹²¹ Both of these compounds are very easy to prepare and it was found that both can be substituted through a diastereoselective lithiation to obtain a single planar-chiral 1,2-disubstituted ferrocene isomer with a high *de*. What is unique about these compounds, compared to other ferrocenes with ODGs, is that the *p*-tolylsulfinyl group can be removed and exchanged with an electrophile (Scheme 2-22).¹²¹

Scheme 2-22. Synthesis of planar-chiral 1,2-disubstituted ferrocenes via (*S_S*)-**75**.



Due to the simplicity of obtaining 1,2-disubstituted ferrocenes from (*R_S*)-**73** and (*S_S*)-**75**, I set out to adapt this chemistry to obtain new dibromoferrocene derivative precursors for the preparation of [1]FCPs. Targeting the synthesis of a 1,1'-disubstituted analog of (*R_S*)-**73** or (*S_S*)-**75**, e.g. **113**, can lead to the preparation of new dibromoferrocene derivatives (**115**) suitable for salt-metathesis reactions (Scheme 2-23). This synthetic pathway is much shorter than the pathway that was used to synthesize **88** and **92**, and there is potentially a wider variety of alkyl groups that can be placed on the ferrocene unit. It is possible that this synthetic pathway for preparing [1]FCPs (**116**) could be shortened by using **114**, instead of **115**, as the precursor for salt-metathesis reactions, assuming that the sulfur containing byproducts would not affect the reaction. The following subsections will discuss my efforts to prepare new dibromoferrocene derivatives using the synthetic pathway outlined in Scheme 2-23.

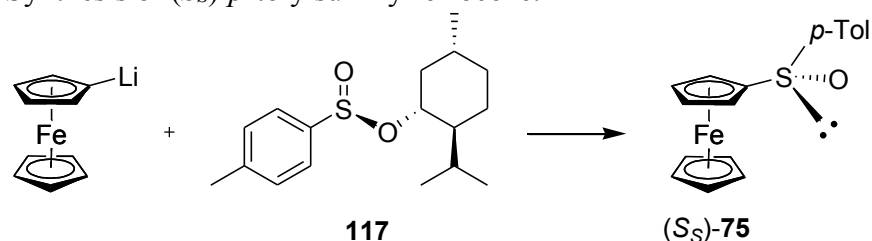
Scheme 2-23. Proposed synthetic pathway for obtaining dibromoferrocene precursors for the preparation of new [1]FCPs via **113**.



2.4.1 Synthesis of (*S,S*)-1,1'-Bis(*p*-tolylsulfinyl)ferrocene

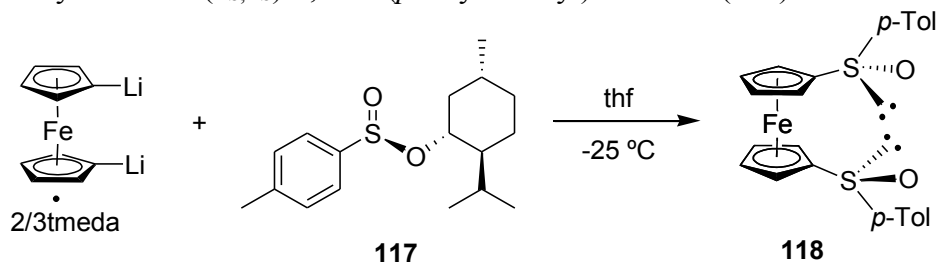
The synthesis of a 1,1'-bis(*p*-tolylsulfinyl)ferrocene (**113**) has not yet been reported in the literature, however, the preparation of ferrocenes (*R_S*)-**73** and (*S_S*)-**75** have been reported. These compounds were obtained by reacting lithioferrocene with an appropriate isomer of menthyl *p*-toluenesulfinate; for instance, (*S_S*)-**75** was obtained by reacting lithioferrocene with (*1R,2S,5R*)-(-)-menthyl (*S_S*)-*p*-tolylsulfinylate (**117**) (Scheme 2-24).¹²⁰ It should be possible to adapt the procedures for synthesizing (*R_S*)-**73** and (*S_S*)-**75** to obtain a 1,1'-bis(*p*-tolylsulfinyl)ferrocene. Due to the well-known synthesis of **117**, I decided to adapt the preparation of (*S_S*)-**75** to synthesize (*S_{S,S}*)-1,1'-bis(*p*-tolylsulfinyl)ferrocene (**118**).

Scheme 2-24. Synthesis of (*S_S*)-*p*-tolylsulfinylferrocene.



To synthesize the 1,1'-bis(*p*-tolylsulfinyl)ferrocene **118**, dilithioferrocene·2/3tmeda was added to **117** in thf at -25 °C (Scheme 2-25). The ^1H NMR spectrum of the crude reaction mixture revealed that significant amounts of the *meso* isomer had formed. In 1998, when Lagneau *et al.* attempted the synthesis of (*S_S*)-**75**, a significant amount of its enantiomer, (*R_S*)-**73** was present.¹³³ It was speculated that the chiral sulfur atom of (*S_S*)-**75** underwent inversion due to the nucleophilic attack of lithioferrocene on (*S_S*)-**75** to give (*R_S*)-**73**. This was confirmed when (*S_S*)-**75** was nearly racemized after reacting with excess lithioferrocene. Based on this study, it is believed that the synthesis of **118** yielded significant amounts of the *meso* isomer due to the nucleophilic attack of dilithioferrocene·2/3tmeda on one of the sulfur atoms of **118**. The amounts of the *meso* isomer can be significantly reduced by slowly adding dilithioferrocene·2/3tmeda to an excess of **117**. After optimizing the reaction conditions to minimize the formation of the *meso* isomer, the remaining amounts of *meso* isomer can be removed through column chromatography to yield a dark yellow solid of **118** in 39% yield. The ^1H NMR spectrum of **118** showed a singlet at 2.37 ppm and two doublets at 7.25 and 7.50 ppm, confirming the presence of the *p*-tolyl groups.

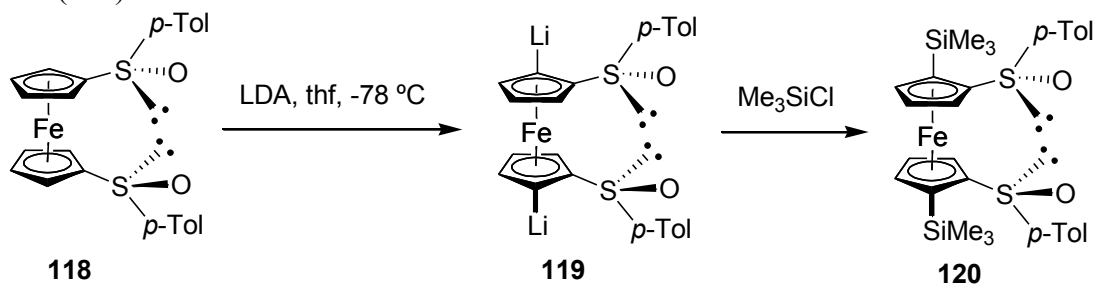
Scheme 2-25. Synthesis of (*S_SS_S*)-1,1'-bis(*p*-tolylsulfinyl)ferrocene (**118**).



2.4.2 Dilithiation of (*S,S*)-1,1'-Bis(*p*-tolylsulfinyl)ferrocene

In 1993, Kagan *et al.* reported that (*R_S*)-**73** could be used to prepare 1,2-disubstituted planar-chiral ferrocenes with a *de* ≥ 98% through a diastereoselective *ortho*-directed lithiation in thf at -78 °C using LDA (Scheme 1-40).¹²⁰ Since **118** is analogous to (*R_S*)-**73** and (*S_S*)-**75**, it should be able to be dilithiated diastereoselectively using similar reaction conditions to obtain the dilithioferrocene **119**. After obtaining **119**, it should be able to react with Me₃SiCl to yield (*S_S,S_S,S_p,S_p*)-2,2'-bis(trimethylsilyl)-1,1'-bis(*p*-tolylsulfinyl)ferrocene (**120**) (Scheme 2-26). However, initial attempts to synthesize **120** through the dilithiation of **118** were unsuccessful.

Scheme 2-26. Attempted synthesis of (*S_S,S_S,S_p,S_p*)-2,2'-bis(trimethylsilyl)-1,1'-bis(*p*-tolylsulfinyl)ferrocene (**120**).

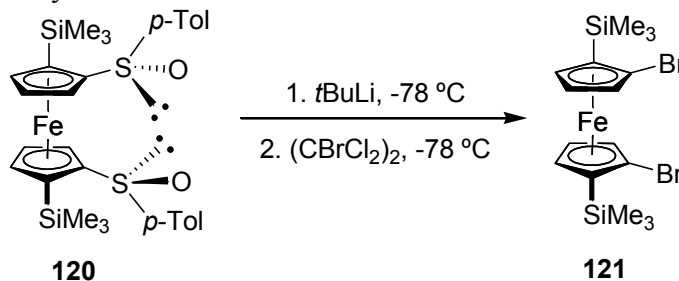


When attempting to synthesize **120**, large amounts of byproducts, including the monosilylated product, were observed in the ¹H NMR spectra of crude reaction mixtures. In order to determine if the problem with the reaction was with this dilithiation or its subsequent silylation, the reaction mixture was quenched with D₂O after dilithiation. After a series of test reactions, it was found that dilute reaction conditions were required to quantitatively dilithiate **118**. The synthesis of **120** was re-attempted using these new conditions for the dilithiation of **118**, unfortunately, **120** was only obtained successfully once on a very small scale. When the scale of the reaction was increased, a mixture of **120** and monosilylated products were obtained.

2.4.3 Future Outlook

Synthesizing new dibromoferrocene derivatives using the pathway described in Scheme 2-23 is very appealing due to its seeming simplicity and flexibility. After successfully synthesizing **118**, only two more steps are needed to obtain new dibromoferrocene derivatives through this synthetic pathway. Ferrocene **120** was successfully synthesized on one occasion, but repeating the reaction gave inconsistent results. Despite these problems, this synthetic pathway for obtaining new dibromoferrocene derivatives for the synthesis of [1]FCPs is still promising. The hurdle of this pathway is optimizing the procedure for the dilithiation of **118**. Once optimized, it will be possible to prepare **120**, leaving only one more synthetic step to synthesize the dibromoferrocene derivative **121** (Figure 2-27). Furthermore, optimizing the dilithiation of **118** potentially opens the door to the synthesis of several new dibromoferrocene derivatives.

Scheme 2-27. Proposed synthesis of dibromoferrocene **121** via ferrocene **120**.

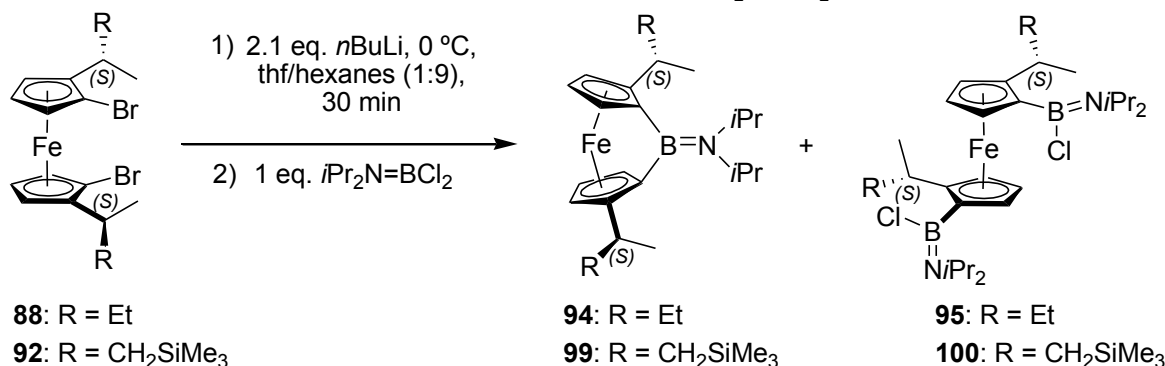


CHAPTER 3: SUMMARY AND CONCLUSIONS

3.1 Synthesis and Application of C_2 -Symmetrical Dibromoferrocene Derivatives in the Synthesis of Strained Bora[1]ferrocenophanes

For the first aim of this thesis, investigations were made into how the steric bulk on ferrocene moieties affects the outcome of salt-metathesis reactions with $i\text{Pr}_2\text{NBCl}_2$ to yield bora[1]FCPs. Following the synthetic pathway outlined in Scheme 2-1, two new dibromoferrocene derivatives, **88** and **92**, were prepared.¹²² These new compounds were successfully used in salt-metathesis reactions with $i\text{Pr}_2\text{NBCl}_2$ to yield bora[1]FCPs **94** and **99** and 1,1'-bis(boryl)ferrocenes **95** and **100** respectively (Scheme 3-1). The product ratios were measured and compared to product ratios obtained from the reaction of dibromoferrocenes **78**, **79**, and **96** with $i\text{Pr}_2\text{NBCl}_2$ ¹²⁵ to gain insight on how the steric bulk on ferrocene moieties affect the outcome of salt-metathesis reactions (see Table 2-2).

Scheme 3-1. Salt-metathesis reactions of **88** and **92** with $i\text{Pr}_2\text{NBCl}_2$.



To better understand the outcome of salt-metathesis reactions for the dibromoferrocene derivatives, the steric effects of the alkyl groups on ferrocenes **78**, **88**, and **92** were investigated through a series of conformational analyses using DFT calculations. The analyses showed that the bulky CH_2SiMe_3 groups in **92** prefer to orient themselves away from the bromine atoms on the Cp rings, whereas the Et groups in **88** have no preferred orientation. As a result, it can be understood

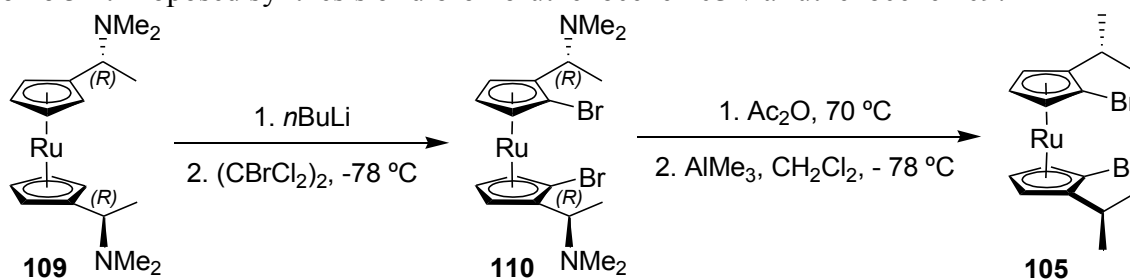
why the product ratio between bora[1]FCPs and 1,1'-bis(boryl)ferrocenes obtained from the reaction of **92** and $i\text{Pr}_2\text{NBCl}_2$ (1.0:0.38) was lower than the product ratio obtained for **88** and $i\text{Pr}_2\text{NBCl}_2$ (1.0:0.30). These calculations helped to show how the sterics of the alkyl groups on ferrocene moieties influence the product ratios of salt-metathesis reactions.

3.2 Synthesis of C_2 -Symmetrical Dibromoruthenocene Derivatives

As mentioned earlier, there are very few [1]RCPs known compared to [1]FCPs, most likely due to the larger Ru atom requiring an increased ring-tilting to obtain [1]RCPs; to synthesize [1]RCPs, bridging elements with bulky ligands are required. Müller *et al.* demonstrated that bulky alkyl groups on ferrocene moieties could be used *in lieu* of bulky ligands on the bridging elements to prepare [1]FCPs.¹²² Adapting this strategy, the second aim of this thesis was to synthesize the dibromoruthenocene **105**, which could potentially be used to facilitate the formation of new [1]RCPs (see Scheme 2-14).

To prepare **105**, the ruthenium analog of the “double Ugi’s amine” (**109**) is required (Scheme 3-2). Compound **109** was successfully prepared for the first time following similar procedures used to synthesize its iron counterpart (see Scheme 2-1).¹¹⁶ Unfortunately, the dilithiation of **109** was not quantitative, and a mixture of **110** and **111** was obtained after bromination. The two compounds could not be separated to isolate the desired dibromoruthenocene **110**. Despite not being able to isolate **110**, the synthesis of **105** was attempted using the mixture of **110** and **111**, which resulted in a mixture of **105** and **112**. This mixture proved to be difficult to separate, thus it was not possible to isolate **105**. For this reason, the synthesis of new [1]RCPs using **105** as a precursor could not be performed.

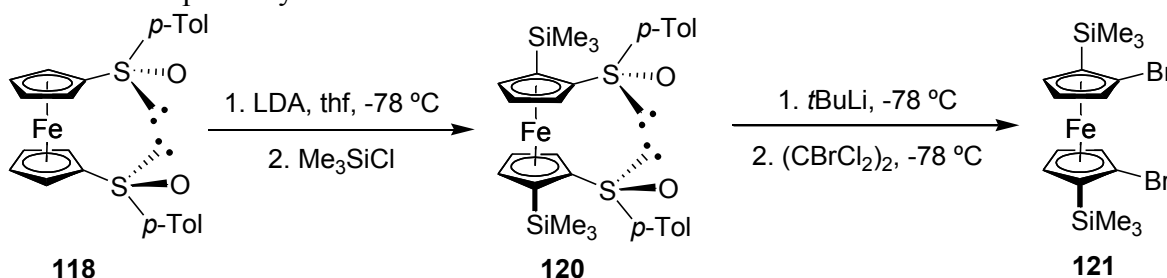
Scheme 3-2. Proposed synthesis of dibromoruthenocene **105** via ruthenocene **109**.



3.3 Alternate Pathway to C₂-Symmetrical Dibromoferrocene Derivatives

As noted earlier, the synthetic pathway for obtaining dibromoferrocenes **88** and **92** is a long process. Secondly, the options for changing the alkyl groups on the ferrocene unit is not very flexible (e.g., see Scheme 2-21). Therefore, another aim of this thesis was to find an alternative synthetic pathway to prepare dibromoferrocene derivatives that is both shorter and more flexible. Using the chemistry that was developed by Kagan *et al.* for synthesizing planar-chiral 1,2-substituted ferrocenes (see Scheme 2-22),¹¹⁹⁻¹²¹ the synthetic pathway in Scheme 3-3 was proposed to obtain the new dibromoferrocene **121**.

Scheme 3-3. Proposed synthesis of dibromoferrocene **121**.



The new ferrocene **118** was successfully prepared by adding dilithioferrocene·2/3tmeda to (*1R,2S,5R*)-(-)-menthyl (*S_S*)-*p*-tolylsulfinat (see Scheme 2-25). The dilithiation of **118** using LDA followed by silylation to yield **120** was successful on a small scale. However, when attempting to synthesize **120** on a larger scale, large amounts of the monosilylated byproduct were obtained. In order to synthesize **121**, an efficient procedure to prepare **120** on a larger scale must be found.

CHAPTER 4: EXPERIMENTAL

4.1 General Procedures

All reactions were performed under nitrogen atmosphere using standard Schlenk techniques, with the exception of [(trimethylsilyl)methyl]lithium, which was performed under argon atmosphere. Solvents were dried using an MBraun Solvent Purification System and stored under nitrogen over 3 Å molecular sieves. Solvents for NMR spectroscopy were prepared through freeze-pump-thaw cycles and stored under nitrogen over 3 Å molecular sieves. ^1H and ^{13}C NMR spectroscopic data were recorded on a 500 MHz Bruker Avance NMR spectrometer at 25 °C. All ^1H chemical shifts were referenced to the signal of residual protons in C_6D_6 and CDCl_3 at $\delta = 7.15$ and 7.26 ppm respectively, and ^{13}C NMR chemical shifts were referenced to the CDCl_3 signal at $\delta = 77.00$ ppm. Assignments for **88**, **92**, **109**, and **118** were supported by additional NMR experiments (DEPT, HMQC, COSY). All signals of Cp protons were assigned as multiplets due to the fine structure of the signals. Mass Spectra were measured on a Jeol AccuTOF GCV 4G using the field desorption (FD) ionization method and were reported in the form m/z (relative intensity) [M^+] where m/z is the observed mass. All intensities are reported relative to the most-intense peak and M^+ is the molecular-ion. For the isotopic pattern, only the mass peak of the isotopologue with the highest natural abundance are listed. Elemental analyses were performed on a Perkin Elmer 2400 CHN Elemental Analyzer.

4.2 Reagents

The following compounds were prepared following literature procedures: (*R,R,S_p,S_p*)-2,2'-bis(α -acetoxyethyl)-1,1'-dibromoferrocene (**85a**),¹²² dilithioferrocene·tmeda,¹³⁴ (*1R,2S,5R*)-(-)-menthyl (*S_S*)-*p*-toluenesulfinate (**117**),¹³⁵ oxazaborolidine catalyst,¹¹⁶ and ruthenocene.¹³⁶ The compounds 1,1'-diacetyl ruthenocene (**106**),¹¹⁶ (*R,R*)-1,1'-bis(α -hydroxyethyl)ruthenocene (**107**),¹¹⁶

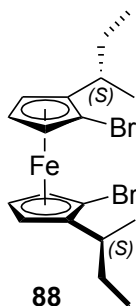
[(trimethylsilyl)methyl]lithium,¹²⁹ and tris[(trimethylsilyl)methyl]aluminum¹³⁰ were synthesized according to procedures in the literature with some alterations; therefore, the syntheses of these compounds are reported below. Acetic anhydride (99%) and sodium potassium tartrate tetrahydrate (Certified ACS Crystalline) were purchased from Fisher Scientific. Acetyl chloride (98%), aluminum(III) bromide ($\geq 98\%$), dimethylamine (40 wt.% in water), ferrocene (98%), lithium diisopropylamide (2.0 M in thf/heptane/ethylbenzene), lithium metal (rod, 99.9%), *n*BuLi (2.5 M in hexanes), triethylaluminum (25 wt.% in toluene), triisobutylaluminum (25 wt.% in toluene), and trimethylaluminum (2.0 M in hexanes) were purchased from Sigma Aldrich. Aluminum(III) chloride (Alfa Aesar; 99.985%), borane-dimethyl sulfide complex (Alfa Aesar; 94%), and 1,2-dibromotetrachloroethane (Alfa Aesar; 98%) were purchased from VWR. Aluminum oxide (Sigma Aldrich, activated, neutral, Brockmann I) and silica gel 60 (EMD, Geduran, particle size 0.040-0.063 mm) were used for column chromatography.

4.3 Computational Details

All DFT calculations were performed by Dr. J. Müller. Geometry optimizations of species **78**, **88**, and **92** were performed on the B3LYP/6-31G(d) level of theory using Gaussian 09.¹³⁷ Calculated vibrational frequencies for all optimized geometries showed that ground-state geometries were obtained. Gibbs free energies (ΔG°) were calculated for standard conditions ($T = 298.15$ K; $P = 1$ atm) using unscaled zero point vibrational energies. Using a Boltzmann distribution between related conformers, equilibrium mixtures of conformers were calculated in percent amounts.

4.4 Syntheses

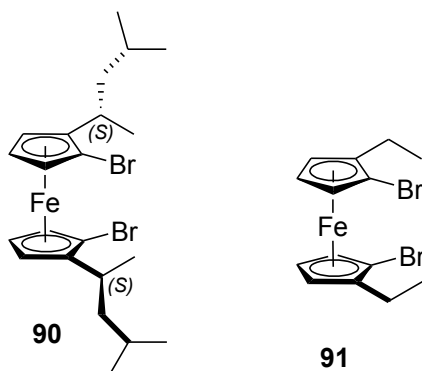
4.4.1 Synthesis of (*S,S,S_p,S_p*)-1,1'-Dibromo-2,2'-di(2-butyl)ferrocene (**88**)



Triethylaluminum (25 wt. % in toluene, 27 mL, 51 mmol) was added dropwise to **85a** (5.214 g, 10.10 mmol) in dry CH₂Cl₂ (100 mL) at -78 °C. The reaction mixture was stirred for 1 h at -78 °C and was warmed to r.t. and stirred for 30 min. The reaction mixture was added dropwise to a saturated aqueous solution of NaHCO₃ (50 mL) at 0 °C via cannula followed by addition of a saturated aqueous solution of sodium potassium tartrate (50 mL). The organic solvents were removed using a rotary evaporator. Diethyl ether (100 mL) was added and the mixture was stirred for 15 min and then 1 M HCl_(aq) (50 mL) was added. The phases were separated and the aqueous phase was extracted with diethyl ether (2x200 mL). The combined organic phases were washed with a saturated aqueous solution of NaHCO₃, water, brine and then dried with Na₂SO₄. All volatiles were removed to yield a red oil which was purified by column chromatography (silica, hexanes), to yield **88** as a red oil (3.899 g, 85%). ¹H NMR (CDCl₃): δ = 0.81 [t, 6H, CH(CH₂CH₃)(CH₃)], 1.24-1.31 [m, 8H, CH(CH₂CH₃)(CH₃)], 1.45-1.53 [m, 2H, CH(CH₂CH₃)(CH₃)], 2.59-2.67 [m, 2H, CH(CH₂CH₃)(CH₃)], 4.02 (m, 2H, CH of Cp), 4.05 (m, 2H, CH of Cp), and 4.22 ppm (m, 2H, CH of Cp); ¹³C NMR (CDCl₃): δ = 11.15 [CH(CH₂CH₃)(CH₃)], 18.32 [CH(CH₂CH₃)(CH₃)], 30.97 [CH(CH₂CH₃)(CH₃)], 31.79 [CH(CH₂CH₃)(CH₃)], 65.19 (CH of Cp), 67.89 (CH of Cp), 74.11 (CH of Cp), 80.80 (*ipso*-Cp), and 94.19 (*ipso*-Cp) ppm; MS: *m/z* (%): 454 (55) [M⁺]; HRMS (FD-TOF): *m/z* calcd for

$C_{18}H_{24}Br_2Fe$: 453.95942; found: 453.95889; elemental anal. calcd (%) for $C_{18}H_{24}Br_2Fe$: C 47.41, H 5.30; found: C 48.05, H 5.29. Partial 1H NMR ($CDCl_3$) assignment of a C_1 -symmetric stereoisomer of **88**: δ = 3.97 (m, 2H, \underline{CH} of Cp), 4.00 (m, 2H, \underline{CH} of Cp), 4.19 (m, 1H, \underline{CH} of Cp), and 4.25 (m, 1H, \underline{CH} of Cp) ppm.

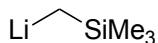
4.4.2 Attempted Synthesis of (*S,S,S_p,S_p*)-1,1'-Dibromo-2,2'-bis[2-(4-methylpentyl)]ferrocene (**90**)



Triisobutylaluminum (25 wt. % in toluene, 24 mL, 26 mmol) was added dropwise to **85a** (2.636 g, 5.108 mmol) in dry CH_2Cl_2 (50 mL) at $-78\text{ }^{\circ}C$. The reaction mixture was stirred for 1 h at $-78\text{ }^{\circ}C$ and was warmed to r.t. and stirred for 30 min. The reaction mixture was added dropwise to a saturated aqueous solution of $NaHCO_3$ (25 mL) at $0\text{ }^{\circ}C$ via cannula followed by a saturated aqueous solution of sodium potassium tartrate (25 mL). The organic solvents were removed using a rotary evaporator. Diethyl ether (50 mL) was added and the mixture was stirred for 15 min and then 1 M $HCl_{(aq)}$ (25 mL) was added. The phases were separated and the aqueous phase was extracted with diethyl ether (2x100 mL). The combined organic phases were washed with a saturated aqueous solution of $NaHCO_3$, water, brine and then dried with Na_2SO_4 . All volatiles were removed to yield a red oil. After analyzing the product by 1H NMR, the oil was identified as

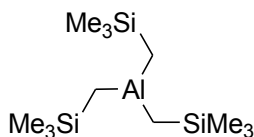
91 and not the expected product **90**. ^1H NMR (CDCl_3): $\delta = 1.14$ (t, 6H, CH_2CH_3), 2.37 (q, 4H, CH_2CH_3), 3.99-4.03 (m, 4H, CH of Cp), and 4.28 ppm (m, 2H, CH of Cp).

4.4.3 Synthesis of [(Trimethylsilyl)methyl]lithium¹²⁹



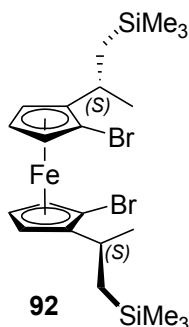
A lithium metal rod (4.87 g, 702 mmol) was cut into slices and hammered into thin plates and suspended in dry hexanes (200 mL). While stirring vigorously under argon, (chloromethyl)trimethylsilane (24.5 mL, 176 mmol) was added dropwise and then heated to reflux for 2 days. The reaction mixture was filtered and the solvent was removed under high vacuum to yield a white solid (14.1 g, 85%). ^1H NMR (C_6D_6): $\delta = -2.09$ (s, 2H, CH_2), and 0.15 ppm (s, 9H, SiMe_3). The ^1H NMR data of [(trimethylsilyl)methyl]lithium were consistent with literature values.

4.4.4 Synthesis of Tris[(trimethylsilyl)methyl]aluminum¹³⁰



A solution of [(trimethylsilyl)methyl]lithium (14.1 g, 150 mmol) in dry hexanes (150 mL) was added to a solution of aluminum(III) bromide (13.3 g, 50.0 mmol) in dry hexanes (215 mL) dropwise via cannula. The reaction mixture was heated to reflux for 12 h, and hexanes was removed by distillation under inert atmosphere. Tris[(trimethylsilyl)methyl]aluminum was isolated by flask-to-flask condensation under high vacuum from the reaction mixture to yield a colourless liquid (13.5 g, 94%). ^1H NMR (C_6D_6): $\delta = -0.41$ (s, 6H, CH_2), and 0.13 ppm (s, 27H, SiMe_3). The ^1H NMR data of tris[(trimethylsilyl)methyl]aluminum were consistent with literature values.

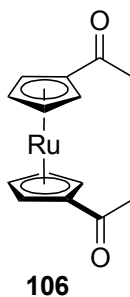
4.4.5 Synthesis of (*S,S,S_p,S_p*)-1,1'-Dibromo-2,2'-bis{2-[1-(trimethylsilyl)propyl]}ferrocene (**92**)



Tris[(trimethylsilyl)methyl]aluminum (4.420 g, 15.31 mmol) in dry hexanes (7 mL) was added dropwise to **85a** (2.626 g, 5.088 mmol) in dry CH₂Cl₂ (50 mL) at -78 °C. The reaction mixture was stirred for 1 h at -78 °C and was warmed to r.t. and stirred for 30 min. The reaction mixture was added dropwise to a saturated aqueous solution of NaHCO₃ (25 mL) at 0 °C via cannula followed by addition of a saturated aqueous solution of sodium potassium tartrate (25 mL). The organic solvents were removed using a rotary evaporator. Diethyl ether (50 mL) was added and the mixture was stirred for 15 min and then 1 M HCl_(aq) (25 mL) was added. The phases were separated and the aqueous phase was extracted with diethyl ether (2x100 mL). The combined organic phases were washed with a saturated aqueous solution of NaHCO₃, water, brine and then dried with Na₂SO₄. All volatiles were removed to yield a red oil which was filtered through an alumina column (3.0 cm x 10.0 cm) using hexanes to obtain **92** as a red oil (2.798 g, 96%). Orange needles of **92** (1.810 g, 62%) were obtained after allowing a solution of **92**, obtained by dissolving **92** in minimal amount of CH₂Cl₂ and adding double the amount of MeOH, to slowly evaporate. The crystallization was repeated to yield orange needles of **92** (1.622 g, 56%). ¹H NMR (CDCl₃): δ = 0.01 [s, 18H, CH(CH₂SiMe₃)(CH₃)], 0.55 [dd, 2H, CH(CH₂SiMe₃)(CH₃)], 0.86 [dd, 2H, CH(CH₂SiMe₃)(CH₃)], 1.33 [d, 6H, CH(CH₂SiMe₃)(CH₃)], 2.82 [ddq, 2H, CH(CH₂SiMe₃)(CH₃)],

4.01 (m, 2H, $\underline{\text{CH}}$ of Cp), 4.04 (m, 2H, $\underline{\text{CH}}$ of Cp), and 4.20 ppm (m, 2H, $\underline{\text{CH}}$ of Cp); ^{13}C NMR (CDCl_3): δ = -0.55 [$\text{CH}(\text{CH}_2\text{SiMe}_3)(\underline{\text{CH}_3})$], 21.37 [$\text{CH}(\text{CH}_2\text{SiMe}_3)(\underline{\text{CH}_3})$], 27.37 [$\underline{\text{CH}}(\text{CH}_2\text{SiMe}_3)(\text{CH}_3)$], 27.73 [$\text{CH}(\underline{\text{CH}_2\text{SiMe}_3})(\text{CH}_3)$], 64.52 ($\underline{\text{CH}}$ of Cp), 67.77 ($\underline{\text{CH}}$ of Cp), 73.89 ($\underline{\text{CH}}$ of Cp), 80.29 (*ipso*-Cp), and 97.34 (*ipso*-Cp) ppm; MS: m/z (%): 570 (52) [M^+]; HRMS (FD-TOF): m/z calcd for $\text{C}_{22}\text{H}_{36}\text{Br}_2\text{FeSi}_2$: 570.00717; found: 570.00609; elemental anal. calcd (%) for $\text{C}_{22}\text{H}_{36}\text{Br}_2\text{Si}_2\text{Fe}$: C 46.17, H 6.34; found: C 46.38, H 6.13. Partial ^1H NMR (CDCl_3) assignment of a C_1 -symmetric stereoisomer of **92**: δ = 3.94 (m, 1H, $\underline{\text{CH}}$ of Cp), 4.17 (m, 1H, $\underline{\text{CH}}$ of Cp), and 4.23 (m, 1H, $\underline{\text{CH}}$ of Cp) ppm. The remaining Cp signals of the stereoisomer are buried under the chemical shifts of **92**, as indicated by the increased integrals for the Cp signals of **92**.

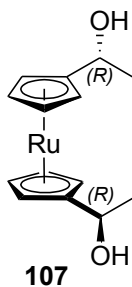
4.4.6 Synthesis of 1,1'-Diacetylruthenocene (**106**)¹¹⁶



Acetyl chloride (5.20 mL, 73.1 mmol) was added dropwise to aluminum(III) chloride (11.5 g, 86.2 mmol) suspended in CH_2Cl_2 (32 mL) at 0 °C. Ruthenocene (5.47 g, 23.2 mmol) in CH_2Cl_2 (126 mL) was added dropwise and then heated to reflux for 48 h. The reaction mixture was cooled to 0 °C and quenched with ice-cold water. The phases were separated and the organic phase was washed with a saturated aqueous solution of NaHCO_3 and brine. The organic phase was dried using Na_2SO_4 and all volatiles were removed. The compound was purified by column chromatography (hexanes/EtOAc 1:2) to yield **106** as a yellow solid (3.99 g, 55%). ^1H NMR

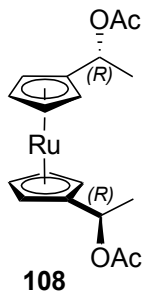
(CDCl₃): δ = 2.20 (s, 6H, CH₃), 4.80 (m, 4H, CH of Cp), and 5.10 ppm (m, 4H, CH of Cp). The ¹H NMR data of **106** were consistent with literature values.

4.4.7 Synthesis of (*R,R*)-1,1'-Bis(α -hydroxyethyl)ruthenocene (**107**)¹¹⁶



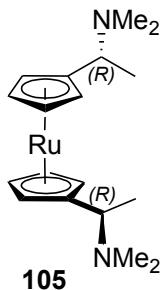
The oxazaborolidine catalyst (1.172 g, 4.228 mmol) was dissolved in dry thf (43 mL) and cooled to 0 °C, and BH₃·SMe₂ (1 M in thf, 3.0 mL, 3.0 mmol) was added dropwise. After stirring for 5 min, more BH₃·SMe₂ (1 M in thf, 11.5 mL, 11.5 mmol) and **106** (2.222 g, 7.047 mmol) in dry thf (115 mL) were added dropwise simultaneously over 20 min at 0 °C. After 15 min of stirring at 0 °C, the reaction was quenched with MeOH (7.5 mL). The reaction mixture was poured into a saturated aqueous solution of NH₄Cl (500 mL) and extracted with ether (600 mL). The phases were separated and the organic phase was washed with water, brine, then dried with Na₂SO₄ and all volatiles were removed to give an oil which was purified by column chromatography (hexanes/EtOAc 1:4) to give **107** as a white solid (2.005 g, 89%). ¹H NMR (CDCl₃): δ = 1.36 (d, 6H, CH₃), 2.42 (br s, 2 H, OH), 4.39 (q, 2H, CH), 4.55 (m, 4H, CH of Cp), 4.64 (m, 2H, CH of Cp), and 4.70 ppm (m, 2H, CH of Cp). The ¹H NMR data of **107** were consistent with literature values.

4.4.8 Synthesis of (*R,R*)-1,1'-Bis(α -acetoxyethyl)ruthenocene (**108**)



The diol **107** (4.678 g, 14.65 mmol) was dissolved in acetic anhydride (10.0 mL, 106 mmol) and pyridine (26.0 mL, 323 mmol) and stirred overnight under nitrogen. All volatiles were removed under high vacuum at 40 °C and yield **108** quantitatively as an oil. ^1H NMR (CDCl_3): δ = 1.44 (d, 6H, CH_3), 2.02 (s, 6H, OAc), 4.47-4.52 (m, 4H, CH of Cp), 4.63 (m, 4H, CH of Cp), and 5.60 ppm (q, 2H, CH).

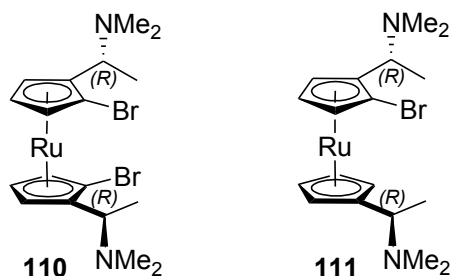
4.4.9 Synthesis of (*R,R*)-1,1'-Bis(α -N,N-dimethylaminoethyl)ruthenocene (**109**)



The diacetate **108** (5.909 g, 14.65 mmol) was dissolved in MeOH (121 mL) and dimethylamine solution (40% in water, 27 mL, 210 mmol) and stirred for 48 h. The reaction mixture was poured into a saturated aqueous solution of NH_4Cl (500 mL) and ether (250 mL). The phases were separated and the organic phase was extracted with a saturated aqueous solution of NH_4Cl (2x200 mL). The aqueous phases were combined and a saturated aqueous solution of NaHCO_3 (200 mL) and 3 M $\text{KOH}_{(\text{aq})}$ (180 mL) was added. The aqueous phase was split into two parts and each portion was extracted with CH_2Cl_2 (3x250 mL). The combined organic phases were dried

with Na₂SO₄ and volatiles were removed to yield **109** as a yellow solid (4.736 g, 87%). ¹H NMR (CDCl₃): δ = 1.27 (d, 6H, CH₃), 2.15 (s, 12H, NMe₂), 3.30 (q, 2H, CH), 4.42 (m, 2H, CH of Cp), 4.44 (m, 2H, CH of Cp), 4.47 (m, 2H, CH of Cp), and 4.51 ppm (m, 2H, CH of Cp); ¹³C NMR (CDCl₃): δ = 17.82 (CH₃), 41.09 (NMe₂), 58.54 (CH), 69.73 (CH of Cp), 70.39 (CH of Cp), 72.96 (CH of Cp), 91.25 (*ipso*-Cp) ppm; MS: *m/z* (%): 374 (100) [M⁺]; HRMS (FD-TOF): *m/z* calcd for C₁₈H₂₈N₂Ru: 374.12960; found: 374.12811; elemental anal. calcd (%) for C₁₈H₂₈N₂Ru: C 57.88, H 7.56, N 7.50; found: C 57.64, H 7.87, N 7.47. To obtain analytically pure samples for MS and elemental analysis, **109** was purified by column chromatography (silica, EtOAc/Et₃N 9:1).

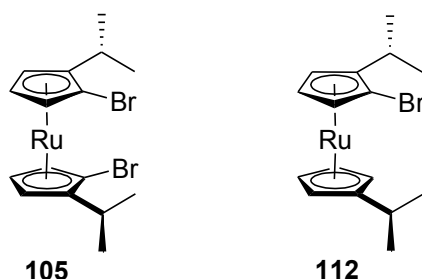
4.4.10 Synthesis of a Mixture of (*R,R,S_p,S_p*)-1,1'-Dibromo-2,2'-bis(*α*-N,N-dimethylaminoethyl)ruthenocene (**110**) and (*R,R,S_p*)-1-Bromo-2,2'-bis(*α*-N,N-dimethylaminoethyl)ruthenocene (**111**)



To a stirred solution of **109** (0.749 g, 2.01 mmol) in dry diethyl ether (8 mL), *n*BuLi (2.5 M in hexanes, 3.2 mL, 8.0 mmol) was added dropwise at r.t. and stirred overnight. The reaction mixture was cooled to -78 °C and 1,2-dibromotetrachloroethane (3.275 g, 10.06 mmol) in dry thf (6 mL) was added dropwise via syringe over 20 min. The resulting reaction mixture was stirred at -78 °C for 1 h, followed by stirring at r.t. for 2 h. The reaction mixture was poured into mixture of a saturated aqueous solution of NH₄Cl (50 mL) and diethyl ether (30 mL). The aqueous phase was removed and the organic phase was extracted with saturated NH₄Cl (2x50 mL). The combined aqueous phase was neutralized with a saturated aqueous solution of NaHCO₃ (30 mL) and basified

with 2 M KOH_(aq) (40 mL) and the aqueous phase was extracted with CH₂Cl₂ (3x50 mL). The organic phase was dried with Na₂SO₄ and all volatiles were removed to yield a 2.2:1.0 mixture of **110** and **111** (1.01 g), respectively. ¹H NMR (CDCl₃) of **110**: δ = 1.35 (d, 6H, CH₃), 2.24 (s, 12H, NMe₂), 3.54 (q, 2H, CH), 4.50 (m, 2H, CH of Cp), 4.58 (m, 2H, CH of Cp), and 4.72 ppm (m, 2H, CH of Cp); ¹H NMR (CDCl₃) of **111**: 1.37 (d, 3H, CH₃), 1.57 (d, 3H, CH₃), 2.24 (s, 6H, NMe₂), 2.29 (s, 6H, NMe₂), 3.38 (q, 1H, CH), 3.59 (q, 1H, CH), 4.37 (m, 1H, CH of Cp), 4.44 (m, 1H, CH of Cp), 4.47-4.54 (m, 2H, CH of Cp), 4.58 (m, 1H, CH of Cp), 4.79 (m, 1H, CH of Cp), and 4.82 ppm (m, 1H, CH of Cp).

4.4.11 Synthesis of a Mixture of (*S_p*,*S_p*)-1,1'-Dibromo-2,2'-di(isopropyl)ruthenocene (**105**) and (*S_p*)-1-Bromo-2,2'-di(isopropyl)ruthenocene (**112**)

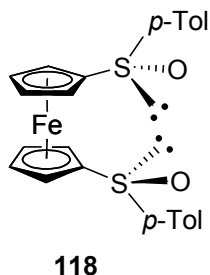


The synthesis of (*S_p*,*S_p*)-1,1'-dibromo-2,2'-di(isopropyl)ruthenocene (**105**) was attempted by using a mixture of **110** and **111**. To calculate the reagents needed for synthesizing **105**, the mixture of **110** and **111** was assumed to be all **110**.

To a mixture of **110** and **111** (approx. 2.2:1.0 ratio) (0.718 g, 1.35 mmol), acetic anhydride (4.1 mL, 43 mmol) was added and the solution was degassed thoroughly via freeze-pump-thaw cycles. The reaction mixture was stirred overnight at 70 °C. All of the volatiles were removed at 40 °C under high vacuum. The oil was dissolved in dry CH₂Cl₂ (13.5 mL) and cooled to -78 °C. Trimethylaluminum (2.0 M in hexanes, 3.4 mL, 6.8 mmol) was added dropwise and the reaction mixture was stirred at -78 °C for 1 h, then at r.t. for 30 min. The reaction mixture was added

dropwise to a saturated aqueous solution of NaHCO₃ (20 mL) at 0 °C via cannula followed by a saturated aqueous solution of sodium potassium tartrate (20 mL). The organic solvents were removed using a rotary evaporator. Diethyl ether (20 mL) was added and the mixture was stirred for 15 min and then 1 M HCl_(aq) (20 mL) was added. The phases were separated and the aqueous phase was extracted with diethyl ether (2x20 mL). The combined organic phases were washed with a saturated aqueous solution of NaHCO₃, water, brine and then dried with Na₂SO₄. All volatiles were removed to yield a yellow oil mixture of **105** and **112** (0.584 g). All attempts to isolate **105**, via column chromatography or recrystallization, failed. ¹H NMR of **105**: δ = 1.15 (d, 6H, CH₃), 1.18 (d, 6H, CH₃), 2.60 (m, 2H, CH), 4.41 (m, 2H, CH of Cp), 4.47 (m, 2H, CH of Cp), and 4.72 ppm (m, 2H, CH of Cp). There was too much overlap of signals to properly identify **112** and determine a composition ratio for the mixture.

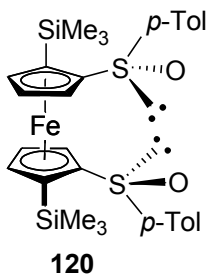
4.4.12 Synthesis of (*S,S*)-1,1'-Bis(*p*-tolylsulfinyl)ferrocene (**118**)



A solution of (*1R,2S,5R*)-(-)-menthyl (*S*)-*p*-toluenesulfinate (**117**) (21.44 g, 72.81 mmol) in thf (200 mL) was cooled to -25 °C and dilithioferrocene·2/3tmeda (5.068 g, 18.40 mmol) in thf (100 mL) was cooled to -78 °C and added via cannula over 30 min. The reaction mixture was stirred at -25 °C for 30 min, then quenched with water. The phases were separated and the organic phase was washed with 1 M NaOH_(aq), water, and brine in succession and dried with Na₂SO₄. All volatiles were removed and the crude solid was purified by column chromatography (CH₂Cl₂/MeOH 95:5) to yield **118** as a dark yellow solid (3.293 g, 39%). ¹H NMR (CDCl₃): δ =

2.36 (s, 6H, $\underline{\text{CH}}_3$), 4.57 (m, 2H, $\underline{\text{CH}}$ of Cp), 4.64 (m, 2H, $\underline{\text{CH}}$ of Cp), 4.71 (m, 2H, $\underline{\text{CH}}$ of Cp), 4.74 (m, 2H, $\underline{\text{CH}}$ of Cp), 7.25 (d, 4H, $\underline{\text{CH}}$ of Ph), and 7.49 ppm (d, 4H, $\underline{\text{CH}}$ of Ph); ^{13}C NMR (CDCl_3): δ = 21.38 ($\underline{\text{CH}}_3$), 66.10 ($\underline{\text{CH}}$ of Cp), 69.84 ($\underline{\text{CH}}$ of Cp), 71.54 ($\underline{\text{CH}}$ of Cp), 72.00 ($\underline{\text{CH}}$ of Cp), 96.66 (*ipso*-Cp), 124.11 ($\underline{\text{CH}}$ of Ph), 129.77 ($\underline{\text{CH}}$ of Ph), 141.27 (*ipso*-Ph), 142.69 (*ipso*-Ph) ppm; MS: m/z (%): 462 (100) [M^+]; HRMS (FD-TOF): m/z calcd for $\text{C}_{24}\text{H}_{22}\text{FeO}_2\text{S}_2$: 462.04106; found: 462.04023; elemental anal. calcd (%) for $\text{C}_{24}\text{H}_{22}\text{O}_2\text{S}_2\text{Fe}$: C 62.34, H 4.80; found: C 62.35, H 4.52.

4.4.13 Attempted Synthesis of (S_S, S_S, S_P, S_P)-2,2'-Bis(trimethylsilyl)-1,1'-bis(*p*-tolylsulfinyl)-ferrocene (**120**)



Lithium diisopropylamide (2.0 M in thf/heptane/ethylbenzene, 0.27 mL, 0.54 mmol) was added dropwise to a solution of **118** (0.115 g, 0.249 mmol) in dry thf (10 mL) at -78°C and stirred for 30 min. Chlorotrimethylsilane (0.06 mL, 0.5 mmol) was added and the reaction mixture was stirred for 1 h at -78°C . The reaction was quenched at -78°C with 1 M $\text{NaOH}_{(\text{aq})}$ and warmed to r.t.. The reaction mixture was poured into diethyl ether and water and then the aqueous phase was removed. The organic phase was washed with water, brined and then dried with Na_2SO_4 . All volatiles were removed to yield a dark brown oil. ^1H NMR (CDCl_3) for **120**: δ = 0.33 (s, 18H, SiMe_3), 2.45 (s, 6H, $\underline{\text{CH}}_3$), 3.91 (m, 2H, $\underline{\text{CH}}$ of Cp), 4.40 (m, 2H, $\underline{\text{CH}}$ of Cp), 4.64 (m, 2H, $\underline{\text{CH}}$ of Cp), 7.25 (d, 4H, $\underline{\text{CH}}$ of Ph), and 7.49 ppm (d, 4H, $\underline{\text{CH}}$ of Ph).

REFERENCES

1. Galli, P.; Haylock, J. C. *Prog. Polym. Sci.* **1991**, 2-3, 443-462.
2. MacDiarmid, A. G. *Synth. Met.* **2001**, 1, 11-22.
3. Mayes, A. G.; Whitcombe, M. J. *Adv. Drug Delivery Rev.* **2005**, 12, 1742-1778.
4. Suriano, F.; Coulembier, O.; Hedrick, J. L.; Dubois, P. *Polym. Chem.* **2011**, 3, 528-533.
5. Bellas, V.; Rehahn, M. *Angew. Chem., Int. Ed.* **2007**, 27, 5082-5104.
6. Rinehart, K. L., Jr.; Frerichs, A. K.; Kittle, P. A.; Westman, L. F.; Gustafson, D. H.; Pruett, R. L.; McMahon, J. E. *J. Am. Chem. Soc.* **1960**, 4111-4112.
7. Osborne, A. G.; Whiteley, R. H. *J. Organomet. Chem.* **1975**, 2, C27-C28.
8. Osborne, A. G.; Whiteley, R. H.; Meads, R. E. *J. Organomet. Chem.* **1980**, 3, 345-357.
9. Seyferth, D.; Withers Jr., H. P. *J. Organomet. Chem.* **1980**, 1, C1-C5.
10. Herberhold, M.; Hofmann, T.; Weinberger, S.; Wrackmeyer, B. *Z. Naturforsch., B: Chem. Sci.* **1997**, 9, 1037-1042.
11. Wrighton, M. S.; Palazzotto, M. C.; Bocarsly, A. B.; Bolts, J. M.; Fischer, A. B.; Nadjio, L. J. *Am. Chem. Soc.* **1978**, 23, 7264-7271.
12. Jäkle, F.; Rulkens, R.; Zech, G.; Foucher, D. A.; Lough, A. J.; Manners, I. *Chem.-Eur. J.* **1998**, 11, 2117-2128.
13. Vogel, U.; Lough, A. J.; Manners, I. *Angew. Chem., Int. Ed.* **2004**, 25, 3321-3325.
14. Pudelski, J. K.; Foucher, D. A.; Honeyman, C. H.; Lough, A. J.; Manners, I.; Barlow, S.; O'Hare, D. *Organometallics* **1995**, 5, 2470-2479.
15. Pudelski, J. K.; Gates, D. P.; Rulkens, R.; Lough, A. J.; Manners, I. *Angew. Chem., Int. Ed. Engl.* **1995**, 13/14, 1506-1508.

16. Bishop, J. J.; Davison, A.; Katcher, M. L.; Lichtenberg, D. W.; Merrill, R. E.; Smart, J. C. *J. Organometal. Chem.* **1971**, *2*, 241-249.
17. Rulkens, R.; Gates, D. P.; Balaishis, D.; Pudelski, J. K.; McIntosh, D. F.; Lough, A. J.; Manners, I. *J. Am. Chem. Soc.* **1997**, *45*, 10976-10986.
18. Green, J. C. *Chem. Soc. Rev.* **1998**, *4*, 263-272.
19. Manners, I. *Adv. Organomet. Chem.* **1995**, 131-168.
20. Foucher, D. A.; Tang, B. Z.; Manners, I. *J. Am. Chem. Soc.* **1992**, *15*, 6246-6248.
21. He, F.; Gädt, T.; Manners, I.; Winnik, M. A. *J. Am. Chem. Soc.* **2011**, *23*, 9095-9103.
22. Patra, S. K.; Ahmed, R.; Whittell, G. R.; Lunn, D. J.; Winnik, M. A.; Manners, I. *Polym. Prepr.* **2011**, *2*, 1002-1003.
23. Rupar, P. A.; Cambridge, G.; Winnik, M. A.; Manners, I. *J. Am. Chem. Soc.* **2011**, *42*, 16947-16957.
24. Rupar, P. A.; Chabanne, L.; Winnik, M. A.; Manners, I. *Science* **2012**, *6094*, 559-562.
25. Qiu, H.; Cambridge, G.; Winnik, M. A.; Manners, I. *J. Am. Chem. Soc.* **2013**, *33*, 12180-12183.
26. Herbert, D. E.; Mayer, U. F. J.; Manners, I. *Angew. Chem., Int. Ed.* **2007**, *27*, 5060-5081.
27. Braunschweig, H.; Dirk, R.; Müller, M.; Nguyen, P.; Resendes, R.; Gates, D. P.; Manners, I. *Angew. Chem., Int. Ed. Engl.* **1997**, *21*, 2338-2340.
28. Berenbaum, A.; Braunschweig, H.; Dirk, R.; Englert, U.; Green, J. C.; Jäkle, F.; Lough, A. J.; Manners, I. *J. Am. Chem. Soc.* **2000**, *24*, 5765-5774.
29. Schachner, J. A.; Lund, C. L.; Quail, J. W.; Müller, J. *Organometallics* **2005**, *5*, 785-787.
30. Schachner, J. A.; Lund, C. L.; Quail, J. W.; Müller, J. *Organometallics* **2005**, *18*, 4483-4488.
31. Lund, C. L.; Schachner, J. A.; Quail, J. W.; Müller, J. *Organometallics* **2006**, *24*, 5817-5823.
32. Bagh, B.; Gilroy, J. B.; Staubitz, A.; Müller, J. *J. Am. Chem. Soc.* **2010**, *6*, 1794-1795.

33. Bagh, B.; Schatte, G.; Green, J. C.; Müller, J. *J. Am. Chem. Soc.* **2012**, *134*, 7924-7936.
34. Braunschweig, H.; Burschka, C.; Clentsmith, G. K. B.; Kupfer, T.; Radacki, K. *Inorg. Chem.* **2005**, *44*, 4906-4908.
35. Schachner, J. A.; Orłowski, G. A.; Quail, J. W.; Kraatz, H.-B.; Müller, J. *Inorg. Chem.* **2006**, *45*, 454-459.
36. Calleja, G.; Carre, F.; Cerveau, G.; Corriu, R. J. P. *C. R. Acad. Sci., Ser. IIC: Chim.* **1998**, *327*, 285-291.
37. Foucher, D. A.; Ziembinski, R.; Tang, B. Z.; Macdonald, P. M.; Massey, J.; Jaeger, C. R.; Vancso, G. J.; Manners, I. *Macromolecules* **1993**, *26*, 2878-2884.
38. Foucher, D.; Ziembinski, R.; Petersen, R.; Pudelski, J.; Edwards, M.; Ni, Y.; Massey, J.; Jaeger, C. R.; Vancso, G. J.; Manners, I. *Macromolecules* **1994**, *27*, 3992-3999.
39. Nguyen, P.; Lough, A. J.; Manners, I. *Macromol. Rapid Commun.* **1997**, *18*, 953-959.
40. Nguyen, P.; Stojcevic, G.; Kulbaba, K.; MacLachlan, M. J.; Liu, X.; Lough, A. J.; Manners, I. *Macromolecules* **1998**, *31*, 5977-5983.
41. Pannell, K. H.; Dementiev, V. V.; Li, H.; Cervantes-Lee, F.; Nguyen, M. T.; Diaz, A. F. *Organometallics* **1994**, *13*, 3644-3650.
42. Pudelski, J. K.; Rulkens, R.; Foucher, D. A.; Lough, A. J.; MacDonald, P. M.; Manners, I. *Macromolecules* **1995**, *28*, 7301-7308.
43. Berenbaum, A.; Lough, A. J.; Manners, I. *Organometallics* **2002**, *21*, 4415-4424.
44. Masson, G.; Beyer, P.; Cyr, P. W.; Lough, A. J.; Manners, I. *Macromolecules* **2006**, *39*, 3720-3730.
45. Peckham, T. J.; Foucher, D. A.; Lough, A. J.; Manners, I. *Can. J. Chem.* **1995**, *73*, 2069-2078.
46. Schultz, M.; Sofield, C. D.; Walter, M. D.; Andersen, R. A. *New J. Chem.* **2005**, *29*, 919-927.

47. Barlow, S.; Drewitt, M. J.; Dijkstra, T.; Green, J. C.; O'Hare, D.; Whittingham, C.; Wynn, H. H.; Gates, D. P.; Manners, I.; Nelson, J. M.; Pudelski, J. K. *Organometallics* **1998**, *10*, 2113-2120.
48. Rulkens, R.; Lough, A. J.; Manners, I. *Angew. Chem., Int. Ed. Engl.* **1996**, *16*, 1805-1807.
49. Sharma, H. K.; Cervantes-Lee, F.; Mahmoud, J. S.; Pannell, K. H. *Organometallics* **1999**, *3*, 399-403.
50. Clearfield, A.; Simmons, C. J.; Withers Jr., H. P.; Seyferth, D. *Inorg. Chim. Acta* **1983**, *1*, 139-144.
51. Seyferth, D.; Withers Jr., H. P. *Organometallics* **1982**, *10*, 1275-1282.
52. Butler, I. R.; Cullen, W. R.; Einstein, F. W. B.; Rettig, S. J.; Willis, A. J. *Organometallics* **1983**, *1*, 128-135.
53. Honeyman, C. H.; Foucher, D. A.; Dahmen, F. Y.; Rulkens, R.; Lough, A. J.; Manners, I. *Organometallics* **1995**, *12*, 5503-5512.
54. Brunner, H.; Klankermayer, J.; Zabel, M. *J. Organomet. Chem.* **2000**, *2*, 211-219.
55. Broussier, R.; Da Rold, A.; Gautheron, B.; Dromzee, Y.; Jeannin, Y. *Inorg. Chem.* **1990**, *10*, 1817-1822.
56. Schachner, J. A.; Tockner, S.; Lund, C. L.; Quail, J. W.; Rehahn, M.; Müller, J. *Organometallics* **2007**, *18*, 4658-4662.
57. Arimoto, F. S.; Haven Jr., A. C. *J. Am. Chem. Soc.* **1955**, 6295-6297.
58. Rosenberg, H.; Rausch, M. D. Patent Application Country: Application: US; US; Priority Application Country: US Patent US3060215, 1962.
59. Rosenberg, H. Patent Application Country: Application: US; US; Priority Application Country: US Patent US3426053, 1969.

60. Withers Jr., H. P.; Seyferth, D.; Fellmann, J. D.; Garrou, P. E.; Martin, S. *Organometallics* **1982**, *10*, 1283-1288.
61. Brandt, P. F.; Rauchfuss, T. B. *J. Am. Chem. Soc.* **1992**, *5*, 1926-1927.
62. Pudelski, J. K.; Manners, I. *J. Am. Chem. Soc.* **1995**, *27*, 7265-7266.
63. Pudelski, J. K.; Foucher, D. A.; Honeyman, C. H.; Macdonald, P. M.; Manners, I.; Barlow, S.; O'Hare, D. *Macromolecules* **1996**, *6*, 1894-1903.
64. Rulken, R.; Lough, A. J.; Manners, I. *J. Am. Chem. Soc.* **1994**, *2*, 797-798.
65. Rulken, R.; Lough, A. J.; Manners, I.; Lovelace, S. R.; Grant, C.; Geiger, W. E. *J. Am. Chem. Soc.* **1996**, *50*, 12683-12695.
66. Ni, Y.; Rulken, R.; Manners, I. *J. Am. Chem. Soc.* **1996**, *17*, 4102-4114.
67. Ni, Y.; Rulken, R.; Pudelski, J. K.; Manners, I. *Macromol. Rapid Commun.* **1995**, *9*, 637-641.
68. Reddy, N. P.; Yamashita, H.; Tanaka, M. *J. Chem. Soc., Chem. Commun.* **1995**, *22*, 2263-2264.
69. Sheridan, J. B.; Temple, K.; Lough, A. J.; Manners, I. *J. Chem. Soc., Dalton Trans.* **1997**, *5*, 711-713.
70. Temple, K.; Jäkle, F.; Sheridan, J. B.; Manners, I. *J. Am. Chem. Soc.* **2001**, *7*, 1355-1364.
71. Mizuta, T.; Onishi, M.; Miyoshi, K. *Organometallics* **2000**, *24*, 5005-5009.
72. Mizuta, T.; Imamura, Y.; Miyoshi, K.; Yorimitsu, H.; Oshima, K. *Organometallics* **2005**, *5*, 990-996.
73. Mizuta, T.; Imamura, Y.; Miyoshi, K. *J. Am. Chem. Soc.* **2003**, *8*, 2068-2069.
74. Tanabe, M.; Manners, I. *J. Am. Chem. Soc.* **2004**, *37*, 11434-11435.
75. Tanabe, M.; Vandermeulen, G. W. M.; Chan, W. Y.; Cyr, P. W.; Vanderark, L.; Rider, D. A.; Manners, I. *Nat. Mater.* **2006**, *6*, 467-470.

76. Temple, K.; Massey, J. A.; Chen, Z.; Vaidya, N.; Berenbaum, A.; Foster, M. D.; Manners, I. *J. Inorg. Organomet. Polym.* **1999**, *4*, 189-198.
77. Nelson, J. M.; Lough, A. J.; Manners, I. *Angew. Chem., Int. Ed. Engl.*, **1994**, *33*(9), 989-91.
78. Blaser, H.; Brieden, W.; Pugin, B.; Spindler, F.; Studer, M.; Togni, A. *Top. Catal.* **2002**, *1*, 3-16.
79. Blaser, H.; Pugin, B.; Spindler, F. *J. Mol. Catal. A: Chem.* **2005**, *1-2*, 1-20.
80. Schaarschmidt, D.; Lang, H. *Organometallics* **2013**, *20*, 5668-5704.
81. Woodward, R. B.; Rosenblum, M.; Whiting, M. C. *J. Am. Chem. Soc.* **1952**, 3458-3459.
82. Rinehart, K. L., Jr.; Motz, K. L.; Moon, S. *J. Am. Chem. Soc.* **1957**, 2749-2754.
83. Sanders, R.; Mueller-Westerhoff, U. T. *J. Organomet. Chem.* **1996**, *1-2*, 219-224.
84. Guillaneux, D.; Kagan, H. B. *J. Org. Chem.* **1995**, *8*, 2502-2505.
85. Rausch, M. D.; Ciappenelli, D. *J. Organomet. Chem.* **1967**, *1*, 127-136.
86. Benkeser, R. A.; Bach, J. L. *J. Am. Chem. Soc.* **1964**, *5*, 890-895.
87. Benkeser, R. A.; Fitzgerald, W. P.; Melzer, M. S. *J. Org. Chem.* **1961**, 2569-2571.
88. Slocum, D. W.; Rockett, B. W.; Hauser, C. R. *J. Am. Chem. Soc.* **1965**, *6*, 1241-1246.
89. Lednicer, D.; Lindsay, J. K.; Hauser, C. R. *J. Org. Chem.* **1958**, 653-655.
90. Lednicer, D.; Hauser, C. R. *J. Org. Chem.* **1959**, 43-46.
91. Slocum, D. W.; Koonsvitsky, B. P. *J. Org. Chem.* **1976**, *23*, 3664-3668.
92. Sawamura, M.; Yamauchi, A.; Takegawa, T.; Ito, Y. *J. Chem. Soc., Chem. Commun.* **1991**, *13*, 874-875.
93. Baillie, C.; Zhang, L.; Xiao, J. *J. Org. Chem.* **2004**, *22*, 7779-7782.
94. Petter, R. C.; Milberg, C. I. *Tetrahedron Lett.* **1989**, *38*, 5085-5088.
95. Carroll, M. A.; Widdowson, D. A.; Williams, D. J. *Synlett* **1994**, *12*, 1025-1026.

96. Carroll, M. A.; White, A. J. P.; Widdowson, D. A.; Williams, D. J. *Perkin I* **2000**, *10*, 1551-1557.
97. Butler, I. R.; Mussig, S.; Plath, M. *Inorg. Chem. Commun.* **1999**, *9*, 424-427.
98. Butler, I. R.; Drew, M. G. B.; Greenwell, C. H.; Lewis, E.; Plath, M.; Mussig, S.; Szewczyk, J. *Inorg. Chem. Commun.* **1999**, *12*, 576-580.
99. Steffen, W.; Laskoski, M.; Collins, G.; Bunz, U. H. F. *J. Organomet. Chem.* **2001**, *1*, 132-138.
100. Mamane, V.; Fort, Y. *J. Org. Chem.* **2005**, *20*, 8220-8223.
101. Breit, B.; Breuninger, D. *Synthesis* **2005**, *16*, 2782-2786.
102. Kumar, S.; Singh, H. B.; Wolmershäuser, G. *Organometallics* **2006**, *2*, 382-393.
103. Kumar, S.; Helt, J. P.; Autschbach, J.; Detty, M. R. *Organometallics* **2009**, *12*, 3426-3436.
104. Albrow, V.; Blake, A. J.; Chapron, A.; Wilson, C.; Woodward, S. *Inorg. Chim. Acta* **2006**, *6*, 1731-1742.
105. Garcia, J.; Moyano, A.; Rosol, M. *Tetrahedron* **2007**, *9*, 1907-1912.
106. Corona-Sánchez, R.; Toscano, R. A.; Ortega-Alfaro, M. C.; Sandoval-Chávez, C.; López-Cortes, J. G. *Dalton Trans.* **2013**, *33*, 11992-12004.
107. Metallinos, C.; Zaifman, J.; Dodge, L. *Org. Lett.* **2008**, *16*, 3527-3530.
108. Connell, A.; Holliman, P. J.; Butler, I. R.; Male, L.; Coles, S. J.; Horton, P. N.; Hursthouse, M. B.; Clegg, W.; Russo, L. *J. Organomet. Chem.* **2009**, *13*, 2020-2028.
109. Schaarschmidt, D.; Lang, H. *Eur. J. Inorg. Chem.* **2010**, *30*, 4811-4821.
110. Chen, C.; Anselment, T. M. J.; Fröhlich, R.; Rieger, B.; Kehr, G.; Erker, G. *Organometallics* **2011**, *19*, 5248-5257.
111. Marquarding, D.; Klusacek, H.; Gokel, G.; Hoffmann, P.; Ugi, I. *J. Amer. Chem. Soc.* **1970**, *18*, 5389-5393.

112. Hayashi, T.; Mise, T.; Fukushima, M.; Kagotani, M.; Nagashima, N.; Hamada, Y.; Matsumoto, A.; Kawakami, S.; Konishi, M. *Bull. Chem. Soc. Jpn.* **1980**, *4*, 1138-1151.
113. Hayashi, T.; Yamamoto, A.; Hojo, M.; Ito, Y. *J. Chem. Soc., Chem. Commun.* **1989**, *8*, 495-496.
114. Hayashi, T.; Yamamoto, A.; Hojo, M.; Kishi, K.; Ito, Y.; Nishioka, E.; Miura, H.; Yanagai, K. *J. Organomet. Chem.* **1989**, *1-3*, 129-139.
115. Schwink, L.; Knochel, P. *Tetrahedron Lett.* **1996**, *1*, 25-28.
116. Schwink, L.; Knochel, P. *Chem.-Eur. J.* **1998**, *5*, 950-968.
117. Gleiter, R.; Bleiholder, C.; Rominger, F. *Organometallics* **2007**, *20*, 4850-4859.
118. Gokel, G. W.; Marquarding, D.; Ugi, I. K. *J. Org. Chem.* **1972**, *20*, 3052-3058.
119. Rebiere, F.; Samuel, O.; Kagan, H. B. *Tetrahedron Lett.* **1990**, *22*, 3121-3124.
120. Rebiere, F.; Riant, O.; Ricard, L.; Kagan, H. B. *Angew. Chem., Int. Ed. Engl.*, **1993**, *32(4)*, 568-70.
121. Riant, O.; Argouarch, G.; Guillaneux, D.; Samuel, O.; Kagan, H. B. *J. Org. Chem.* **1998**, *10*, 3511-3514.
122. Sadeh, S.; Schatte, G.; Müller, J. *Chem.-Eur. J.* **2013**, *40*, 13408-13417.
123. Bagh, B.; Sadeh, S.; Green, J. C.; Müller, J. *Chem.-Eur. J.* **2014**, *8*, 2318-2327.
124. Khozeimeh Sarbisheh, E.; Green, J. C.; Müller, J. *Organometallics* **2014**, *22*, 6708.
125. Sadeh, S.; Bhattacharjee, H.; Khozeimeh Sarbisheh, E.; Quail, J. W.; Müller, J. *Chem.-Eur. J.* **2014**, *49*, 16320-16330.
126. Kang, J.; Lee, J. H.; Choi, J. S. *Tetrahedron: Asymmetry* **2001**, *1*, 33-35.
127. Kang, J.; Lee, J. H.; Im, K. S. *J. Mol. Catal. A: Chem.* **2003**, *1-2*, 55-63.
128. Bailey, W. F.; Luderer, M. R.; Jordan, K. P. *J. Org. Chem.* **2006**, *7*, 2825-2828.

129. Vaughn, G. D.; Krein, K. A.; Gladysz, J. A. *Organometallics* **1986**, *5*, 936-942.
130. Beachley, O. T., Jr.; Tessier-Youngs, C.; Simmons, R. G.; Hallock, R. B. *Inorg. Chem.* **1982**, *5*, 1970-1973.
131. Lemay, G.; Kaliaguine, S.; Adnot, A.; Nahar, S.; Cozak, D.; Monnier, J. *Can. J. Chem.* **1986**, *9*, 1943-1948.
132. Toma, S.; Federic, J.; Solcaniova, E. *Collect. Czech. Chem. Commun.* **1981**, *10*, 2531-2539.
133. Lagneau, N. M.; Chen, Y.; Robben, P. M.; Sin, H.; Takasu, K.; Chen, J.; Robinson, P. D.; Hua, D. H. *Tetrahedron* **1998**, *26*, 7301-7334.
134. Butler, I. R.; Cullen, W. R.; Ni, J.; Rettig, S. J. *Organometallics* **1985**, *12*, 2196-2201.
135. Rayner, P. J.; O'Brien, P.; Horan, R. A. J. *J. Am. Chem. Soc.* **2013**, *21*, 8071-8077.
136. Liu, D.; Xie, F.; Zhang, W. *J. Org. Chem.* **2007**, *18*, 6992-6997.
137. Gaussian 09, Revision D.01, Frisch, M. J.; Trucks, G. W.; Schlegel, H. B.; Scuseria, G. E.; Robb, M. A.; Cheeseman, J. R.; Scalmani, G.; Barone, V.; Mennucci, B.; Petersson, G. A.; Nakatsuji, H.; Caricato, M.; Li, X.; Hratchian, H. P.; Izmaylov, A. F.; Bloino, J.; Zheng, G.; Sonnenberg, J. L.; Hada, M.; Ehara, M.; Toyota, K.; Fukuda, R.; Hasegawa, J.; Ishida, M.; Nakajima, T.; Honda, Y.; Kitao, O.; Nakai, H.; Vreven, T.; Montgomery, Jr., J. A.; Peralta, J. E.; Ogliaro, F.; Bearpark, M.; Heyd, J. J.; Brothers, E.; Kudin, K. N.; Staroverov, V. N.; Keith, T.; Kobayashi, R.; Normand, J.; Raghavachari, K.; Rendell, A.; Burant, J.C.; Iyengar, S. S.; Tomasi, J.; Cossi, M.; Rega, N.; Millam, J. M.; Klene, M.; Knox, J. E.; Cross, J. B.; Bakken, V.; Adamo, C.; Jaramillo, J.; Gomperts, R.; Stratmann, R. E.; Yazyev, O.; Austin, A. J.; Cammi, R.; Pomelli, C.; Ochterski, J. W.; Martin, R. L.; Morokuma, K.; Zakrzewski, V. G.; Voth, G. A.; Salvador, P.; Dannenberg, J. J.; Dapprich, S.; Daniels, A. D.; Farkas, O.;

Foresman, J. B.; Ortiz, J. V.; Cioslowski, J.; Fox, D, J., Gaussian, Inc., Wallingford CT, 2013.